Cross–Layer Optimization for Multihop Wireless Visual Sensor Networks

Η ΜΕΤΑΠΤΥΧΙΑΚΗ ΕΡΓΑΣΙΑ ΕΞΕΙΔΙΚΕΥΣΗΣ

υποβάλλεται στην

ορισθείσα από την Γενική Συνέλευση Ειδικής Σύνθεσης

του Τμήματος Πληροφορικής Εξεταστική Επιτροπή

από την

Ευτυχία Δάτσικα

ως μέρος των Υποχρεώσεων για τη λήψη του

ΜΕΤΑΠΤΥΧΙΑΚΟΥ ΔΙΠΛΩΜΑΤΟΣ ΣΤΗΝ ΠΛΗΡΟΦΟΡΙΚΗ

ΜΕ ΕΞΕΙΔΙΚΕΥΣΗ

ΣΤΙΣ ΤΕΧΝΟΛΟΓΙΕΣ - ΕΦΑΡΜΟΓΕΣ

Απρίλιος 2012

Dedication

The present thesis is dedicated to my family.

Acknowledgements

I would like to thank my supervisor Assistant Professor Lisimachos Paul Kondi for his continuous guidance, encouragement and patience until the completion of this thesis. I would also like to thank Assistant Professors Konstantinos Parsopoulos and Evangelos Papapetrou for their valuable advice in many technical matters. Special thanks to Angeliki Katsenou, Katerina Pandremmenou and my other colleagues for the excellent collaboration. Finally, I would like to thank my family and my friends for their unconditional support.

Table of Contents

List of Figures

List of Tables

Abstract

Eftychia G. Datsika. MSc, Department of Computer Science, University of Ioannina, Greece. April, 2012. Cross–Layer Optimization for Multihop Wireless Visual Sensor Networks. Thesis Supervisor: Lisimachos Paul Kondi.

Traditional Wireless Visual Sensor Networks (WVSN) consist of low–weight, energy–constrained sensors with wireless communication capability that are equipped with video cameras, and a Centralized Control Unit (CCU) that collects the information from the visual sensors, applies channel and source decoding to the received video of each sensor and manages the resource allocation among all the network nodes. Since the transmission range of a sensor is limited, the recorded video sequences may need to be transmitted using relay nodes until they reach the CCU via a multihop path.

In addition, a node's transmissions cause interference to other transmitting nodes within its transmission range, leading to degradation of the quality of the received videos. Also, the nodes may record scenes with different amounts of motion, so their resource requirements are different. Due to all these factors, resources (transmitted power, source coding rate, channel coding rate) have to be optimally allocated using a quality–aware joint strategy, in order to maintain the end–to–end distortion at a low level for all nodes.

We propose a cross–layer approach that enables the optimal control of the transmitted power and the use of the available network resources, namely the source coding rates and channel coding rates of a multihop DS–CDMA WVSN. The WVSN nodes can either monitor different scenes (source nodes) or retransmit videos of other sensors (relay nodes). Moreover, in real environments the source nodes monitor different scenes that may be of dissimilar motion levels and importance. Hence a higher end–to–end quality is demanded for those nodes that are assigned a higher priority. Overall, each node has different power and resource requirements, and therefore a global optimization approach is required.

For the purpose of enhancing the delivered video quality of the source nodes with respect to their priorities, we suggest the use of two priority–based optimization criteria; the w.NBS (Nash Bargaining Solution with different bargaining powers) criterion maximizes the distortion–related Nash Product by using motion–based bargaining powers, while the MWAD (Minimization of Weighted Aggregation of the Expected Distortion) criterion minimizes the weighted aggregation of the expected end–to–end video distortions by using motion–based weights. Both priority–based criteria achieve their goal even in the case that the background noise is considered, resulting in higher video quality (in

terms of PSNR) for the source nodes that view scenes of high motion. However, MWAD achieves higher average PSNR, whereas w.NBS demands lower transmitted power.

Furthermore, three other criteria that are not taking into account the motion levels of the videos were tested. The e.NBS (Nash Bargaining Solution with equal bargaining powers) criterion uses the Nash Bargaining Solution with equal bargaining powers. The MAD (Minimization of the Average Distortion) criterion aims at minimizing the average distortion of the videos transmitted through the network, while the MMD (Minimization of the Maximum Distortion) criterion minimizes the maximum distortion so as to achieve an overall good quality for the videos. MAD and e.NBS generally favor low motion scenes, and MMD offers the same quality to all scenes. Thus, the appropriate criterion should be chosen according to the requirements of each application.

The employed criteria result in global mixed–integer optimization problems that are resolved by using Particle Swarm Optimization (PSO). The transmitted powers are allowed to take continuous values while the source and channel coding rates are allowed to have only discrete values.

Εκτεταμενη Περιληψη στα Ελληνικα

Ευτυχία Δάτσικα του Γεωργίου και της Σταματίας. MSc, Τμήμα Πληροφορικής, Πανεπιστήμιο Ιωαννίνων, Απρίλιος, 2012. Διαστρωματική Βελτιστοποίηση σε Ασύρματα Δίκτυα Οπτικών Αισθητήρων με Πολλαπλά Άλματα. Επιβλέπων καθηγητής: Λυσίμαχος Παύλος Κόντης.

Τα ασύρματα δίκτυα οπτικών αισθητήρων αξιοποιούνται τα τελευταία χρόνια σε πολλές υπηρεσίες πολυμέσων, όπως σε συστήματα παρακολούθησης και αυτόματου εντοπισμού. Συνήθως αποτελούνται από δύο λειτουργικά μέρη: έναν αριθμό από συσκευές καμερών κατανεμημένων σε ένα χώρο από τον οποίο καταγράφουν σκηνές και μια κεντρική μονάδα ελέγχου που συλλέγει και επεξεργάζεται τις πληροφορίες από τις κάμερες. Δεδομένου ότι η ισχύς μετάδοσης μιας κάμερας μπορεί να μην είναι επαρκής για να γίνει σωστή μετάδοση των σκηνών στην κεντρική μονάδα ελέγχου, είναι απαραίτητες οι αναμεταδόσεις μέσω ενδιάμεσων κόμβων (relay nodes). Επιπλέον, οι μεταδόσεις ενός κόμβου προκαλούν παρεμβολές στις μεταδόσεις κόμβων που βρίσκονται μέσα στην εμβέλειά του, γεγονός που οδηγεί σε υποβάθμιση της ποιότητας των βιντεοακολουθιών που μεταδίδονται.

Επίσης, οι κάμερες ενός ασύρματου δικτύου οπτικών αισθητήρων μπορεί να καταγράφουν σκηνές με διαφορετικά επίπεδα κίνησης. Επομένως, οι απαιτήσεις τους όσον αφορά τους πόρους που τους ανατίθενται, όπως ρυθμός κωδικοποίησης πηγής και καναλιού και ισχύς μετάδοσης, είναι διαφορετικές για κάθε κάμερα. Για παράδειγμα, σκηνές υψηλής κίνησης χρειάζονται περισσότερα bits για την κωδικοποίηση πηγής ώστε να έχουν μια καλή τελική ποιότητα. Αντίθετα, σκηνές χαμηλής κίνησης χρειάζονται λιγότερα bits για την κωδικοποίηση πηγής, άρα μπορούν να χρησιμοποιούν μικρότερη ισχύ μετάδοσης. Έτσι, εξοικονομούν ενέργεια και μειώνονται ταυτόχρονα οι παρεμβολές στους γειτονικούς κόμβους.

Εξαιτίας όλων αυτών των παραγόντων, οι αναφερθέντες πόροι πρέπει να κατανέμονται βέλτιστα μεταξύ των καμερών και των ενδιάμεσων κόμβων με βάση μια κοινή στρατηγική, στοχεύοντας στη διατήρηση της παραμόρφωσης των βινετοακολουθιών σε χαμηλά επίπεδα. Στην παρούσα εργασία προτείνουμε μια μέθοδο κατανομής πόρων σε ασύρματα δίκτυα οπτικών αισθητήρων με πολλαπλά άλματα που χρησιμοποιούν το πρωτόκολλο πρόσβασης DS–CDMA. Η μέθοδος αυτή βασίζεται σε ένα σχεδιασμό ως προς πολλά επίπεδα της στοίβας πρωτοκόλλων OSI, τα οποία ανταλλάσσουν μεταξύ τους πληροφορίες με σκοπό την καλύτερη απόδοση του δικτύου. Για τη βέλτιστη κατανομή των πόρων μεταξύ των καμερών και των ενδιάμεσων κόμβων του δικτύου, χρησιμοποιήσαμε πέντε διαφορετικά κριτήρια. Τα δύο από αυτά, συγκεκριμένα το w.NBS (Nash Bargaining Solution with

different bargaining powers) και το MWAD (Minimization of Weighted Aggregation of the Expected Distortion) επιτυγχάνουν την κατανομή των πόρων σύμφωνα με το επίπεδο κίνησης των μεταδιδόμενων σκηνών. Συγκεκριμένα, το κριτήριο w.NBS βασίζεται στη λύση διαπραγμάτευσης του Nash και μεγιστοποιεί το γινόμενο Nash με χρήση διαφορετικών διαπραγματευτικών ισχύων. Το κριτήριο MWAD ελαχιστοποιεί ένα γραμμικό συνδυασμό των αναμε-νόμενων παραμορφώσεων των σκηνών, δίνοντας σε καθεμία από αυτές βάρος ανάλογα με το επίπεδο κίνησής της. Τα άλλα τρία κριτήρια δε λαμβάνουν υπόψη τα επίπεδα κίνησης των σκηνών. Τα δύο κριτήρια MAD (Minimization of the Average Distortion) και MMD (Minimization of the Maximum Distortion) ελαχιστοποιούν αντίστοιχα τη μέση και τη μέγιστη παραμόρφωση των μεταδιδόμενων σκηνών. Το κριτήριο e.NBS (Nash Bargaining Solution with equal bargaining powers) βασίζεται και αυτό στη λύση διαπραγμάτευσης του Nash και μεγιστοποιεί το γινόμενο Nash με χρήση όμως της ίδιας διαπραγματευτικής ισχύος για όλες τις σκηνές.

Τα προβλήματα βελτιστοποίησης μικτών ακεραίων που προέκυψαν επιλύθηκαν με τη μέθοδο Particle Swarm Optimization (PSO). Οι ισχύες μετάδοσης μπορούν να παίρνουν συνεχείς τιμές από ένα καθορισμένο σύνολο ενώ το σύνολο των τιμών που μπορούν να έχουν οι ρυθμοί κωδικοποίησης πηγής και καναλιού είναι διακριτό.

Τα αποτελέσματα των πειραμάτων που πραγματοποιήθηκαν έδειξαν πως κάθε κριτήριο προσφέρει διαφορετική ποιότητα σε κάθε βιντεοακολουθία σύμφωνα με τα επίπεδα κίνησής της. Τα κριτήρια w.NBS και MWAD προτείνονται για την περίπτωση που απαιτείται ενίσχυση της ποιότητας των σκηνών σύμφωνα με το επίπεδο κίνησής τους και την προτεραιότητά τους, καθώς βελτιώνουν την ποιότητα των σκηνών υψηλής κίνησης ακόμα και με την επίδραση θορύβου κατά τη μετάδοση. Το MWAD επιτυγχάνει υψηλότερο μέσο PSNR, ενώ το w.NBS απαιτεί χαμηλότερη ισχύ μετάδοσης. Όσον αφορά τα άλλα τρία κριτήρια, διαπιστώθηκε ότι το MAD και το e.NBS γενικά ευνοούν τις σκηνές χαμηλής κίνησης, ενώ το MMD προσφέρει ίδιο PSNR για όλες τις σκηνές. Ανάλογα λοιπόν με τις απαιτήσεις για την ποιότητα των σκηνών που θέτει κάθε εφαρμογή, προτείνεται η χρήση διαφορετικού κριτηρίου.

Chapter 1

INTRODUCTION

1.1 Wireless Networking–Wireless Visual Sensor Networks

Due to recent technological advances wireless networks are an active research area in computer science and telecommunications. Wireless telecommunications permit the transfer of information between two or more points that are not physically connected and are useful for a plethora of applications. Thanks to many new wireless technologies and industrial standards, wireless networks have been employed for many real-time video communication services such as video telephony, video conferencing, video games and mobile TV broadcasting. In order to connect different computing devices with varying specifications, like laptop computers, personal digital assistants, smart phones, sensors, automotive computing devices, wireless networks are nowadays of great use.

In the past few years very common networks infrastructures are the *multihop wireless networks* that are utilized by multiple users, e.g. peers that transmit and/or receive content, stations, applications or simple relay nodes. These networks often support the function of various real–time multimedia applications used by the numerous interconnected nodes. These multi–user multimedia applications have generally high demands regarding the delivered QoS (*Quality of Service*). Providing video content of high quality through a wireless network is not a trivial task due to both generic restrictions of this type of networking and the requirements imposed by the loss–intolerant applications that are served by the wireless network.

First of all, resources (transmitted power, bandwidth, source and channel coding rate, bandwidth, transmission time slots, etc.) are usually constrained in a wireless communication channel and should be distributed carefully. The conditions of the physical connections and the fact that the wireless medium is shared lead to fluctuations over time of the transmission bit rates, the bandwidth and the bit error probabilities of the links, especially in wireless networks that change dynamically. Of course, even in static wireless connections, interference among transmitting nodes and signal attenuation due to multipath fading, diffusion, shadowing and similar phenomena reduce the received signal strength and, in consequence, the end–to–end quality.

Additionally, the inherent features of the multimedia transmission impose strict delivery deadlines. Unpredictable demands in terms of QoS by nodes of a dynamically changing topology as well as varied levels of interference often lead to packet collisions and out of order transmissions of real–time flows. Delay–sensitive and bandwidth–intensive applications require an scheme that allocates the provided resources in a timely manner.

The resource allocation problem becomes more crucial in the case of *Wireless Visual Sensor Networks* (WVSN), which are useful in many remote sensing applications, such as video surveillance, environmental tracking, etc [1]. They consist of battery–powered sensors with embedded cameras and small–scale wireless communication capability. Each sensor can capture digital visual information of a specific area and/or relay collected video content through multihop wireless paths to a central control station. For the assignment of the available resources a compromise between two aspects is essential: on the one hand, the energy consumption has to be minimized in order to prolong the WVSN's lifespan and simultaneously reduce the interference among the transmitted signals; on the other hand, the distortion of the delivered video sequences has to be minimized as well so that the QoS requirements of an application are satisfied.

Towards this direction, a series of studies have been implemented in the last decade [18], [22], [24], [8], [37], [23]. A considerable number of them adopts a *cross–layer* approach for the resource allocation in wireless networks and WVSN in particular. The optimization of transmission parameters of the OSI layers separately is not suitable for this type of networking as a fixed allocation of resources does not fit the varied wireless connections and there is a strict interdependence among the layers. With the *cross–layer optimization* lower layers are able to communicate with each other so that the experienced quality at the application layer is enhanced.

1.2 Related Work

A distributed cross–layer technique for multi–user video streaming over multihop wireless networks was proposed by [31]. It assumes that video content is encoded using a scalable video codec that permits users with different demands and resources to transmit/receive videos with different quality by decoding a different part of a a bit stream that was encoded only once. Under this assumption, the packets of each flow are of different

importance , thus different priority must be given to them when it comes to application layer scheduling, routing and MAC layer retransmission strategy as implied by the priority queueing. This technique aims at minimizing the end–to–end packet loss probabilities by selecting the appropriate relay node for each packet according to its priority and choosing the modulation and coding scheme in order to meet the packets' deadlines.

Another technique is the one presented in [14] that considers the wireless transmission of prioritized elastic real–time flows with different end–to–end requirements. A distributed rate control algorithm was proposed, which allocates the transmission bit rates to the flows so that the throughput is maximized under the delay constraints of the flows. This optimization problem is proven to be a global Network Utility Maximization problem where utility maximization ensures that the deadlines of all packets that belong to the transmitted flows are met by adjusting the traffic generation rate.

A popular approach used to increase the performance of multihop wireless networks with dynamically changing network characteristics is machine learning. The initial machine learning schemes that were proposed focused on the allocation the network layer parameters only. Other schemes employed a centralized approach but they demonstrated poor performance when applied in delay–sensitive applications due to large communication overheads and latency in propagation of network information from the control station to the nodes. As an alternative, various distributed approaches were presented aiming at the maximization of network performance, as those of [10] and [11]. However, they did not perform cross–layer optimization.

One of the first cross–layer distributed techniques that are based on machine learning is the one proposed by [21]. It uses reinforcement learning in case of restricted knowledge of the network dynamics and permits the adaptation of transmission parameters and allocation of resources to the varied conditions autonomously for each node. The joint routing and power control problem was modeled as a Markov Decision process that leads to the selection of the optimal policy for all nodes.

Also, several studies that implement game–theoretic analysis have been presented [17], [25], [26]. Cooperative or non–cooperative games allocate efficiently the resources in a centralized or distributed way. The cross–layer scheme described in [5] suggests a distributed non–cooperative game that allows the nodes of a DS–CDMA multihop wireless network to select their transmitted powers and the linear receiver design so that the number of bits sent per unit of power is maximized. Along with the transmitted power, each node has to choose among three types of receiver: a matched filter (MF), a linear minimum mean–squared error receiver (MMSE) and a decorrelator (DE). In this work, the resource allocation is derived by the Nash Equilibrium of the non–cooperative game.

Another alternative for power allocation in DS–CDMA multihop wireless networks is analyzed in [20]. A joint allocation of power levels of the relay nodes under group–based power constraints and the design of linear receivers for interference suppression are proposed. The resulting optimization problem are solved with recursive alternating least squares algorithms (RALS) which allocate the parameters of the receiver, the channels

and the power levels, after creating a group of users according to the power levels.

Furthermore, a lot of research studies have focused on resource allocation techniques especially designed for WVSN. The initial target was to minimize the energy consumption with a cross–layer approach as the one presented in [12]. In this work, after survey of topology, medium access control (MAC) and transceiver energy consumption models, it is shown that regular sleep periods achieve a reduction of the absolute energy consumption per useful transmitted bit in accordance with the data transmission rates. Nevertheless, the scheme does not incorporate any content–aware approach as it is limited to the parameters of physical, data link and network layer.

Of course, for large–scale WVSN, limited resources such as battery power and bandwidth of the wireless links have to be taken into consideration also for the development of an efficient routing scheme. In networks with hundreds of sensors, the routing process is affected by the following parameters that are analyzed in [2]:

(a) Node deployment

(b) Energy consumption without losing accuracy

(c) Data reporting method

(d) Node/link heterogeneity

(e) Fault tolerance

(f) Adaptation to environmental events

(g) Modification of network dynamics

(h) Transmission media (MAC design)

(i) Connectivity and node distribution

(j) Area coverage

(k) Data aggregation and data fusion

(l) QoS demands

According the WVSN structure and routing operation, the routing protocols that have been proposed can be separated into several categories. Depending on the WVSN structure, a routing protocol can be *flat–based*, *hierarchical–based* or *location–based*. As for the routing operation, the protocols can be characterized as *multipath–based*, *query–based*, *negotiation–based*, *QoS–based* and *coherent–based*. Another classification depends on the way that a node finds a path to its destination; a routing protocol can be proactive, reactive or hybrid. Last, the *cooperative* protocols that permit the nodes to send their data to central nodes for aggregation and processing.

Lately, works that are published in the field of WVSN suggest resource allocation approaches oriented to multimedia systems. Some of them include routing–like process that allocates paths to video flows with respect to their priority and impact on multimedia quality.

For instance, the study deployed in [32] analyzes three different approaches for determining the optimal paths and transmission time allocation among the video streams transmitted over the links by the nodes, which maximize the end–to–end video quality. The first approach is a *Centralized optimization* approach for resource allocation per video flows;a central control unit gathers network information and allocates the resources. Although it can reach a global optimal solution, its complexity increases significantly with the number of nodes and suffers from great delay when the network dynamics change and timely adaptation is required. For a static network with high transmission bit rates, the *Congestion Game Modeling* approach is proved to be preferable; a prioritized congestion game is played among the nodes that compete with each other for network resources. They can make autonomous decisions for their video flows in order to maximize their own utility, i.e. minimize the video distortion. The optimal allocation is guaranteed as the modeling always converges to a Nash Equilibrium. The third approach, namely the *Distributed Greedy* approach outperforms the others for networks with varied conditions. This approach allows both the source and relay nodes to decide on the resource allocation and makes use of the network information in order to apply local optimization. Even if the allocation is not optimal and the information overhead may be large, the distributed approach demonstrates high adaptability to varied source characteristics and network dynamics.

Finally, it is worth mentioning a different scheme investigated in [19]. It employs joint coding/routing optimization of network costs (lifetime) and capacity (video distortion) based on link rate allocation and multipath routing that is based on *Network Coding* (NC) for correlated data and *Distributed Video Coding* (DVC). With NC the maximum possible information flow in an network can be achieved because the nodes of a network take several packets and combine them together for transmission instead of simply relaying the packets they receive. DVC models the correlation between multiple sources at the decoder side together with channel codes, therefore the computational complexity is shifted from encoder side to decoder side. It is suitable for applications with complexity-constrained sender, such as sensor networks and video/multimedia compression. The initial optimization problem refers to the wireless link capacity allocation and the choice of NC–subgraph at the transport layer. It results in four cross–layer subproblems; a rate control problem at the transport layer, a channel contention resolution problem at the MAC layer of the data link layer, a distortion control problem and an energy conservation problem that are affected by the choices at the transport and MAC layer respectively.

Without a doubt, many problems need to be tackled in the field of multimedia wireless networks and WVSN in particular. There are already many open research issues at the application, transport, data link and physical layers of the communication stack which

require cross–layer optimization so that better QoS is achieved.

1.3 Scope of Thesis

In this thesis we assume a multihop WVSN where all nodes communicate with each other using DS–CDMA at the physical layer. The WVSN consists of a number of spatially distributed smart low–power sensors with wireless communication capability. The sensors (source nodes) are equipped with video cameras and are capable of recording scenes of a specific field of view. Relay nodes are used in order to deliver the videos received by sensors (source nodes) to the Centralized Control Unit (CCU), as the transmission range of each sensor is limited. The CCU gathers information from all the nodes of the network, applies channel and source decoding to the received videos and manages the resource allocation among all nodes.

Additionally, the transmission of each node causes interference to neighboring nodes that transmit simultaneously. In other words, if a node increases its transmitted power aiming at improving the quality of the video it transmits, the quality of other transmitted videos might deteriorate due to interference. Moreover, in a real environment, the sensors of the network monitor scenes with different motion levels. Some sensors may image a relatively stationary field while others may image scenes with a high level of motion. Thus, not all videos have the same demands as far as the source and channel coding rate are concerned; a node that transmits low motion video can use a lower source coding rate and still yield a good quality for the transmitted video. As can be expected, lower demands in source and channel coding rates lead to lower energy consumption. Given that each video has different motion level, it is of dissimilar importance and can be assigned a different priority when it comes to resource allocation.

Under these assumptions, a cross–layer optimization scheme across the physical, network and application layer is proposed that aims at achieving optimal video transmission over multihop DS–CDMA WVSNs. It is assumed that the transmitted power is defined at the physical layer, the channel coding rate at the data link layer and the source coding rate at the application layer. Along with the problem of efficiently allocating the transmitted power, our scheme appropriately assigns the source coding rate and channel coding rate to each visual sensor while at the same time the transmitted power and the channel coding rate are determined for each relay node. Low bit error rates at each link are necessary, so that the good quality of the transmitted video is maintained. However, the optimization is quality–driven, i.e. the objective is to optimize a function of the received video qualities for each visual sensor, as opposed to optimizing network parameters such as bit error rate, throughput, etc.

Furthermore, we employ five different optimization criteria. First, two priority–based optimization criteria were used that take into account the different priorities of the transmitted videos. The w.NBS criterion (*Weighted Nash Bargaining Solution*) maximizes the distortion–related Nash Product by using motion–based bargaining powers. The aim of

the maximization is to find the Nash Bargaining Solution so that the resources are allocated after the negotiation among the nodes of the network. Next, the MWAD criterion (*Minimization of the Weighted Aggregation of Distortions*) minimizes the weighted aggregation of the expected end–to–end video distortions by using weights that demonstrate the motion level of each transmitted video. With these two criteria, the resource allocation can be determined not only according to the available resources but also the video content characteristics (motion level) of the participating nodes.

Three criteria that treat all videos in a non content–aware manner were tested as well. The e.NBS criterion uses the Nash Bargaining Solution with the same bargaining power for all nodes that join the bargaining game. Thus, it is assumed that all nodes are treated equally. Another criterion is MAD (*Minimization of the Average Distortion*) that aims at minimizing the average distortion of the videos transmitted through the network. The last employed criterion is MMD (*Minimization of the Maximum Distortion*) that minimizes the maximum distortion of all transmitted videos so as to achieve an overall good quality for all of them.

All the aforementioned criteria result in global mixed–integer optimization problems that are resolved by using the Particle Swarm Optimization algorithm (PSO). The transmitted powers are allowed to take continuous values while the source and channel coding rates are allowed to have only discrete values. The only constraint imposed in all optimization problems is that all interfering nodes of a specific hop along a multihop path have the same transmission bit rate.

1.4 Thesis Outline

The rest of the present thesis is structured as follows. In Chapter 2 we describe our network model, the joint source and channel coding and the estimation of the expected distortion. In Chapter 3 the resource allocation problems and the employed optimization criteria are analyzed. Experimental results are presented in Chapter 4. In Chapter 5 conclusions are drawn and future work is outlined.

Chapter 2

FUNDAMENTALS

In this chapter, the considered model for WVSNs is described and some fundamental notions are explained for the better understanding of the proposed cross–layer optimization method.

2.1 System Model

This section presents the basic structure of a WVSN and analyzes the notion of the cross–layer design that is employed by our method.

2.1.1 Network Architecture

Wireless Visual Sensor Networks have emerged as an important class of sensor-based distributed intelligent systems. These networks are comprised of a large number of low–weight energy–constrained sensors that monitor a specific area. The sensors are equipped with video cameras and are able to provide information from a monitored site, performing distributed and collaborative processing of their collected data. Using multiple cameras in the network provides different views of the scene, which enhances the reliability of the captured events. In such case, the sensors can be organized in clusters that have the same

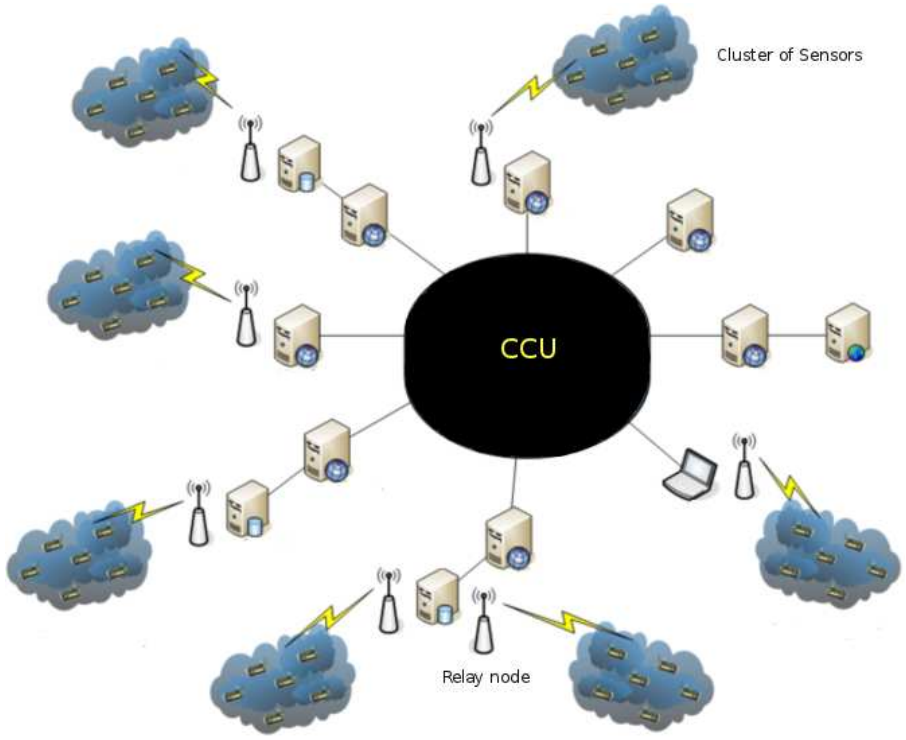

Figure 2.1: Example of a WVSN.

field of view. In a typical WVSN as the one depicted in Fig. 2.1, a Centralized Control Unit (CCU) collects the information from the visual sensors and performs channel and source decoding so as to obtain the received video of each sensor (source node). All sensors communicate with the CCU at the network layer either directly or via other intermediate nodes, i.e. relay nodes. Since the transmission range of a sensor is limited, its recorded video sequences may need to be transmitted using a number of relay nodes until they reach the CCU via a multihop path. The CCU of the WVSN transmits information to all types of nodes and requests changes in transmission parameters, such as source and channel coding rates and transmitted power, aiming at the optimal performance for all nodes.

A WVSN is organized similarly with a wireless network; the network operations of a WVSN are separated in different layers as imposed by the OSI. The OSI, or *Open System Interconnection*, is a model that defines a networking framework for implementing protocols in seven logical layers that group different types of communication functions [4]. Each layer executes specific operations and its services are implemented over the services provided by the layer below it; a layer serves the layer above it and is served by the layer below it. Control is passed from one layer to the next, starting at the application layer in one node, proceeding to the bottom layer, over the channel to the next node and back up the hierarchy [35]. More specifically, the seven layers of OSI are the following (Fig. 2.2):

(a) *Physical layer*: this layer defines the electrical and physical specifications for devices and the relationship between a device and a transmission medium. Its major func-

tions are the establishment and termination of a connection to a communications medium and the modulation or conversion between the representation of digital data in user equipment and the corresponding signals transmitted over a communications channel.

(*b*) *Data Link layer*: this layer provides the functional and procedural means to transfer data between network entities and to detect and possibly correct errors that may occur in the physical layer. It offers methods for exchanging data frames between devices over a common media.

(*c*) *Network layer*: this layer provides the functional and procedural means of transferring variable length data sequences from a source host on one network to a destination host on a different network, while maintaining the quality of service requested by the transport layer (in contrast to the Data Link layer which connects hosts within the same network). The Network layer performs network routing functions, and might also perform fragmentation and reassembly and report delivery errors.

(*d*) *Transport layer*: this layer provides transparent transfer of data between end users, providing reliable data transfer services to the upper layers. Also, it controls the reliability of a given link through flow control, segmentation/desegmentation and error control.

(*e*) *Session layer*: this layer controls the dialogues (connections) between computers. It establishes, manages and terminates the connections between the local and remote application using the services offered by the Transport layer.

(*f*) *Presentation layer*: this layer establishes context between application-layer entities, in which the higher-layer entities may use different syntax and semantics, if the presentation service provides a mapping between them. It provides independence from data representation (e.g., encryption) by translating between application and network formats.

(*g*) *Application layer*: the last layer is the OSI layer closest to the end user, which means that both the OSI application layer and the user interact directly with the software application. This layer implements many well-known communication services and components, such as File Transfer Protocol (FTP), Hypertext Transfer Protocol (HTTP), Domain Name System (DNS), etc.

The most successful implementation of the OSI reference model is today the Transfer Control Protocol/Internet Protocol version 4 (TCP/IPv4) and Fig. 2.3 shows how its layers relate to the layers defined by OSI. Since TCP/IP is loosely based on the layered design of the OSI reference model, its stack design is highly rigid and strict and each layer cooperates only with the layer directly above it or the one directly below it. This results in a non–existent collaboration between the different layers. The weaknesses of

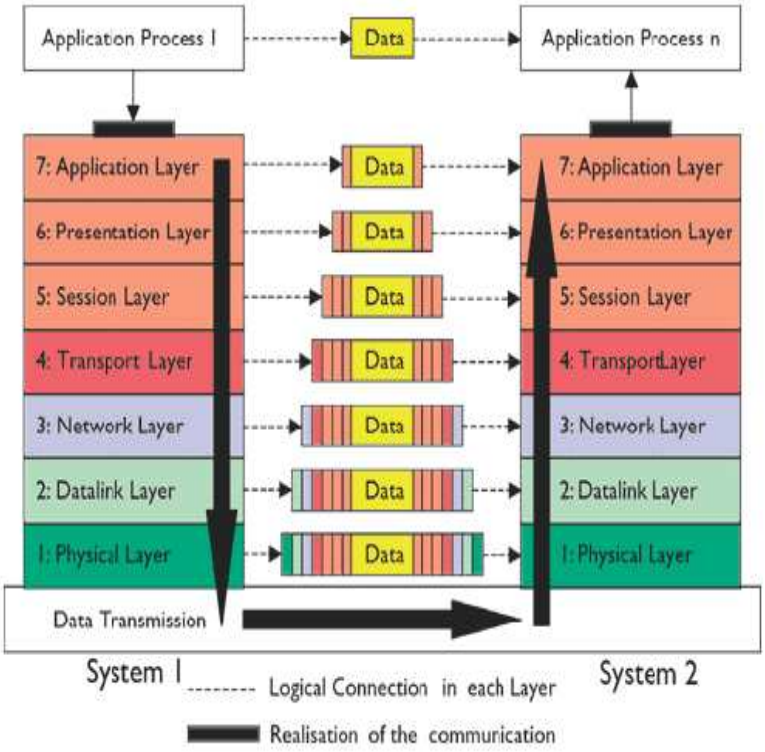

Figure 2.2: The Open Systems Interconnection reference model.

the OSI design are obvious in the case of wireless communications that have different infrastructure and demands comparing to the wired communication.

2.1.2 Cross–Layer Design

To fully optimize wireless broadband networks, both the challenges from the physical medium and the QoS (*Quality of Service*) demands from the applications have to be taken into account. Low throughput, dropped or corrupted packets, jitter and out-of-order delivery affect the offered QoS. The degradation of the end–to–end quality due to these factors is worse in the case of transmission over wireless network, due to the perpetual changes of its state. Owing to this, rate, power and coding at the physical layer should be adapted to meet the requirements of the applications conforming to the current channel and network conditions.

Therefore, information has to be shared between all layers so that the highest possible adaptivity is obtained. Feedback can be transported dynamically via the layer boundaries to enable the compensation for overload, latency or other mismatch of requirements and resources in case that a layer is affected by a deficiency detected in another layer. The cross-layer control mechanism provides a feedback on concurrent quality information for the adaptive setting of control parameters. Cross–layer adaptation has become a popular solution for optimizing the performance of real–time multimedia applications implemented on resource constrained systems. By jointly optimizing parameters, configurations and

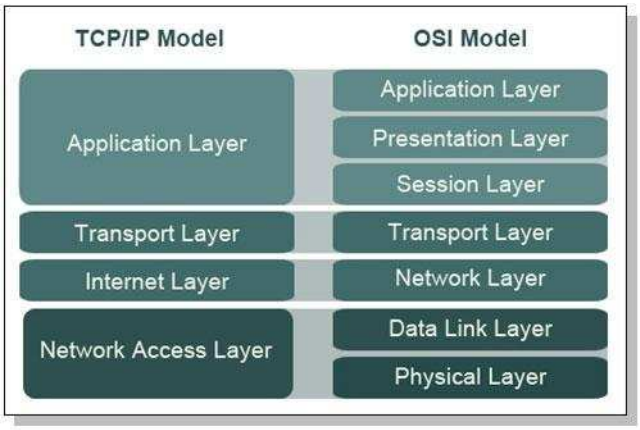

Figure 2.3: The TCP/IP stack.

algorithms across two or more system layers, rather than optimizing them in isolation, system performance can be significantly improved.

Taking these facts into consideration, we applied a multi–node cross–layer optimization technique on multihop DS–CDMA based WVSNs that operates across the physical, data link and application layers of the system. The employed method accounts for network performances all the way from the physical layer up to the application layer. All of the source and relay nodes of the considered WVSN are jointly optimized as the following parameters are allocated simultaneously to them by the optimization scheme:

(a) **Transmitted power** at the physical layer.

(b) **Channel coding rate** at the data link layer.

(c) **Source coding rate** at the application layer.

2.2 Radio Propagation Models

In reality, the signal strength or energy level decays as the distance from the transmitter to the receiver increases. The propagation of the signal across a link decreases its energy. With any communications system, the signal that is received differs from the signal that is transmitted, due to various transmission impairments. For analog signals, these impairments introduce various random modifications whereas for digital signals bit errors may corrupt the transmitted data; a binary 1 is transformed into a binary 0 and vice versa.

Generally, the radio waves travel between two points in four different ways. They either propagate directly from one point to another or follow the curvature of the earth or even refract off the ionosphere back to earth. Sometimes they might become trapped in the atmosphere and travel long distances. For the WVSNs deployed in this thesis, the transmitted signal uses a frequency equal to 315 MHz. Therefore, we assume line–of–sight wireless transmission [33]. For this kind of transmission the most significant impairments that degrade the signal quality are the following:

(*a*) Attenuation and Attenuation distortion

(*b*) Free space loss

(*c*) Noise

(*d*) Atmospheric absorption

(*e*) Multipath

(*f*) Refraction

In our method either the free space loss or the multipath and the noise affect the level of the received power of a node. *Free space loss* is the type of attenuation of a transmitted signal that occurs while the signal is being spread over a larger and larger area, even if no other sources of attenuation or impairment are assumed. Next, the *multipath* is the effect that takes place when the signal is reflected by obstacles so that multiple copies of the signal with varied delays can be received. There are cases that the receiver may capture only reflected signals or a composite signal that can be either larger or smaller than the direct signal, depending on the differences in the path lengths of the direct and reflected waves. As far as the noise is concerned, it can be defined as additional unwanted signals inserted between transmission and reception of an original signal. For our model, noise is considered to be the interference caused to a node's transmission by the simultaneous transmissions of other nodes and the background noise.

These propagation effects influence system performance, particularly when dealing with power control. Although the mechanisms are diverse, they are usually characterized by these effects. The propagation models have traditionally focused on predicting the average received signal strength at a given distance from the transmitter, as well as the variability of the signal strength in close spatial proximity to a particular location. There are two general categories of propagation models [29]:

(*a*) The *large–scale* propagation models that predict the mean signal strength for an arbitrary transmitter–receiver(T-R) separation distance (of several hundreds or thousand meters) and are useful in estimating the radio coverage area of a transmitter.

(*b*) The *small–scale* or *fading* models that characterize the rapid fluctuations of the received signal strength over very short travel distances (a few wavelengths) or short–time durations (on the order of seconds).

Moreover, different models have been developed to meet the needs of realizing the propagation behavior in different conditions. Types of models for radio propagation include the models for indoor or outdoor applications, the ground wave propagation models, the sky wave propagation models, the environmental attenuation models, the point-to-point propagation models, the terrain models and the city models.

In our work we employed two different propagation models, described in sections 2.2.1 and 2.2.2, so as to predict the received power at a specific distance from a node, namely the *Free Space* and the *Two Ray Ground Reflection* Model. We take into account both the free space model (direct path) and the multipath fading model (reflection path) depending on the distance between transmitter and receiver. If this distance is less than a certain distance known as the *cross–over distance* d_0, the Free Space model should be used, else the Two Ray Ground model is used. The cross–over distance is defined as follows:

$$d_0 = \frac{4\pi h_r h_t \sqrt{l}}{\lambda}, \tag{2.1}$$

where $l \leqslant 1$ is the system loss factor, λ is the wavelength of the carrier signal, h_t is the transmitter antenna height and h_r is the receiver antenna height.

2.2.1 Free Space Propagation Model

The Free Space Propagation Model is used to predict received signal strength when the transmitter and receiver have a clear, unobstructed line–of–sight path between them. As with most large–scale radio wave propagation models, this model predicts that received power decays as a function of the T-R separation distance raised to some power. It basically represents the communication range as a circle around the transmitter, which radiates in all directions uniformly (isotropic radiator). Letting S^{trans} be the power at the transmitted antenna, $S^{\text{rec}(d)}$ the power at the receiver antenna, d the distance between the two antennas, λ the wavelength of the carrier signal, the free space loss for an ideal isotropic transmitter is:

$$\frac{S^{\text{trans}}(d)}{S^{\text{rec}}(d)} = \frac{(4\pi)^2 d^2}{\lambda^2}. \tag{2.2}$$

The received power $S_n^{\text{rec}}(d)$ at a receiver node in distance d from a node n that transmits power S_n^{trans} is given by the Friis formula for transmitters that are not isotropic, thus the antenna gains have to be taken into account:

$$S_n^{\text{rec}}(d) = S_n^{\text{trans}} \frac{G_t G_r \lambda^2}{(4\pi)^2 d^2 l} = S_n^{\text{trans}} \frac{G_t G_r c^2}{(4\pi)^2 f^2 d^2 l}, \tag{2.3}$$

where $l \geqslant 1$ is the system loss factor not related to propagation, λ is the wavelength of the carrier signal in meters, f is the carrier frequency in Hz, G_t is the transmitter antenna gain and G_r is the receiver antenna gain. The value λ is related to the carrier frequency by $\lambda = c/f$, where c is the speed of light which is equal to 3×10^8 m/sec. The values for S_n^{trans} and $S_n^{\text{rec}}(d)$ must be expressed in the same units while G_t and G_r are dimensionless quantities. The miscellaneous losses l are usually due to transmission line attenuation, filter losses as well as antenna losses in the communication system. A value of $l = 1$ indicates no loss in the system hardware.

The Eq. (2.3) shows that the received power falls off as the square of the T-R separation distance. It has been proved that for the same antenna dimensions and separation, the

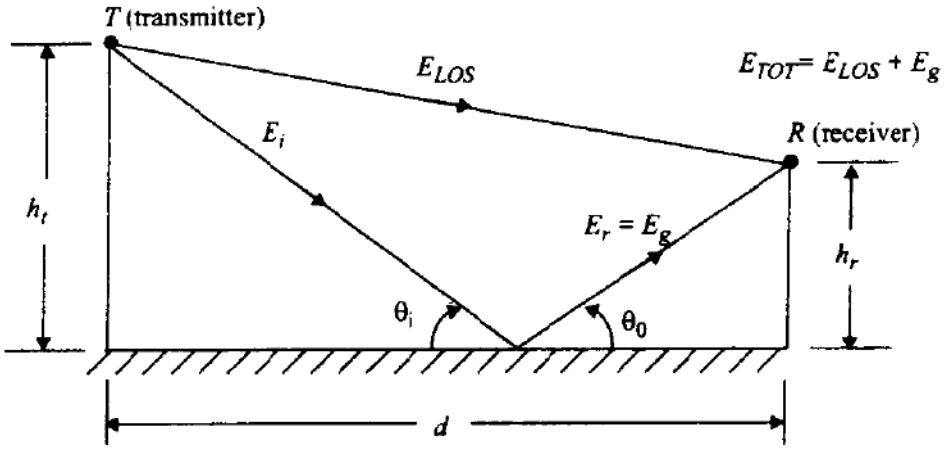

Figure 2.4: The Two Ray Ground Reflection Model.

higher the frequency f is, the higher is the free space path loss. As the frequency increases, losses become more burdensome.

2.2.2 Two Ray Ground Reflection Model

A single line–of–sight between two nodes may not always be the only means of propagation. Hence, the Free Space Propagation Model can be inaccurate and the Two Ray Ground Reflection Model is preferable. This model is based on geometric optics and considers both the direct line–of–sight path (component E_{LOS}) and a ground reflection path (component E_g) between transmitter and receiver, as depicted in Fig. 2.4. Assuming the Earth to be flat, the received power $S_n^{\text{rec}}(d)$ at a receiver node in distance d from a transmitting node n is predicted by:

$$S_n^{\text{rec}}(d) = S_n^{\text{trans}} \frac{G_t G_r h_t^2 h_r^2}{d^4 l}, \tag{2.4}$$

where S_n^{trans} is the transmitted power of node n, $l \geqslant 1$ is the system loss factor not related to propagation, G_t is the transmitter antenna gain, G_r is the receiver antenna gain, h_t is the transmitter antenna height and h_r is the receiver antenna height. This model has been found to be reasonably accurate for predicting the large–scale signal strength over distances of several kilometers, comparing to the Free Space Model which gives better results for small distances. Although the Eq. (2.4) demonstrates a faster power loss than Eq. (2.3) as the T-R separation distance increases, the Two Ray Ground Reflection Model does not perform well for short distances. This is caused by the oscillation due to the constructive and destructive combination of the two rays. It should also be noted that at large values of d ($d \gg \sqrt{h_t h_r}$), the received power and the path loss become independent of the frequency.

2.3 Joint Source and Channel Coding

Regarding the efficient transmission of data through a channel, coding theory has formed essentially two aspects. The first one is the *data compression* or *source coding* that involves encoding information using fewer bits than the original representation. The second is the *error correction* or *channel coding*, a technique used for controlling errors in data transmission over unreliable or noisy communication channels.

Shannon's separation theorem states that source coding and channel coding can be performed separately and sequentially, while maintaining optimality, if the source coding rate does not exceed channel capacity. However, this is true only in the case of asymptotically long block lengths of data. In many practical applications, the conditions of the Shannon's separation theorem neither hold, nor can be used as a good approximation. The two employed coders do not actually have infinite delay and complexity so that the the source and channel coding are optimized independently. To make matters worse, this theorem can be applied only in point–to–point communication so it does not fit the modern multiuser communications systems with continuously variable channel conditions and high QoS demands.

As a consequence, considerable interest has developed in various schemes of joint source-channel coding as it has the ability to cope with varied channel qualities and to approach the theoretical bounds of transmission rates. In information theory, *joint source–channel coding* is the encoding of a redundant information source for transmission over a noisy channel, and the corresponding decoding, using a single code instead of the more conventional steps of source coding followed by channel coding.

In our model we employ joint source–channel coding under the assumption that the two encoders exchange information that they are able to communicate with the physical layer. Figure 2.5 illustrates the considered DS–CDMA wireless system. The Centralized Control Unit (CCU) uses a rate–controller that allocates efficiently the source and channel coding rates and the transmitted powers to the users of the network. It is obviously necessary that the application layer should communicate with the physical and the data link layer so that parameters of all layers are tuned conforming to the users' requirements (distortion) and the network conditions (bit error rate); the source coding rate must be chosen aiming at the minimization of the video distortion; the channel coding rate should offer a good level of protection to the transmitted data; the transmitted power affects is equally important to the other parameters as it affects the performance of the layers above the physical layer.

2.3.1 Source Coding – H.264/AVC standard

Video compression is the process of converting digital video into a format that takes up less capacity when it needs to be stored or transmitted. It is useful because it helps reduce the consumption of data space or transmission capacity. Because compressed data must be decompressed to be used, this extra processing imposes computational or other

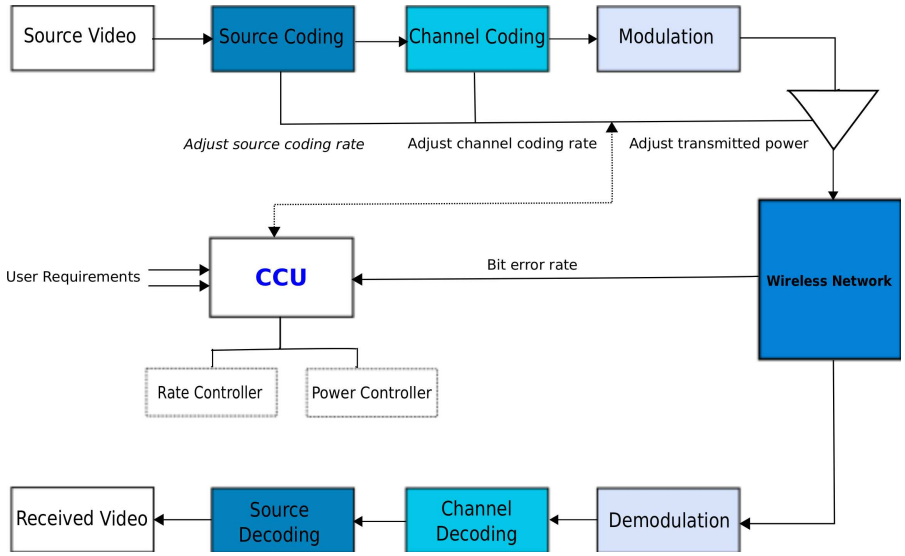

Figure 2.5: The cross–layer design of a wireless system that supports joint source and channel coding.

costs through decompression. For instance, a compression scheme for video may require expensive hardware for the video to be decompressed fast enough to be viewed as it is being decompressed, and the option to decompress the video in full before watching it may be inconvenient or require additional storage.

The design of data compression schemes involve trade-offs among various factors, including the degree of compression, the amount of distortion introduced, e.g. when using lossy data compression, and the computational resources required to compress and uncompress the data. Especially for the case the video transmission, a high level of compression is required with the less possible impact on the offered quality. It is therefore essential that a compression algorithm causes the least possible distortion to the decoded video for a certain bit rate that is used for the encoding process.

For the compression of the video sequences used for transmission in the WVSN topologies tested with our method the H.264/AVC (Advanced Video Coding) standard was preferred. It is currently one of the most commonly used formats for the recording, compression, and distribution of high definition video. This codec is adopted for an increasing range of applications including:

(a) High Definition DVDs (HD–DVD and Blu–Ray formats)

(b) High Definition TV Broadcast in Europe

(c) Apple products including iTunes video downloads, iPod video and MacOS

(d) Mobile TV broadcasting

(e) Internet video

(f) Videoconferencing

Figure 2.6 shows the encoding and decoding process and highlights the parts that are covered by the H.264/AVC standard. The encoder performs *block motion compensation*, i.e. it processes a frame of video in units of a *macroblock* (16×16 displayed pixels). It forms a prediction of the macroblock based on previously coded data, either from the current frame (*intra prediction*) or from other frames that have already been coded and transmitted (*inter prediction*). The encoder subtracts the prediction from the current macroblock to form a residual.

The H.264/AVC standard also covers two layers in order to achieve a "network–friendly" video representation addressing "conversational" (video telephony) and "non conversational" (storage, broadcast, or streaming) applications; the *Video Coding Layer* (VCL) which creates a coded representation of the source content and the *Network Abstraction Layer* (NAL) to format the VCL data and provide header information about how to use the data for video delivering over network [30].

The coded video data are organized into *NAL units*, which are packets that each contains an integer number of bytes [34]. A NAL unit starts with a one–byte header, which signals the type of the data it contains. The remaining bytes represent payload data. NAL units are classified into *VCL NAL units*, which contain coded slices or coded slice data partitions, and *non–VCL NAL units*, which contain associated additional information. The most important non–VCL NAL units are parameter sets and Supplemental Enhancement Information (SEI). The sequence and picture parameter sets contain infrequently changing information for a video sequence. SEI messages are not required for decoding the samples of a video sequence. They provide additional information which can assist the decoding process or related processes like bit stream manipulation or display. A set of consecutive NAL units with specific properties forms an *access unit*. The decoding of an access unit results in exactly one decoded picture. A set of consecutive access units with certain properties is a coded video sequence; these access units are sequential in the NAL unit stream and use only one sequence parameter set. A coded video sequence represents an independently decodable part of a NAL unit bit stream. It always starts with an *instantaneous decoding refresh access unit* (IDR), which signals that the IDR access unit and all the following access units can be decoded without decoding any previous pictures of the bit stream. An IDR access unit contains an intra picture which is a coded picture that can be decoded without decoding any previous pictures in the NAL unit stream. A NAL unit stream may contain one or more coded video sequences.

The VCL of H.264/AVC follows the so–called block–based hybrid video coding approach. The way pictures are partitioned into smaller coding units follow the traditional concept of subdivision into *macroblocks* and *slices*. Each picture is partitioned into macroblocks and slices that each covers a rectangular picture area of 16×16 luma sample and 8×8 samples of the two chroma components, in the case of a video in a 4:2:0 chroma sampling format. The samples of a macroblock are either specially or temporally predicted and the resulting prediction residual signal is represented using transform coding. The macroblocks of a picture are organized in slices, each of which can be parsed inde-

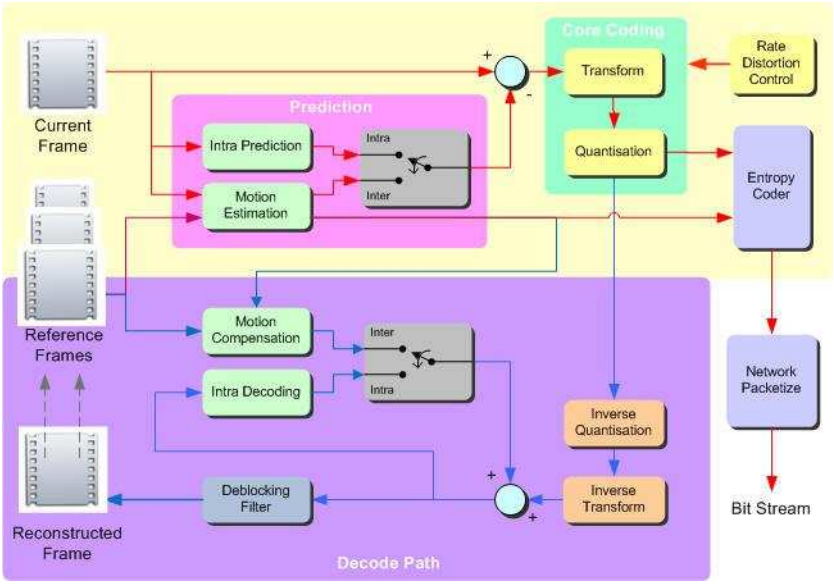

Figure 2.6: The H.264/AVC encoder and decoder structure.

pendently of other slices in a picture. Depending on the degree of freedom for generating the prediction signal, H.264/AVC supports three basic slice coding types:

(a) I-slice: intra picture predictive coding using spatial prediction from neighboring regions,

(b) P-slice: intra picture predictive coding and inter picture predictive coding with one prediction signal for each predicted region,

(c) B-slice: intra picture predictive coding, inter picture predictive coding and inter picture bipredictive coding with two prediction signals that are combined with a weighted average to form the region prediction.

The prediction methods supported by H.264/AVC are more flexible than those in previous standards, enabling accurate predictions and hence efficient video compression. Intra prediction uses 16×16 and 4×4 block sizes to predict the macroblock from surrounding previously coded pixels within the same frame (Fig. 2.7). Inter prediction uses a range of block sizes (from 16×16 down to 4×4) to predict pixels in the current frame from similar regions in previously coded frames (Fig. 2.8).

For transform coding, H.264/AVC specifies a set of integer transforms of different block sizes. While for intra macroblocks the transform size is directly coupled to the intra prediction block size, the luma signal of motion–compensated macroblocks that do not contain blocks smaller than 8×8 can be coded by using either 4×4 or 8×8 transform. For the chroma components a two–stage transform, consisting of 4×4 transforms and a Hadamard transform of the resulting DC coefficients is employed. A similar hierarchical transform is also used for the luma component of macroblocks coded in intra 16×16. All

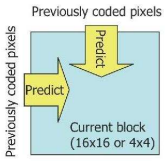

Figure 2.7: The intra prediction

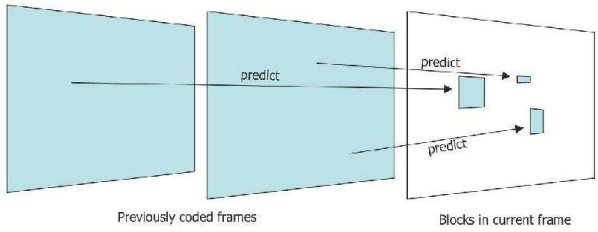

Figure 2.8: The inter prediction.

inverse–transforms are specified by exact integer operations, so that inverse–transform mismatches are avoided.

In the step of quantization, the output of the transform, a block of transform coefficients, is quantized, i.e. each coefficient is divided by an integer value. H.264/AVC uses *uniform reconstruction quantizers*. Quantization reduces the precision of the transform coefficients according to a quantization parameter QP which is selected for each macroblock. One of 52 quantization step sizes can be chosen per macroblock. Typically, the result is a block in which most or all of the coefficients are zero, with a few non–zero coefficients. Setting QP to a high value means that more coefficients are set to zero, resulting in high compression at the expense of poor decoded video quality. Setting QP to a low value means that more non–zero coefficients remain after quantization, resulting in better quality but lower compression.

The video coding process produces a number of values that must be encoded to form the compressed stream. These values are the quantized transform coefficients, information to enable the decoder to recreate the prediction, information about the structure of the compressed data and the compression tools used during encoding and information about the complete video sequence. These values and parameters (syntax elements) are converted into binary codes using variable length coding and/or arithmetic coding. In particular, for the entropy coding two lossless compression algorithms are preferred; *the Context-adaptive binary arithmetic coding* (CABAC) and the *Context-adaptive variable-length coding* (CAVLC). While CAVLC uses variable length codes and its adaptivity is restricted to the coding of transform coefficient levels, CABAC utilizes arithmetic coding and a more sophisticated mechanism for employing statistical dependencies, which leads to typical bit rate savings of 10-15 % comparing to CAVLC. Each of these encoding methods produces an efficient, compact binary representation of the information. The encoded bit stream can be stored or transmitted after this process.

In the decoding process the video decoder that receives the compressed H.264 bit stream decodes each of the syntax elements and extracts the necessary information (quantized transform coefficients, prediction information, etc). This information is then used to reverse the coding process and recreate a sequence of video pictures.

The quantized transform coefficients are re–scaled and each of them is multiplied by an integer value so that its original scale is restored. An inverse transform combines the standard basis patterns, weighted by the re–scaled coefficients, to re–create each block of

residual data. These blocks are combined together to form a residual macroblock. For each macroblock, the decoder forms a prediction which is added to the decoded residual. A decoded macroblock is next reconstructed and can be displayed as part of a video frame.

The biggest advantage of the H.264/AVC standard over previous standards is its compression performance. It can deliver better image quality at the same compressed bit rate or a lower compressed bit rate for the same image quality, comparing to other standards such as MPEG-2 and MPEG-4 Visual.

2.3.2 Channel Coding – Rate Compatible Punctured Convolutional Codes

Many communication channels are subject to channel noise, and thus errors may be introduced to the transmitted data during transmission from the source to a receiver. In information theory and coding theory with applications in computer science and telecommunication two techniques that enable reliable delivery of digital data over unreliable communication channels are employed: the *error detection* and the *error correction*. Error detection techniques allow detecting errors caused by noise or other impairments during transmission, while error correction enables the detection of errors and the reconstruction of the original error–free data. The general idea for achieving error detection and correction is to add some redundancy (i.e. some extra data) to a message, which receivers can use to check the consistency of the delivered message, and to recover data determined to be erroneous.

In telecommunications, the error detection is most commonly realized using a suitable hash function or a checksum algorithm. A *hash function* adds a fixed-length tag to a message, which enables receivers to verify the delivered message by recomputing the tag and comparing it with the one provided. A *checksum algorithm* is the procedure that yields the *checksum* (fixed-size datum computed from an arbitrary block of digital data) from the data. A good checksum algorithm will yield a different result with high probability when the data is accidentally corrupted; if the checksums match, the data is very likely to be free of accidental errors. The error correction may be realized in two different ways:

(*a*) *Automatic repeat request* (ARQ): This is an error control technique whereby an error detection scheme is combined with requests for retransmission of erroneous data. Every block of data received is checked using the error detection code used, and if the check fails, retransmission of the data is requested. This may be done repeatedly, until the data can be verified.

(*b*) *Forward error correction* (FEC): The sender encodes the data using an *error-correcting code* (ECC) prior to transmission. The additional information (redundancy) added by the code is used by the receiver to recover the original data. In general, the reconstructed data is what is deemed the "most likely" original data.

In addition, there are three main categories of FEC codes. On the one hand, there are the *Block codes* that work on fixed-size blocks (packets) of bits or symbols of predetermined size. Practical block codes can generally be decoded in polynomial time to their block length. On the other hand, there are the *Convolutional codes* which work on bit or symbol streams of arbitrary length. A convolutional code can be turned into a block code, if desired, by a technique called "tail-biting". The third category is the *Turbo codes*. Their performance is close to the Shannon theoretical limit. The encoder is formed by the parallel concatenation of two convolutional codes separated by an interleaver or permuter and the two corresponding decoders decode the received data through an iterative process.

The convolutional codes are used extensively in numerous applications in order to achieve reliable data transfer. They map information to code bits sequentially by convolving a sequence of information bits with "generator" sequences. The encoder has a certain structure such that the encoding process can be expressed as convolution. Usually they are defined by three parameters (n, m, k); n is the number of output bits, m is the number of input bits and k is the number of the registers. The ratio m/n is the *code rate* and demonstrates the efficiency of a convolutional code. Also, the *constraint length* $L = m(k-1)$ represents the number of bits in the registers that affect the output of the n bits.

To convolutionally encode data, k memory registers, each holding 1 input bit, are employed. The encoder has n modulo-2 adders and n generator polynomials, one for each adder. These polynomials decide which bits will be added so that each output bit is derived. An input bit $m1$ is fed into the leftmost register. Using the generator polynomials and the existing values in the remaining registers, the encoder outputs n bits. Now all register values are shifted bitwise to the right ($m1$ moves to $m0$, $m0$ moves to $m-1$) and the registers wait for the next input bit. If there are no remaining input bits, the encoder continues output until all registers have returned to the zero state.

Figure 2.9 depicts an encoder with code rate equal to 1/3 and constraint length L equal to three. Generator polynomials are $G1 = (1,1,1)$, $G2 = (0,1,1)$, and $G3 = (1,0,1)$. Therefore, output bits are calculated as follows:

$$n1 = m1 + m0 + m - 1$$
$$n2 = m0 + m - 1$$
$$n3 = m1 + m - 1$$

Several algorithms exist for decoding convolutional codes. For relatively small values of k, the *Viterbi* algorithm is universally used as it provides maximum likelihood performance and is highly parallelizable. Codes with bigger constraint length are more practically decoded with any of several sequential decoding algorithms, of which the *Fano* algorithm is the best known. Unlike Viterbi decoding, sequential decoding is not maximum likelihood but its complexity increases slightly with constraint length, allowing the use of strong, long-constraint-length codes.

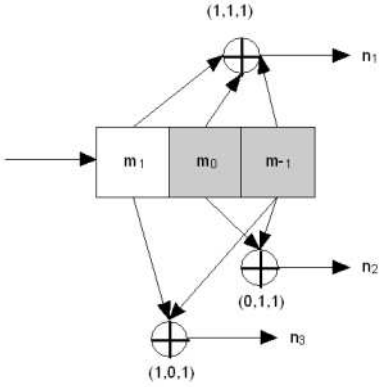

Figure 2.9: A convolutional encoder with rate 1/3 and $L = 3$.

The Viterbi algorithm employed for channel decoding in our model finds the most likely sequence of hidden states called the Viterbi path. It computes a specific metric, e.g. the Hamming distance, for each path. The path that has the higher value of that metric is the path to be chosen. This results in a sequence of observed events. The algorithm compares the received sequence with all possible transmitted sequences and selects the path of the trellis that results in a sequence that is similar to the received sequence in most of the places. This algorithm assumes that the error probabilities are very low and that the errors are randomly distributed. Considering the convolutional code with (n, m, k) = (2, 1, 3) of Fig. 2.10 and its corresponding *trellis* (a state diagram with a vertical layout) Fig. 2.11, a valid path through the trellis is a-b-d-c-a-b-c-a that was generated by the input sequence 1100100 and produces the output sequence 11 10 01 01 11 11 10 11. In case of an invalid path, the decoder tries to apply error correction by determining the input that most likely generated the invalid output.

For a simpler implementation of the decoding process using the Viterbi algorithm for rate m/n with two branches arriving at each node instead of 2^m branches, the *punctured* convolutional codes were introduced. These codes are based on *puncturing*, a technique that makes a m/n rate code from a "basic" code with rate equal to 1/2. The new rate code is reached by deletion of some bits in the encoder output. Bits are deleted according to a *puncturing matrix*. For example, if a code with rate 2/3 has to be derived using the matrix $\left[\begin{smallmatrix}1 & 0\\ 1 & 1\end{smallmatrix}\right]$ the output of a basic encoder should be taken; every second bit from the first branch and every bit from the second one are transmitted.

An extension to the puncturing technique is the utilization of the *Rate Compatible Punctured Convolutional codes* (RCPC). A low rate $1/N$ code is punctured periodically with a period P so that a family of codes with rate $P/(P + l)$, where $l \in [1, (N - 1)P]$. A rate compatibility restriction on the puncturing tables ensured that all code bits of high rate codes (mother codes) are used by the lower rate codes. In other words, a code with higher rate must be a subset of a code with a lower rate. If these codes are used, the transmitted signal can be encoded at different rates without increasing the decoder complexity.

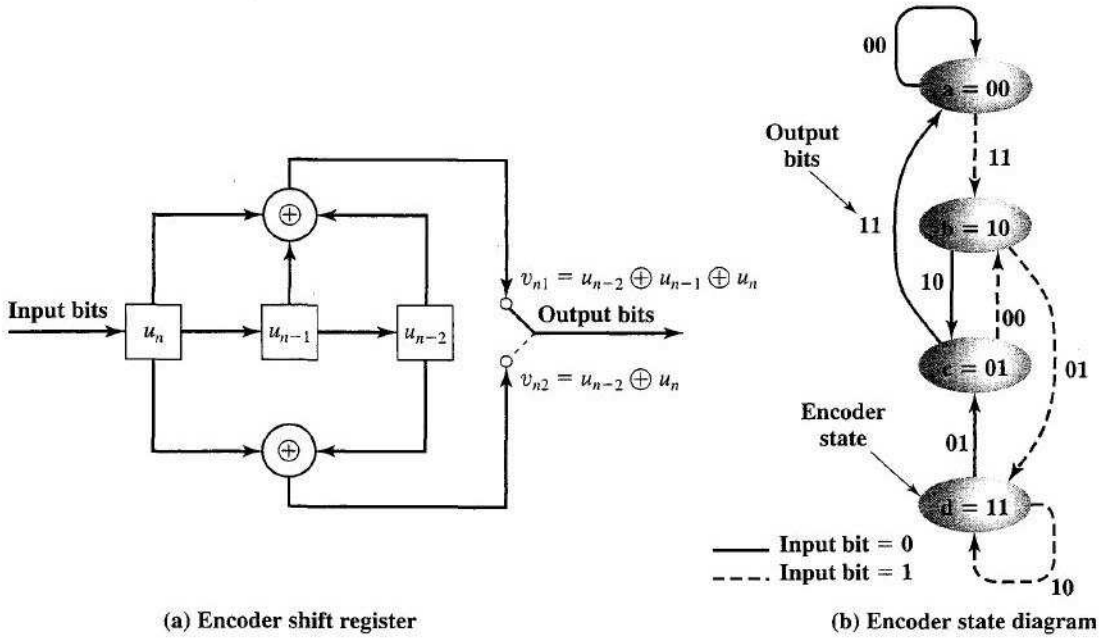

Figure 2.10: A convolutional encoder with $(n, m, k) = (2, 1, 3)$.

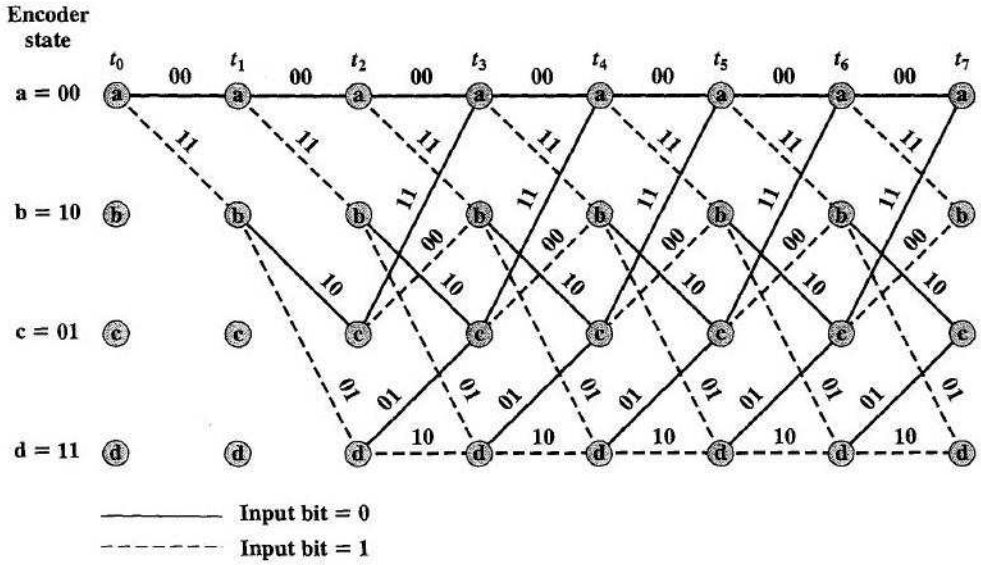

Figure 2.11: Trellis Diagram for a convolutional encoder with $(n, m, k) = (2, 1, 3)$.

RCPC CODE: M=4 P=8

d	8/9 8/9	8/10 4/5	8/12 2/3	8/14 4/7	8/16 1/2	8/18 4/9	8/20 4/10	8/22 4/11	8/24 1/3	8/26 4/13	8/28 2/7	8/30 4/15	8/32 1/4
	1111 0111 1000 1000 0000 0000	1111 1111 1000 1000 0000 0000	1111 1111 1010 1010 0000 0000	1111 1111 1110 1110 0000 0000	1111 1111 1111 1111 0000 0000	1111 1111 1111 1111 1000 1000	1111 1111 1111 1111 1100 1100	1111 1111 1111 1111 1110 1110	1111 1111 1111 1111 1111 1111	1111 1111 1111 1111 1000 1000	1111 1111 1111 1111 1010 1010	1111 1111 1111 1111 1110 1110	1111 1111 1111 1111 1111 1111
2	1												
3	242	42											
4	4199	274	4										
5	63521	2688	0	2		c_d							CODE
6	885318	21692	496	62									10011
7	11678199	154684	0	144	32	2							11101
8		1103894	10884	350	96	36	2						10111
9			0	2006	160	60	34	10					11011
10				5394	576	82	28	8					
11					1800	354	66	36	8	2			
12					4000	856	226	72	48	4			
13							354	114	72	56	20	2	
14								228	48	40	20	16	
15									104	38	36	38	32
16									256	104	24	0	16
17											56	18	0
18											184	74	32
19													48
20													96

Figure 2.12: Puncturing tables with c_d values for RCPC codes with $P = 8$, $k = 4$ and rates $\frac{8}{8+l}, l = 1, 2, 4, 6 \ldots 24$.

Another advantage of the RCPC codes is that the same Viterbi decoder can be used for all RCPC codes of the same number of registers. Furthermore, the Viterbi upper bounds can be found for the bit error probability P_b that is given by:

$$P_b \leqslant \frac{1}{P} \sum_{d=d_{\text{free}}}^{\infty} c_d P_d \tag{2.5}$$

where P is the period of code, P_d is the pairwise error probability in choosing between two paths of mutual Hamming distance d, d_{free} is the minimum Hamming distance between two different coded sequences (free distance of the code) and c_d is the distance spectra, i.e. the average number of bit errors resulting from an erroneous choice between two paths with distance d.

For the RCPC codes used in our model, we set $P = 8$ and $k = 4$. A family of codes with rates $\frac{8}{8+l}, l = 1, 2, 4, 6 \ldots 24$ is derived. The necessary values for c_d and d_{free} are given by the table shown in Fig. 2.12.

2.4 Direct-Sequence Code Division Multiple Access (DS–CDMA)

In the present thesis the nodes of the considered WVSNs access the channel by employing *Direct-Sequence Code Division Multiple Access* (DS–CDMA), the most widely used type of *Code Division Multiple Access* (CDMA).

CDMA

First of all, CDMA is a multiplexing technique used with *spread spectrum*. Spread spectrum is actually a method by which a signal generated in a particular bandwidth is deliberately spread in the frequency domain, resulting in a signal with a wider bandwidth. CDMA employs spread-spectrum technology and a special coding scheme where each transmitter is assigned a different code sequence. Popular codes are the maximum length or "pseudo-noise" sequences, the Walsh the Hadamard codes, the Gold codes and the Kasami codes. In that way *multiple access* is provided which means multiple users are allowed to be multiplexed over the same physical channel, so that they all transmit their signals simultaneously on the same frequency.

Two main approaches exist for the implementation of spread spectrum modulation in multiple access schemes such as CDMA: the *Direct Sequence Spread Spectrum* (DSSS) and the *Frequency Hopping Spread Spectrum* (FHSS). In CDMA based systems that use FSSS (FH–CDMA) the data of each user are transmitted over a carrier that switches rapidly among many frequency channels. The bandwidth spectrum is split in a number of frequencies so that many users are able to transmit simultaneously. On the contrary, in the CDMA systems that employ DSSS (DS–CDMA) the data of all users can be transmitted at the same time over the same bandwidth spectrum. The final transmitted signal of each user occupies more bandwidth than the information signal that is modulated.

Supposing we have an original signal with a bit data rate D that is transmitted using CDMA. Each bit is broken into k *chips* according to a pattern which is specific for each user (*user's code*). The resulting channel will have a *chip rate* equal to kD chips/sec. For Fig. 2.13 three users A, B, C with codes $c_a = (1, 0, 0, 1)$, $c_b = (1, 1, 0, 0)$ and $c_c = (1, 1, 0, 1)$ respectively are assumed. Letting $k = 4$, a decoder that receives a chip sequence $d = (d1, d2, d3, d4)$ and tries to communicate with a user u that has a code $c = (c1, c2, c3, c4)$ applies the following decoding process:

$$S_u(d) = d1 \times c1 + d2 \times c2 + d3 \times c3 + d4 \times c4. \tag{2.6}$$

If the user A wants to send a 1 bit, it transmits its code as a chip pattern (1, 0, 0, 1), else it uses the complement of this pattern, (0, 1, 1, 0), in order to transmit a 0 bit. For the respective cases, it is derived from Eq. (2.6) that $S_A(1, 0, 0, 1) = 2$ and $S_A(0, 1, 1, 0) = 0$. If the decoder computes for $S_A(d)$ a value equal to 2 or 0 then a bit 1 or 0 is received. In any other case, either information from the wrong user has been decoded or a transmission error has occurred.

Generally, there are two basic categories of a CDMA system. It can either be synchronous or asynchronous. *Synchronous* CDMA exploits orthogonal codes; since each user has a code orthogonal to others' codes, they do not cause interference to each other. As opposed to synchronous CDMA, *asynchronous* CDMA uses *PN codes*. These are "pseudo-random" or "pseudo-noise" (PN) binary sequences that appear randomly, although each of them can be reproduced in a deterministic manner by intended receivers.

Since the number of PN codes is not fixed, there is no strict limit to the number of

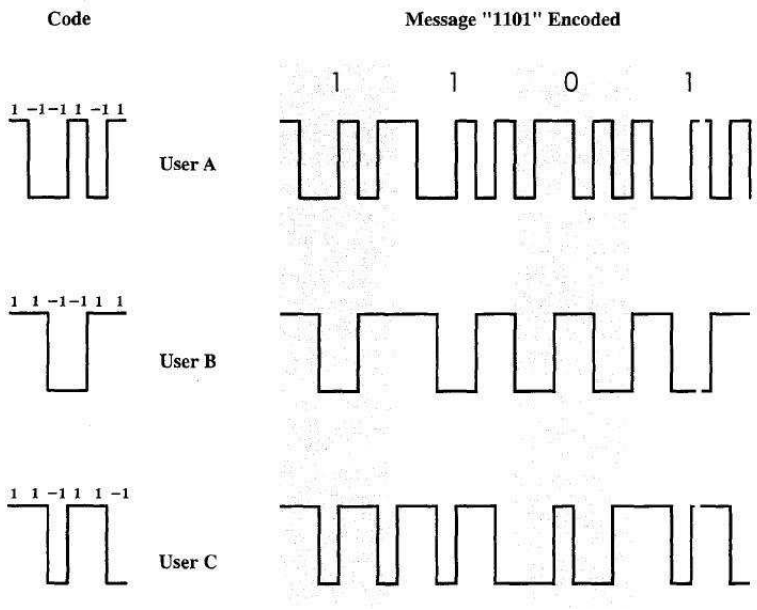

Figure 2.13: CDMA example.

users that can be supported in an asynchronous CDMA system, only a practical limit governed by the desired bit error probability, since the SINR (*Signal to Interference and Noise Ratio*) varies inversely with the number of simultaneous users. What is more, with asynchronous CDMA a certain level of privacy is achieved as a receiver cannot demodulate the received data without knowledge of the pseudo-random sequence used to encode the data.

The selection of the codes used to modulate the users' signal is very important for the performance of an asynchronous CDMA system. The good separation between the signal of a desired user and the signals of other users is essential. Unlike synchronous CDMA, the signals of other users will appear as noise to the signal of interest and interfere slightly with the desired signal in proportion to number of users. In fact, the sum of a large number of PN sequences, which are statistically uncorrelated, results in *multiple access interference* (MAI) that is approximated by a Gaussian noise process.

Additionally, if the signals of all users are received with the same power, the noise power of the MAI increases in proportion to the number of users. CDMA performance is also sensitive to relative received powers of the signals. The offered QoS is affected by the *near-far problem*; if signal of one user is too strong, it generates too much interference to the signals of other nodes. Thus, a transmitted power control scheme is necessary for maintaining good performance in terms of QoS for all users.

Especially for the case of WVSNs, the transmitted power control is applied so that the energy consumption is minimized. The goal is not only to prolong the lifespan of the WVSN but also to suppress as much as possible the interference among the users that transmit over the same frequency. Nevertheless, in the particular case of WVSNs that transmit video content, the reduction of the transmitted power of each node should not lead to the degradation of the video quality.

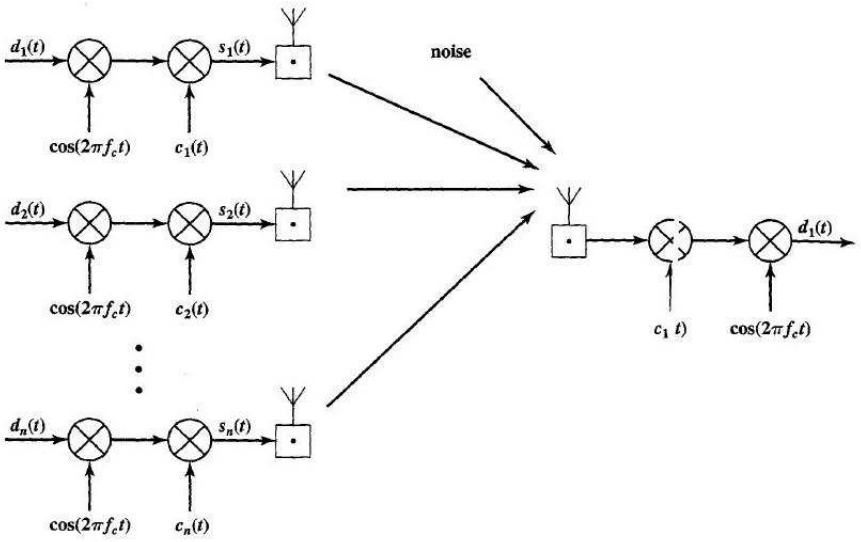

Figure 2.14: CDMA in a DSSS BPSK Environment with n users transmitting with n orthogonal PN codes.

DS–CDMA

The *Direct Sequence Code Division Multiple Access* (DS–CDMA) technique is adopted in this thesis, which applies DSSS and offers high spectrum efficiency. With this method, each bit of user information is represented by L bits in the transmitted signal, using a unique spreading code s_k of length L. These added bits are pseudonoise (PN) code symbols called "chips", each of which has a much shorter duration than an information bit (*chip time*). For the transmission of the ith bit of a bit stream a user k transmits $b_k(i)s_k$, namely a vector of L chips where the value $b_k(i)$ is either 1 or -1 according to the value of the ith bit.

The deriving chip rate is higher than the original signal bit rate (Fig. 2.15). The ratio between the user information time and the chip time is the *spread factor* that indicates the increase of the bandwidth finally used for the transmission. For instance, using a spreading code with 5 bits the transmitted signal occupies bandwidth that is 5 times greater than it would be if a spreading code with 1 bit was used. A receiver can retrieve the desired signal by multiplying the received signal with the same code as the one used for the transmission. Assumimg the set–up depicted in Fig. 2.14, consisting of n users with n different orthogonal PN sequences, the signals from all users along with the background noise reach the receiver. If it is interested in data from user 1 only ($d_1(t)$), it multiplies the received signal with the spreading code of user 1 ($c_1(t)$). Eventually, the useless energy of other users' signals is spreaded over a large bandwidth whereas the receiver can recover the signal of user 1 which is concentrated in a smaller bandwidth.

For the modulation of the transmitted data, the *Binary Phase Shift Keying* (BPSK) technique was preferred in this work. In this type of phase–shift keying that shifts the phase of the carrier signal two different phases which represent the two binary digits are used. These phases are separated by 180° (Fig. 2.16). Let N be the number of users in a

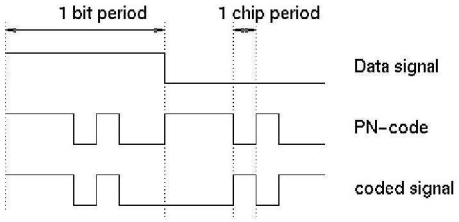

Figure 2.15: A DS-CDMA signal generated by multiplication of a user data signal by a PN code.

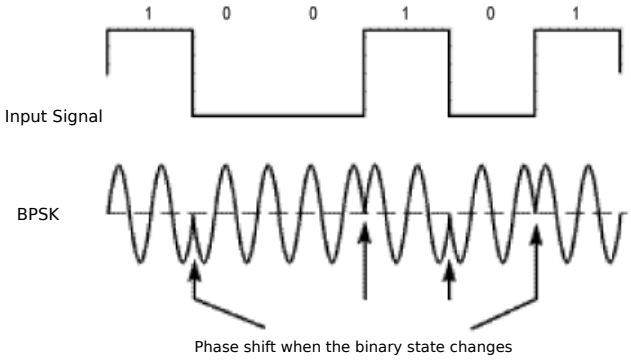

Figure 2.16: BPSK example.

synchronous single–path BPSK channel, A_n, $b_n(i)$, $\mathbf{s}_n$, $\mathbf{u}_n$ the amplitude, symbol stream, spreading code and noise of user n respectively and $\mathbf{r}(i)$, $\mathbf{s}_k(i)$ and $\mathbf{u}_n$ vectors of length L. The received signal can be expressed as:

$$\mathbf{r}(i) = A_1 b_1(i)\mathbf{s}_1 + \sum_{n=2}^{N} A_n b_n(i)\mathbf{s}_n + \mathbf{u}_n. \tag{2.7}$$

We consider a multihop WVSN with K source nodes and M relay nodes. As all nodes communicate with each other using DS–CDMA at the physical layer, each node uses L chips for a single bit transmission. Thus, a node n is associated with a spreading sequence of length L. As in [7], the interference from other nodes to the node of interest is modeled as Additive White Gaussian Noise (AWGN). This means that the noise n_0 gets added an not multiplied to the received signal, its spectrum is flat for all frequencies and its values follow the Gaussian probability distribution function:

$$p\,(x) = \frac{e^{\dfrac{-(x-\mu)^2}{2\sigma^2}}}{\sqrt{2\pi\sigma^2}}, \tag{2.8}$$

where $\mu = 0$ and $\sigma^2 = n_0/2$.

For a WVSN with $N = K + M$ nodes, a node's received power at a specific distance from node n is $S_n^{\text{rec}} = E_n R_n$ in Watts. E_n is the energy–per–bit and the total transmission bit rate for source and channel coding in bits/sec is given by:

$$R_n = \frac{R_{\mathrm{s},n}}{R_{\mathrm{c},n}},\ n = 1, 2, \ldots, N, \tag{2.9}$$

where $R_{\mathrm{s},n}$ is the source coding rate in bits/sec and the dimensionless number $R_{\mathrm{c},n}$ is the channel coding rate. A node that transmits with a lower source coding rate is able to use more bits for the channel coding. It can transmit with lower power and as a consequence it causes less interference to other nodes' transmissions.

We assume that interference exists on each link across the path to the CCU from nodes that are in the effective transmission range. Letting $\mathbf{J}$ be the set of interfering nodes for each hop h, it is assumed that $|\mathbf{J}| \leqslant N$, where $|.|$ denotes the cardinality of a set. The energy–per–bit to (MAI) ratio is different in each link, depending on the nodes causing interference to the considered node n and can be expressed for the h–th hop of a path as follows:

$$\frac{E_n}{I_0 + N_0} = \frac{\frac{S_n^{\mathrm{rec}}}{R_n}}{\sum\limits_{j=1, j\neq n}^{|\mathbf{J}|} \frac{S_j^{\mathrm{rec}}}{W_{\mathrm{t}}} + N_0}, \tag{2.10}$$

where $I_0/2$ is the two sided noise power spectral density due to MAI, $N_0/2$ is the two sided noise power spectral density of background noise in W/Hz, W_{t} is the total bandwidth in Hz and $S_{\mathrm{j}}^{\mathrm{rec}}$ is the received power of node $j \in \mathbf{J}$ that causes interference to node n. For a given received signal power $S_{\mathrm{n}}^{\mathrm{rec}}$ at a distance d from a node n, the required transmitted power $S_{\mathrm{n}}^{\mathrm{trans}}$ for the node n can be determined by a suitable Radio Propagation Model, as described in section 2.2.

Given that the transmission bit rate is:

$$R_n = \frac{R_{\mathrm{chip}}}{L}, \tag{2.11}$$

where the chip rate R_{chip} is the same for all nodes of the network, we can obtain different values for the transmission bit rates of each hop using a different spreading code length L. A smaller L increases the transmission bit rate but it also decreases the energy per bit. Thus, the bit error rate is also increased.

2.5 Description of the proposed Resource Allocation method for multihop DS–CDMA WVSNs

In this section, the considered resource allocation problem is formulated and the process of estimating the expected distortion needed for the optimization is analyzed.

2.5.1 Problem Formulation

As mentioned in section 1.3, our method aims at allocating optimally the source and channel coding rates and the received powers among the source nodes of a WVSN and

simultaneously allocate the necessary channel coding rates and received powers to the relay nodes of this network. The quality–based optimization actually minimizes a function of the distortions of the videos transmitted by all of the source nodes of the WVSN, hence it optimizes the video quality of all users.

We first define the following vectors for the received powers, source and channel coding rates of source nodes $k = 1, 2, \ldots, K$ and relay nodes $m = 1, 2, \ldots, M$, respectively:

(a) $S^{\text{rec}} \doteq (S^{\text{rec}}_{\text{S},1}, \ldots, S^{\text{rec}}_{\text{S},K}, S^{\text{rec}}_{\text{R},1}, ..., S^{\text{rec}}_{\text{R},M})^{\top}$,

(b) $R_{\text{s}} \doteq (R_{\text{s},1}, \ldots, R_{\text{s},K})^{\top}$,

(c) $R_{\text{c}} \doteq (R_{\text{c,S},1}, \ldots, R_{\text{c,S},K}, R_{\text{c,R},1}, \ldots, R_{\text{c,R},M})^{\top}$.

Under the constraint that imposes the same transmission bit rate R_j, $j \in \mathbf{J}$, for the interfering nodes of hop h, for each source node k the source coding rate $R_{\text{s},k}$, the channel coding rate $R_{\text{c},k}$ and the received power $S^{\text{rec}}_{\text{S},k} \in [S^{min}_{\text{S}}, S^{max}_{\text{S}}]$, and for each relay node m the channel coding rate $R_{\text{c},m}$ and the received power $S^{\text{rec}}_{\text{R},m} \in [S^{min}_{\text{R}}, S^{max}_{\text{R}}]$ are determined, so that a function of the overall end–to–end expected video distortion $E\{D_{\text{s+c},k}\}$ for each source node k is minimized, i.e.

$$(R^*_{\text{s}}, R^*_{\text{c}}, S^{\text{rec}*}) = \arg \min_{R_{\text{s}}, R_{\text{c}}, S^{\text{rec}}} f(E\{D_{\text{s+c},1}\}, \ldots, E\{D_{\text{s+c},K}\}),$$

The type of the function $f(.)$ is different for each one of the deployed optimization criteria that will be presented in the next chapter. The $E\{D_{\text{s+c},1}\}, \ldots, E\{D_{\text{s+c},K}\}$ values are obtained by the model described in the following section.

2.5.2 Expected Video Distortion Estimation

As a matter of fact, the expected distortion of a video transmitted by a specific source node depends on the bit error rates of the links across the path to the final receiver of the video. In order to calculate the expected distortion as a function of the bit error probabilities P_b after channel decoding, we use *Universal Rate– Distortion Characteristics* (URDCs), as in [3]. It should be noted that the errors occurring in the channel are random, thus the video distortion $D_{\text{s+c},k}$ of a user k is a random variable. Due to that fact we have to calculate the value of the expected distortion $E\{D_{\text{s+c},k}\}$ for various realizations of the channel.

A video encoded using the H.264/AVC standard can only handle packet errors and not bit errors. For the purpose of estimating the video distortion with URDCs, we followed the process described below in order to derive a correlation between the packet loss rate PLR_{RTP} of the *Real–Time Transport Protocol* (RTP) and a certain bit error rate BER. The RTP provides a packet format for real–time data transmissions and allows the error detection in a packet. Let us also define the packet size of the packet of the lowest layer in bits LL_{size}, the packet loss rate of the lowest layer PLR_{LL} for a packet of size LL_{size} and the size of an RTP packet RTP_{size}.

(a) Encode video with an H.264/AVC encoder.

(b) Estimate $PLR_{RTP} = 1 - (1 - PLR_{LL})^{RTP_{size}}$.

(c) Drop packets with errors from the encoded stream according to the PLR_{RTP}.

(d) Decode the corrupted H.264 video stream.

(e) Estimate the distortion of the decoded video stream.

After creating a relation between the BER and the distortion of a packet–based video stream, we define the total bit error probability for a multihop transmission of the video of a source node k. Assuming that $Pb_{h,k}$ is the bit error probability for hop h and the source node k, the end–to–end bit error probability across an H–hop path for k is [36]:

$$Pb_k = 1 - \prod_{h=1}^{H}(1 - Pb_{h,k}). \tag{2.12}$$

Owing to Eq. (2.12), the expected distortion due to lossy compression and channel errors can be derived by the model for the URDC of each user k used in [16]:

$$E\{D_{\mathrm{s+c},k}\} = \alpha_k \left[\log_{10} \left(\frac{1}{1 - \prod_{h=1}^{H}(1 - Pb_{h,k})} \right) \right]^{-\beta_k}, \tag{2.13}$$

where parameters α_k and β_k are positive numbers that depend on the motion level of the transmitted video sequence and the source coding rate. Values of α_k for high motion video sequences are generally greater than those for low motion video sequences. These parameters are determined using mean square optimization from a few ($E\{D_{\mathrm{s+c},k}\}$, Pb_k) pairs and the $E\{D_{\mathrm{s+c},k}\}$ values are estimated at the encoder using the *Recursive Optimal Per–pixel Estimate* model (ROPE)[38]. The choice of α_k and β_k minimizes the square of the approximation error so that there is no need to calculate the URDCs based on experimental results for every possible value of $P_b's$. In contrast, we computed the expected distortion for a small number of packet loss rates associated with specific BERs. Since the BER needed for the URDCs is the BER after channel decoding and the distortion caused to the packet–based video stream is related to the BER, we let P_b be equal to BER.

Considering a AWGN channel with BPSK modulation, the pairwise error probability from Eq. (2.5) is given by:

$$P_d = Q\left(\sqrt{2dR_{\mathrm{c}} \left[\frac{E_n}{I_0 + N_0} \right]} \right), \tag{2.14}$$

where R_c is the channel coding rate and $E_n/(I_0 + N_0)$ is the energy/bit MAI ratio.

Therefore, as an estimate of the bit error probabilities for the transmitting node n at the h–th hop (after channel decoding), we can use the Viterbi upper bound for RCPC codes as follows:

$$Pb_{h,n} = \frac{1}{P} \sum_{d=d_{\text{free}}}^{\infty} c_d \frac{1}{2} \text{erfc} \left(\sqrt{dR_{\text{c},n} \left[\frac{E_n}{I_0 + N_0} \right]} \right), \tag{2.15}$$

where P is the period of the used code, d_{free} is the free distance of the code and c_d is the information error weight. The node n can either be the source node k or a relay node m that retransmits the video of k. The function Q can be replaced by erfc(.) which is the complementary error function given by:

$$erfc(z) = \left(2 \int_{z}^{\infty} \exp(-t^2) dt \right) / \sqrt{\pi}. \tag{2.16}$$

From Equations (2.12), (2.13) and (2.15) it follows that $E\{D_{\text{s+c},k}\}$ of the video of user k is a function of the source coding rate $R_{\text{s},k}$, the channel coding rate $R_{\text{c,S},k}$, the received power $S^{\text{rec}}_{\text{S},k}$ and the channel coding rate $R_{\text{c,R},m}$ and the received power $S^{\text{rec}}_{\text{R},m}$ of each relay node m that retransmits the video of k across its path to the CCU:

$$E\{D_{\text{s+c},k}\}(R_{\text{s},k}, R_{\text{c,S},k}, S^{\text{rec}}_{\text{S},k}, R_{\text{c,R},m}, S^{\text{rec}}_{\text{R},m}) =$$

$$\alpha_k \left[\log_{10} \left(\frac{1}{1 - \prod_{h=1}^{H} \left(1 - \frac{1}{P} \sum_{d=d_{\text{free}}}^{\infty} c_d \frac{1}{2} \text{erfc} \left(\sqrt{dR_{\text{c},n} \left[\frac{E_n}{I_0 + N_0} \right]} \right) \right)} \right) \right]^{-\beta_k}, \tag{2.17}$$

where $n = k$ for the first hop and $n = m$, $m \in [1, M]$ for the next hops.

Chapter 3

OPTIMAL RESOURCE ALLOCATION FOR MULTIHOP DS–CDMA WIRELESS VISUAL SENSOR NETWORKS

In this chapter, the employed optimization criteria are presented and formulated. Moreover, the necessary notions of Game Theory are explained for the better comprehension of the criteria that are solved using the Nash Bargaining Solution (NBS). In all resulting optimization problems, the goal is to minimize the expected end–to–end distortion $E\{D_{\mathrm{s+c},k}\}$ of each node k of the WVSN. In other words, the *Peak Signal–to–Noise Ratio* (PSNR) of each user has to be maximized:

$$PSNR_k = 10 \log_{10} \frac{255^2}{E\{D_{\mathrm{s+c},k}\}}. \tag{3.1}$$

PSNR is the ratio between the maximum possible power of a signal and the power of corrupting noise that affects the fidelity of its representation. It is a measure of the quality of a reconstructed signal reconstruction after the compression of the signal using lossy codecs and its transmission through a lossy channel. If the expected distortion $E\{D_{\mathrm{s+c},k}\}$ of the transmitted video of a source node k is known, the PSNR in dB for the video is calculated by Eq. (3.1).

3.1 Resource Allocation using the Nash Bargaining Solution (NBS)

In game theory, the Nash Bargaining Solution is the solution of a *bargaining game*, namely a multiple-player cooperative game used to model bargaining interactions. In the *Nash Bargaining Game* two or more players demand a portion of a resource. If the portion requested by the players is less than that available, both players' request is satisfied; in the opposite case neither player gets the requested portion. In such bargaining problems, it is implied that if a player cooperates with the other players, he will eventually have a better payoff than he would achieve on its own, independent of a negotiation. John Nash defined a bargaining problem as a pair (X, ξ), where X represents the set of feasible payoff pairs on which two players can agree and ξ as a payoff pair in X that reflects the consequences of a disagreement.

In fact, the Nash Bargaining Solution is a solution concept of a game involving two or more players, in which each player is assumed to know the strategies of the other players, and no player has anything to gain by changing only his own strategy unilaterally. If each player has chosen a strategy and no player can benefit by changing his strategy while the other players keep theirs unchanged, then the current set of strategy choices and the corresponding payoffs constitute a Nash equilibrium. Finally, each player achieves an optimal strategy as response to the strategies of the other players.

In the present thesis, a bargaining game is used for the resource allocation. The nodes of a DS–CDMA based multihop WVSN interfere with each other, as they all transmit simultaneously. Each node tries to increase its transmitted power, aiming at a better quality for its video, but this also can lead to the degradation of the quality of the other nodes' videos. It is therefore essential that cooperation should exist among the nodes through the CCU. In this way, the resources will be allocated so that a good quality, namely PSNR, is achieved for all nodes. For the arising bargaining problem a measure of satisfaction of the demands of a source node k in terms of quality is the *utility function*. It can be defined similarly as the PSNR of the video of the source node k (Eq. (3.1)):

$$U_k = 10 \log_{10} \frac{255^2}{E\{D_{\mathrm{s+c},k}\}}. \tag{3.2}$$

Due to the fact that $E\{D_{\mathrm{s+c},k}\}$ depends on the source coding rate, the channel coding rate and the received power of a source node k, the defined utility function depends on the same parameters, as well. For each source node, the greater the value of U_k is, the better the quality of its transmitted video becomes.

Furthermore, the *feasible set* $\mathbf{U}$ is the set of all possible vectors $(U1, U2, ..., U_k)$ that represent the feasible payoffs (allocations) of the players (source nodes). It is mandatory that this set is convex, closed and bounded above and that the free disposal is allowed. First, letting $\mathbf{V}$ be a vector space over the real numbers, a set $\mathbf{S}$ in $\mathbf{V}$ is said to be *convex* if, for all x and y in $\mathbf{S}$ and all t in the interval [0,1], the point $(1-t)x + ty$ is in $\mathbf{S}$ so that every point on the line segment connecting x and y is in $\mathbf{S}$. Next, a set $\mathbf{S}$ is *closed* if and only if it contains all of its limit points. If there is an element p in $\mathbf{S}$ such that $p \geqslant q$ for

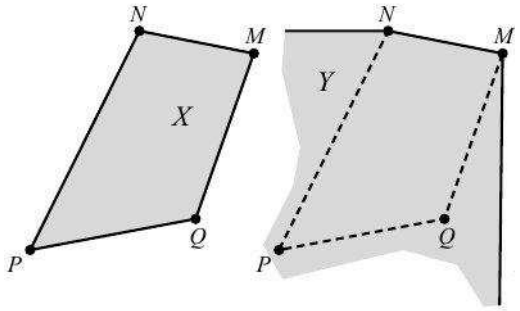

Figure 3.1: Cooperative payoff regions without and with free disposal.

all q in $\mathbf{S}$, then the set $\mathbf{S}$ is bounded above.

In a cooperative game, *free disposal* is the ability of each player to dispose of some portion of utility. If x is a strategy on which the players can agree and $x \geqslant y$, then they can achieve y if they agree that each of them will dispose an amount after the implementation of x. Although the free disposal does not seem reasonable, it should be used mainly for the reason that in this way no strategies are excluded from the feasible set of the players. If there are strategies that are never chosen, the optimal choice for the players cannot be defined. The difference between a game that permits the free disposal and one that does not permit it is depicted in Fig. 3.1. The *cooperative payoff region* is the set of payoffs which can be obtained by the players through cooperative play. It can be derived from the convex hull of the points that define the players' strategies. With the free disposal the cooperative payoff region X must be replaced by the region Y. If all the points y located to the southwest of a point x in the set X are gathered, the set Y can be obtained [6].

The *disagreement point* $d = (d_1, \ldots, d_K)^\top$ is defined as the vector of the utility functions the players can expect to receive if negotiations break down. The utility of each player after the cooperation must not be smaller than it would be if the player did not join the bargaining game. Every player should either have a gain or remain with the same utility he had before the cooperation. Moreover, the elements of the set $\mathbf{U}$ that assign to the players the utilities they would gain if negotiations failed are called the *Pareto–efficient payoff profiles*. The *bargaining set* consists of all the Pareto–efficient payoff profiles.

In cooperative game theory it is assumed that an agreement will be Pareto–efficient. This means that for the Nash Bargaining Solution there can be no other agreement that would lead to the increase of a player's utility (value of utility function) without reducing the utilities of the other players. An allocation that is not Pareto efficient implies that a certain change in allocation of utility functions may result in some players being made "better off" with no player being made worse off, and thus it can be made more Pareto efficient through a Pareto improvement. As shown in Fig. 3.2, the points B, C and D are Pareto efficient. The point A is not Pareto efficient whereas the point X reflects an allocation that is not feasible.

In the bargaining game used for our resource allocation problem can be written as a function $F(.)$ of $\mathbf{U}$ and d. It belongs to the bargaining set and must satisfy three axioms.

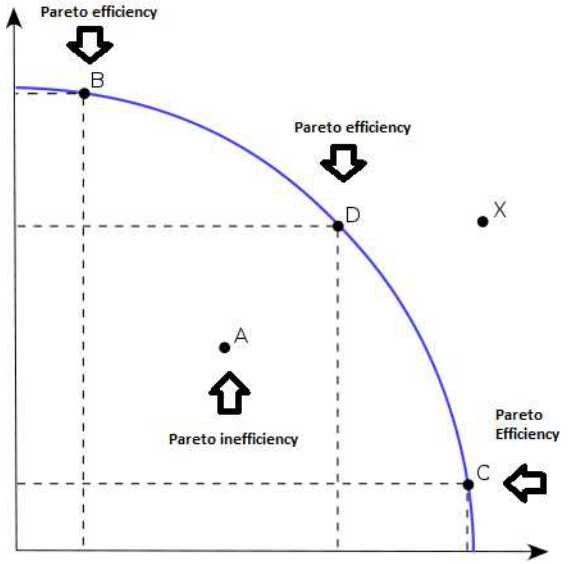

Figure 3.2: Pareto–efficient and Pareto–inefficient points.

These axioms guarantee that it is invariant to affine transformations, independent from irrelevant alternatives and Pareto optimal [6]:

(*a*) $F(\mathbf{U}, d) \geqslant d$ and $y > F(\mathbf{U}, d) \Rightarrow y \notin U$.

(*b*) Given any strictly increasing affine transformation $\tau(.)$, $F(\tau(U), \tau(d)) = \tau(F(\mathbf{U}, d))$.

(*c*) If $d \in Y \subseteq U$, then $F(\mathbf{U}, d) \in Y \Rightarrow F(Y, d) = F(\mathbf{U}, d)$.

With the first axiom it is guaranteed that the Nash Bargaining solution lies in the bargaining set. The second axiom says that if the utility u is scaled according to an affine transformation and an outcome is assigned the new utility $U = Au + b$ with $A \geqslant 0$, the bargaining solution will not be affected. The last axiom is a formalization of the *Independence of Irrelevant Alternatives*. A bargaining solution satisfies the Independence of Irrelevant Alternatives if $F(X, d) = F(Y, d) \cap Y$ for two sets X and Y with $Y \subseteq X$ and $F(X, d) \cap Y \neq \emptyset$, where $d \in Y$. As depicted in Fig. 3.3, $F(X, d)$ lies in Y and the elements of X that are not in Y are considered to be irrelevant alternatives. The selection of a bargaining solution should not depend on the availability (or unavailability) of the irrelevant solutions. To put things differently, if the bargaining solution of a set belongs to a subset of this set, then the bargaining solution will not be affected if the subset is extended. Hence, if the solution chooses $F(X, d)$ for the bargaining problem (X, d), then $F(X, d)$ should be chosen for the bargaining problem (Y, d) as well.

Based on the Nash Bargaining Solution we define the bargaining game deployed in our resource allocation scheme as a pair $(\mathbf{U}, d)$, where the *feasible set* $\mathbf{U} \subseteq \mathbb{R}^K$ is the set of all possible vectors $(U1, U2, ..., U_k)$ resulting from different combinations of the vectors of the received power from the K source nodes and the M relay nodes $S^{\text{rec}} = (S^{\text{rec}}_{\text{S},1}, \ldots, S^{\text{rec}}_{\text{S},K}, S^{\text{rec}}_{\text{R},1}, \ldots, S^{\text{rec}}_{\text{R},M})^{\top}$, the source coding rate of the source nodes $R_{\text{s}} =$

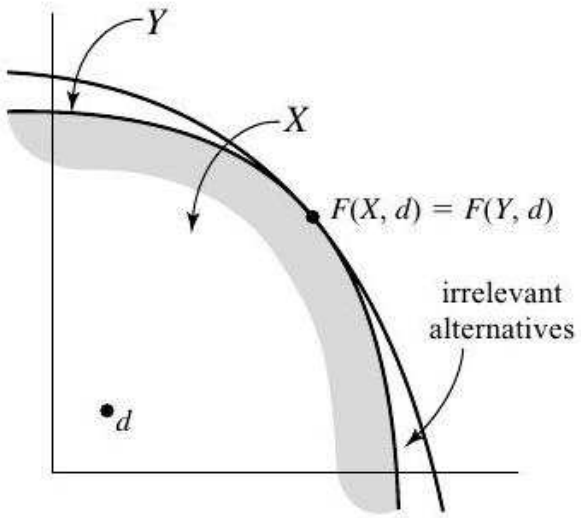

Figure 3.3: Irrelevant Alternatives.

Criterion Name	Bargaining Power per Source Node
e.NBS	$bp_k = 1/K$
w.NBS	$bp_k = \alpha_k / \sum_{j=1}^{K} \alpha_j; j = 1, 2, \ldots, K$

Table 3.1: Bargaining powers for the e.NBS and w.NBS criteria.

$(R_{\mathrm{S},1}, \ldots, R_{\mathrm{S},K})^\top$ and the channel coding rate $R_{\mathrm{c}} = (R_{\mathrm{c,S},1}, \ldots, R_{\mathrm{c,S},K}, R_{\mathrm{c,R},1}, \ldots, R_{\mathrm{c,R},K})^\top$ for all nodes, and $d \in \mathbb{R}^K$ which is the vector of all the disagreement points, namely $d = (d_1, \ldots, d_K)^\top$. The Nash Bargaining Solution of this multi–player bargaining game can be found by maximizing the Nash Product:

$$F(\mathbf{U}, d) = \arg\max_{U} (U_1 - d_1)^{bp_1} (U_2 - d_2)^{bp_2} \ldots (U_K - d_K)^{bp_K}, \tag{3.3}$$

subject to the constraints: $(U_k - d_k) > 0$ and $\sum_{k=1}^{K} bp_k = 1$. The value bp_k is the *bargaining power* of a source node k. In this particular bargaining game, the disagreement point $d \in \mathbf{U}$ is the minimum acceptable PSNR for each video. It conforms to the QoS requirements of each application and can be determined by the system designer.

The bargaining power bp_k of each node indicates the advantage it has in the bargaining game. It is assigned in accordance with the rules of the bargaining game and determines which player is more advantaged. A node with a higher bargaining power is favored by the rules of the bargaining game compared to a node with a lower bargaining power. Furthermore, the players can have the same or different bargaining powers that reflect their impact on the bargaining game. According to the choice of values of the bargaining powers of the nodes (Table 3.1), we considered two different criteria; the *e.NBS* criterion and the *w.NBS* criterion [15].

3.1.1 NBS with Equal Bargaining Powers (e.NBS)

The *e.NBS* criterion assumes that all bargaining powers are assigned the same values. In our resource allocation problem, if there is no reason to assume that some videos should have a higher priority in the bargaining game, all of the transmitted videos are treated as of equal importance. In this case, we set to each source node k a bargaining power equal to $bp_k = \frac{1}{K}$. The Nash Bargaining Solution can be found by:

$$F(\mathbf{U}, d) = \arg\max_{U}[(U_1 - d_1)(U_2 - d_2)\dots(U_K - d_K)]^{\frac{1}{K}}, \tag{3.4}$$

under the constraints: $(U_k - d_k) > 0 \; \forall \; k$ and $\sum_{k=1}^{K} bp_k = 1$ that are imposed for the general case of the bargaining game (Eq. (3.3)).

3.1.2 NBS with Different Bargaining Powers (w.NBS)

The *w.NBS* criterion assigns to each node a different bargaining power which is motion–related. The resources are allocated according to the motion level of the transmitted videos of the source nodes, as it is reflected by parameters α_k that are given by Eq. (2.13) and depend on the motion level of each video sequence and the source coding rate. The bargaining power of a source node k can be defined as:

$$bp_k = \frac{\alpha_k}{\sum_{j=1}^{K} \alpha_j}; \; j = 1, 2, \dots, K. \tag{3.5}$$

Then the Nash Bargaining Solution is:

$$F(\mathbf{U}, d) = \arg\max_{U}(U_1 - d_1)^{bp_1}(U_2 - d_2)^{bp_2}\dots(U_K - d_K)^{bp_K}, \tag{3.6}$$

under the same constraints imposed for the general case of the bargaining game (Eq. (3.3)). A source node with higher motion level has a higher bargaining power, thus it is more advantaged by the rules of the bargaining game. A high priority in the resource allocation scheme is assigned to high motion videos as it is more difficult to keep their quality at a good level in comparison with the low motion videos. Consequently, the content–aware approach of w.NBS favors the nodes that transmit high motion videos.

3.2 Resource Allocation with Minimization of the Expected Distortion

Besides the former criteria that are based on the Nash Bargaining Solution, two other criteria have been proposed that aim at the minimization of the expected distortion.

3.2.1 Minimization of the Average Distortion (MAD)

The MAD criterion results in an optimization problem that minimizes the average video distortion of K source nodes of a WVSN by assigning optimally the received powers and channel coding rates of all nodes along with the source coding rates of the source nodes. It can be formulated as follows:

Given a total transmission bit rate R_j for the interfering source and relay nodes of each hop, the vectors of optimal received powers $S^{\text{rec}\,*}$, source coding rates R_{s}^* and channel coding rates R_{c}^* are determined so that the overall end–to–end average distortion $D_{\text{ave}}(R_{\text{s}}, R_{\text{c}}, S^{\text{rec}})$ of all source nodes is minimized:

$$(R_{\text{s}}^*, R_{\text{c}}^*, S^{\text{rec}\,*}) = \arg \min_{R_{\text{s}}, R_{\text{c}}, S^{\text{rec}}} D_{\text{ave}}(R_{\text{s}}, R_{\text{c}}, S^{\text{rec}}), \tag{3.7}$$

subject to the constraints that $R_j = \dfrac{R_{\text{s},j}}{R_{\text{c},j}}$ and that all the interfering nodes of a specific hop have the same transmission bit rate R_j. The average distortion is given by: $D_{\text{ave}}(R_{\text{s}}, R_{\text{c}}, S^{\text{rec}}) = \dfrac{1}{K} \sum_{k=1}^{K} E\{D_{\text{s+c},k}\}(R_{\text{s}}, R_{\text{c}}, S^{\text{rec}})$.

This criterion tries to achieve on average a good quality for all the videos transmitted in the WVSN and it does not assign priorities to them.

3.2.2 Minimization of the Maximum Distortion (MMD)

The MMD criterion results in an optimization problem that minimizes the maximum video distortion of K source nodes of a WVSN by assigning optimally the received powers and channel coding rates of all nodes along with the source coding rates of the source nodes. It can be formulated as follows:

Given a total transmission bit rate R_j for the interfering source and relay nodes of each hop, the vectors of optimal received powers $S^{\text{rec}\,*}$, source coding rates R_{s}^* and channel coding rates R_{c}^* are determined so that the overall end–to–end maximum distortion $D_{\text{ave}}(R_{\text{s}}, R_{\text{c}}, S^{\text{rec}})$ of all source nodes is minimized:

$$(R_{\text{s}}^*, R_{\text{c}}^*, S^{\text{rec}\,*}) = \arg \min_{R_{\text{s}}, R_{\text{c}}, S^{\text{rec}}} \max_{k} E\{D_{\text{s+c},k}\}(R_{\text{s}}, R_{\text{c}}, S^{\text{rec}}), \tag{3.8}$$

subject to the constraints that $R_j = \dfrac{R_{\text{s},j}}{R_{\text{c},j}}$ and that all the interfering nodes of a specific hop have the same transmission bit rate R_j.

This criterion treats all the videos as if they were of equal importance and manages to deliver the same levels of quality for all of them.

3.3 Resource Allocation with Minimization of the Weighted Aggregation of the Expected Distortion (MWAD)

According to the MWAD criterion we form a function that expresses the weighted aggregation of the expected distortion of all source nodes. The objective is to determine the vectors of the received power S^{rec}, the source coding rate R_{s} and the channel coding rate R_{c} for all nodes, so that this function is minimized. To put it formally:

$$(R_{\text{s}}^*, R_{\text{c}}^*, S^{\text{rec}\,*}) = \arg \min_{R_{\text{s}}, R_{\text{c}}, S^{\text{rec}}} \sum_{k=1}^{K} w_k E\{D_{\text{s+c},k}\}, \tag{3.9}$$

where the weight for each source node k is:

$$w_k = \frac{\alpha_k}{\sum_{j=1}^{K} \alpha_j}, \tag{3.10}$$

given that $\sum_{k=1}^{K} w_k = 1$. The weights can be tuned according to parameters α_k, which reflect the motion level of each recorded video. Hence, high motion nodes have a higher priority in the minimization of their distortion, and as a result in the enhancement of the delivered video quality.

3.4 Particle Swarm Optimization

In our scheme the received and transmitted powers are assumed to take continuous values within a specified range whereas the source and channel coding rates can only have discrete values. As the arising multi–variable optimization problems are mixed–integer problems, a stochastic optimization technique was preferred, called *Particle Swarm Optimization* (PSO) [28].

PSO is an efficient and adjustable population–based optimization algorithm that is easy to implement and can provide globally optimal solutions with low computational complexity. It was inspired by aggregate behavior of living organisms, e.g., flocks of birds or schools of fish. This technique actually mimics the behavior of a population, the *swarm*, that consists of a number of individuals, the *particles*. For the PSO, the swarm has a fixed size and the particles are search agents that wander around in a multidimensional search space, aiming at minimizing a function and reaching a globally optimal solution. They are characterized by a *position* and a *velocity* and have a dynamic memory so as to store at each iteration of the algorithm the position that so far minimizes the optimization function. The best position of a particle is updated as soon as a position with lower function value is discovered. The particles can also communicate to each other good positions or other information; by following the currently best particles, the other particles will continue exploring the search space towards the direction that will most likely lead

to the global solution. Each particle changes its position and velocity according to other particles belonging to its *neighborhood*. The interconnections among the particles of a neighborhood can be described with a graph where the nodes represent the particles and form a topology. The information flow within a swarm is greatly affected by the structure of the neighborhood. A common type of a neighborhood topology is the ring topology [27].

Next, let $\mathcal{S} = \{x_1, x_2, \ldots, x_N\}$ denote a swarm consisting of N particles, each one defined as an n–dimensional vector $x_i \in \mathbb{S}$, $i = 1, 2, \ldots, N$ in the search space $\mathbb{S}$ and v_i and $p_i \in \mathbb{S}$ denote the corresponding velocity and best position of the i–th particle. Let also t be the current iteration of the algorithm, χ a parameter called the *constriction coefficient*, c_1 and c_2 two positive acceleration parameters called *cognitive* and *social* parameter, respectively and R_1, R_2 two vectors with components uniformly distributed in the range $[0, 1]$. Assuming that a function $f(x)$ has to be minimized, the basic loop of the PSO algorithm includes the following steps:

In the iteration t for a particle i:

(a) Find the best known position p_{g_i} in the neighborhood of the particle x_i that gives the lowest value of $f(x)$.

(b) Update the velocity of particle i according to the equation:

$$v_i(t+1) = \chi\Big[v_i(t) + c_1 R_1\big(p_i(t) - x_i(t)\big) + c_2 R_2\big(p_{g_i}(t) - x_i(t)\big)\Big] \tag{3.11}$$

(c) Update the position of particle i as:

$$x_i(t+1) = x_i(t) + v_i(t+1) \tag{3.12}$$

(d) Evaluate the corresponding value of the objective function for each particle in iteration t: $f(x_1(t+1)), f(x_2(t+1)), ..., f(x_N(t+1))$.

(e) Update the best known position of the particle if $f(x_i(t+1)) \leqslant f(p_i(t+1))$.

(f) Check for convergence; if maximum number of iterations is not reached or the particles have not converged to an optimum solution, update iteration number as $t = t + 1$ and repeat step 1.

As for the convergence of the algorithm towards solutions in the search space of the problem, Clerc and Kennedy [9] investigated the stability of PSO and proposed a set of parameters which lead the algorithm to convergence. These parameters, which control the acceleration of the swarm and balance its particles' need for local and global search, are set to the values $\chi = 0.729$ and $c_1 = c_2 = 2.05$.

Chapter 4

EXPERIMENTAL RESULTS

In this chapter, the set–up of the experimental evaluation of the proposed method is described and the experimental results are presented and analyzed.

4.1 Experimental Setting

We tested our resource allocation optimization technique in various multihop DS–CDMA based WVSN topologies. In order to evaluate the effectiveness of all priority and non-priority based criteria for different visual sensors' resource requirements, we applied our method in several cases with different motion amounts per transmitted video. Also, various levels of power spectral density of background noise were considered for all of our test cases.

For the case of priority–based resource allocation, we employed the two weighted criteria; the w.NBS criterion assigns to each source node a motion-related bargaining power that indicates the advantage this node has when it joins the bargaining game; the MWAD criterion minimizes the weighted aggregation of distortions. The criteria e.NBS, MAD and MMD were used for avoiding giving priority to any source node of the considered topologies. The source nodes may transmit video with different motion levels, namely high, medium or low. The notions "low", "medium" and "high" motion are used for video sequences of similar motion levels with "Akiyo", "Salesman" and "Foreman" QCIF video sequences of 15 fps, respectively. For each video sequence, the α_k and β_k of Eq. (2.13) were estimated for a specific source coding rate as follows : after being encoded

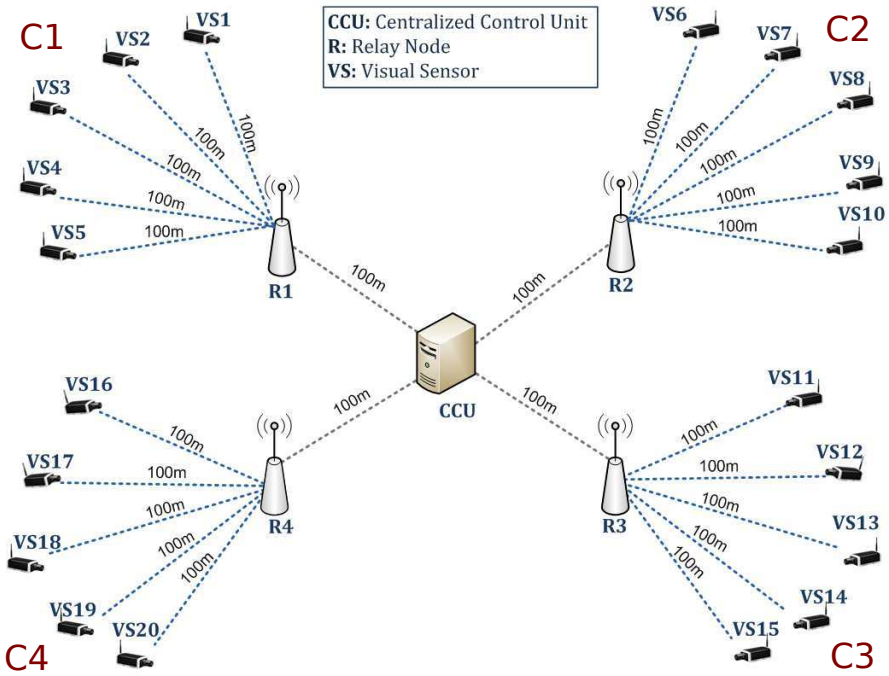

Figure 4.1: Example of a WVSN topology with two hops.

using H.264/MPEG–4 AVC, we estimated the packet loss rate for RTP with a range of bit error rate probabilities, i.e. $[10^{-8} - 10^{-3}]$; according to this rate, packets were extracted randomly from the video sequences. Finally, each video was decoded and its distortion was computed. 300 iterations of this computation were conducted, thus an average of distortion was kept for each video. Moreover, the BPSK modulation scheme was used for all transmissions along with RCPC codes with mother code 1/4 for the channel coding and packets of 400 bits. In all cases, two different transmission bit rates were tested, which correspond to the following valid source and channel coding sets:

(a) $CS1 \in \{1 : (32\text{kbps}, 1/3), 2 : (48\text{kbps}, 1/2), 3 : (64\text{kbps}, 2/3)\}$ with R_k=96kbps

(b) $CS2 \in \{1 : (48\text{kbps}, 1/3), 2 : (72\text{kbps}, 1/2), 3 : (96\text{kbps}, 2/3)\}$ with R_k=144kbps

Our resource allocation method was applied to the two WVSN topologies depicted in Figures 4.1 and 4.2. In both of them, the source nodes are organized in clusters, under the consideration that neighboring visual sensors monitor the same area. Hence, they record scenes with the same motion level. We tested each topology for cases with different motion amounts, so as to demonstrate the effectiveness of the criteria for different visual sensors resource requirements. Aiming at evaluating the performance of our scheme under several noise levels, different values of N_0 of Eq. (2.10) were chosen. Furthermore, the ranges for the used transmitted powers were given by the Propagation Models described in section 2.3. For a certain range of transmitted powers of a node and the parameters of the Propagation Models shown in Table (4.1), the range of the received powers of a node in distance d from the transmitting node is derived. Using these parameters, the

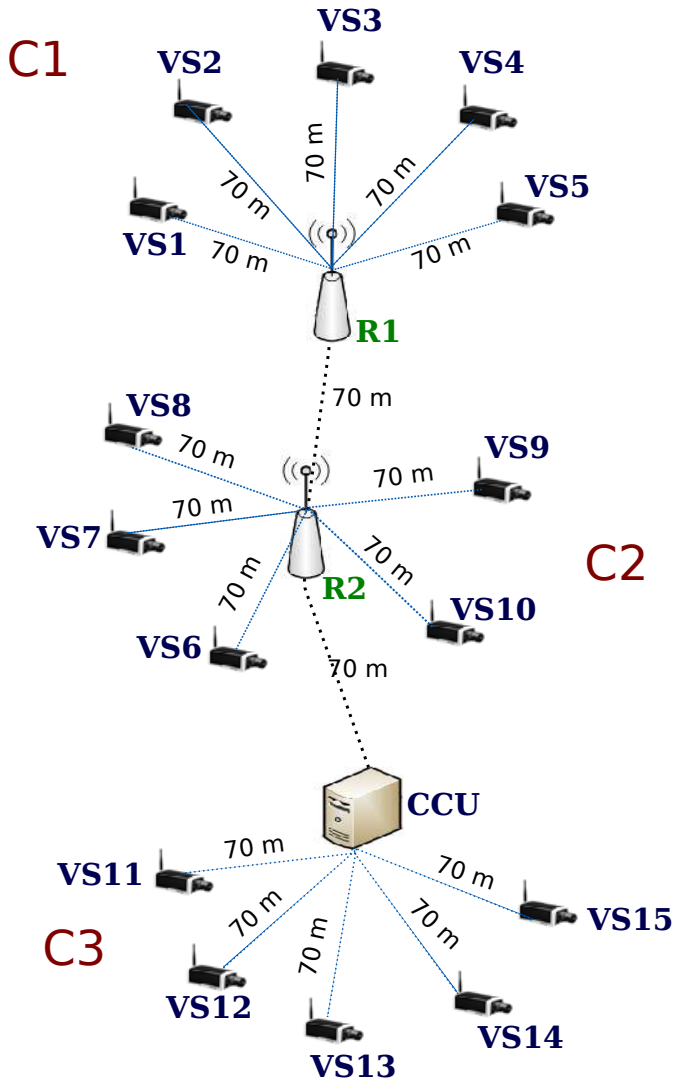

Figure 4.2: Example of a WVSN topology with more hops.

cross–over distance d_0 given by Eq. (2.1) is equal to 113.0973 m. Thus, for the distances 70 and 100 m of the two topologies, the ranges of received powers are derived by the Free Space Propagation Model. The range, thus the maximum available transmitted power, for the relay nodes needs to be bigger as they transmit video sequences of more than one source node.

In our implementation of PSO, the discrete parameters were allowed to take continuous values for the velocity and position update but they were rounded to the nearest integer for the evaluation of each particle. The swarm size and the number of iterations depend on the considered test case. The acceptable values of received powers in the optimization problems are the ranges which derive from the Propagation Models for each topology and test case. The parameters χ, $c1$ and $c2$ were set to the default values 0.729, 2.05 and 2.05 as mentioned in [9] and a ring topology with radius equal to 1 was preferred. For the criteria e.NBS and w.NBS that employ the Nash Bargaining Solution, the disagreement point d was to 24, which is the minimum acceptable PSNR.

Parameters	
G_t	3 dB
G_r	3 dB
h_t	3 m
h_r	3 m
l	1
f	315 MHz

Table 4.1: Parameters used by the Free Space and Two Ray Ground Propagation Models

Additionally, 30 independent experiments were conducted for each criterion used in a specific test case. This was necessary as PSO is a stochastic algorithm. Its performance has to be evaluated for a number of experiments which result in different solutions that minimize the used function. It should be pointed out that the power allocation is not always unique. After a series of experiments it was observed that the level of the power spectral density of the background noise N_0 can determine whether there is or not a unique solution to the resource allocation problem in question. If N_0 equal to 0 or very close to it, e.g. 0.01 pW/Hz or less, the ratio $E_k/(I_0 + N_0)$ tends to be equal to E_k/I_0. In this case, the ratio remains the same if all the received powers are multiplied with the same constant. Therefore, PSO is actually searching for the optimal power ratio that minimizes the function. In our results, we have normalized the received and transmitted powers so that the minimum available power is used from the ranges defined for each test case.

- **WVSN topology 1**

In the first topology, 20 nodes are organized in four clusters of the same cardinality $\{C1, C2, C3, C4\}$. As the CCU is out of the transmission range of the source nodes, four relay nodes $\{R1, R2, R3, R4\}$ retransmit the received videos of each cluster to the CCU as shown in Fig. 4.1. Interference exists among the nodes in the clusters as they transmit their videos to their corresponding relay node. Moreover, the four relay nodes interfere with each other when they retransmit videos to the CCU. The five nodes of each cluster transmit video sequences of the same motion level, thus (α_k,β_k) parameters within a cluster's nodes are assumed to be equal. Three different set–ups $\mathbf{V} = \{V1, V2, V3, V4\}$ for the transmitted videos' motion levels were tested for the cases of $N_0 = 0$ pW/Hz and $N_0 = 0.1$ pW/Hz or $N_0 = 1$ pW/Hz, with transmission bit rates equal to 96 and 144 kbps. For the first set–up, let $\mathbf{V} = \{high, low, medium, medium\}$; for the second set–up, let $\mathbf{V} = \{high, low, high, low\}$; for the third set–up, let $\mathbf{V} = \{high, medium, high, low\}$. The dimension of the deriving optimization problem is equal to 12, as the received powers of four relay nodes and four clusters, along with the source and channel coding rates of the source nodes in clusters, have to be allocated. Thus, each particle consists of eight constant values, namely the received powers of the nodes and four discrete values

corresponding to the source and channel coding rates of the source nodes. Preliminary experiments showed that PSO optimization performs efficiently for all employed criteria and test cases in this topology using a number of particles equal to 80 and a maximum number of iterations equal to 500.

For the first topology, when the transmission bit rate is set to 96 kbps, the total bandwidth W_t for all links is 5 MHz. The range of $[100, 500]$ mW is used for the transmitted powers of all source nodes and the range $[100, 5000]$ mW for the relay nodes. The corresponding ranges of received powers are respectively $[0.22867, 1.1433]$ μW and $[0.22867, 11.433]$ μW, as derived by the Free Space Propagation Model for distance d=100 m. For the source nodes in clusters, the valid source and channel coding set is $CS \in \{1 : (32\text{kbps}, 1/3), 2 : (48\text{kbps}, 1/2), 3 : (64\text{kbps}, 2/3)\}$. For the relay nodes the transmission bit rate is 480 kbps and the source and channel coding rates are set to $(64\text{kbps}, 2/3)$.

When the transmission bit rate is set to 144 kbps, the total bandwidth W_t is 2 MHz for the first hop and 10 MHz for the second hop. The range of $[100, 500]$ mW is used for the transmitted powers of all source nodes and the range $[100, 5000]$ mW for the relay nodes. The corresponding ranges of received powers are respectively $[0.22867, 1.1433]$ μW and $[0.22867, 22.866]$ μW, as derived by the Free Space Propagation Model for distance d=100 m. For the source nodes in clusters, the valid source and channel coding set is $CS \in \{1 : (48\text{kbps}, 1/3), 2 : (72\text{kbps}, 1/2), 3 : (96\text{kbps}, 2/3)\}$. For the relay nodes the transmission bit rate is 720 kbps and the source and channel coding rates are set to $(96\text{kbps}, 2/3)$.

- **WVSN topology 2**

In the second topology, 15 nodes are organized in three clusters of the same cardinality $\{C1, C2, C3\}$. As the CCU is out of the transmission range of the source nodes in clusters $C1$ and $C2$, two relay nodes $\{R1, R2\}$ retransmit the received videos of each cluster to the CCU as shown in Fig. 4.2. Interference exists among the nodes in the clusters as they transmit their videos to their corresponding relay node. Additionally, the relay nodes $R1$ and $R2$ interfere with the source nodes in clusters $C2$ and $C3$ respectively. The five nodes of each cluster transmit video sequences of the same motion level. Two different set–ups $\mathbf{V} = \{V1, V2, V3\}$ for the transmitted videos' motion levels were tested for the cases of $N_0 = 0$ pW/Hz and $N_0 = 0.1$ pW/Hz with transmission bit rates equal to 96 and 144 kbps. For the first set–up, let $\mathbf{V} = \{low, low, high\}$; for the second set–up, let $\mathbf{V} = \{low, high, medium\}$. For this topology, the dimension of the optimization problem is equal to eight, as the received powers of two relay nodes and three clusters, along with the source and channel coding rates of the source nodes in clusters, have to be allocated. Thus, each particle consists of five constant values, namely the received powers of the nodes and three discrete values corresponding to the source and channel coding rates of the source nodes. In this topology a number of particles equal to 100 and a maximum number of iterations equal to 1000 were used for the PSO.

For the second topology, when the transmission bit rate is set to 96 kbps, the total bandwidth W_t for all links is 4 MHz. The range of $[100, 500]$ mW is used for the transmitted powers of all source nodes. The range $[100, 2500]$ mW is used for the relay node $R1$, while the range for the relay node $R2$ is $[100, 5000]$ mW. The corresponding ranges of received powers are respectively $[0.46667, 2.3333]$ μW, $[0.46667, 11.667]$ μW and $[0.46667, 23.333]$ μW, as derived by the Free Space Propagation Model for distance d=70 m. For the source nodes in clusters, the valid source and channel coding set is $CS \in \{1 : (32\text{kbps}, 1/3), 2 : (48\text{kbps}, 1/2), 3 : (64\text{kbps}, 2/3)\}$. For the relay node $R1$ the transmission bit rate is 480 kbps and the source and channel coding rates are set to $(64\text{kbps}, 2/3)$; for the relay node $R2$ the transmission bit rate is 960 kbps and the source and channel coding rate are set to $(64\text{kbps}, 2/3)$.

When the transmission bit rate is set to 144 kbps, the total bandwidth W_t is 6 MHz for all hops. The range of $[100, 500]$ mW is used for the transmitted powers of all source nodes. The range $[100, 5000]$ mW is used for the relay node $R1$, while the range for the relay node $R2$ is $[100, 10000]$ mW. The corresponding ranges of received powers are respectively $[0.46667, 2.3333]$ μW, $[0.46667, 23.3333]$ μW and $[0.46667, 46.6666]$ μW. For the source nodes in clusters, the valid source and channel coding set is $CS \in \{1 : (48\text{kbps}, 1/3), 2 : (72\text{kbps}, 1/2), 3 : (96\text{kbps}, 2/3)\}$. For the relay node $R1$ the transmission bit rate is 720 kbps and the source and channel coding rates are set to $(96\text{kbps}, 2/3)$; for the relay node $R2$ the transmission bit rate is 1440 kbps and the source and channel coding rates are set to $(96\text{kbps}, 2/3)$.

4.2 Priority–based Resource Allocation in Multihop DS–CDMA Visual Sensor Networks

Firstly, two priority–based optimization criteria, namely MWAD and w.NBS, were tested in both of the topologies. These criteria are preferred for a priority aware approach of the resource allocation. When w.NBS is employed, the high motion nodes join the bargaining game with a bigger advantage than the others. Thus, they have higher priority when it comes to the assignment of received power and source and channel coding rates. Likewise, the use of MWAD favors the high motion users more as indicated by the weights of Eq. (3.9).

WVSN topology 1:

Tables (4.2) to (4.25) depict the achieved PSNRs, the allocated CS and the received and transmitted powers for all the cases that employ MWAD and w.NBS. It can be seen both criteria generally achieve to enhance the PSNRs according to the motion level, i.e. they offer better quality to nodes that transmit high motion video. Nonetheless, MWAD treats more fairly the low and medium motion nodes as it offers higher PSNR than w.NBS can achieve.

More specifically, when N_0 is equal to 0 pW/Hz, if w.NBS is used, the high motion nodes have a gain of 0.024–2.44 dB in comparison with the case that MWAD is used. The low and medium motion nodes have a gain of 0.024–2.87 dB when MWAD is employed. On the contrary, if N_0 is equal to 0.1 or 1 pW/Hz the difference of gain between the two criteria is smaller. The high motion nodes have a gain of 0.04–0.24 dB in comparison with the case that MWAD is used; the low and medium motion nodes have a gain of 0.04–0.73 dB when MWAD is employed. This criterion achieves higher average PSNR compared to w.NBS for both values of N_0. In general, an increase of the transmission bit rate reduces the average PSNR of both criteria. Also, the differences between the two criteria that concern the offered PSNRs are less evident when the bit rate is equal to 144 kbps.

Furthermore, observing Tables (4.2), (4.4), (4.6), (4.8), (4.10), (4.12), (4.14), (4.16), (4.18), (4.20), (4.22) and (4.24), it can be pointed out that when the transmission bit rate is 96kbps, w.NBS and MWAD choose the source and channel coding rate combination that offers the highest available source coding rate to the high motion nodes. In fact, the quality of the video is more affected by the errors due to encoding than the errors due to channel coding. On the contrary, a higher channel coding rate is preferred for the low and medium motion nodes. Videos of relatively low motion are less prone to errors, thus it is easier to achieve good quality for them. Similar values for the source and channel coding rates are chosen if the transmission bit rate is 144 kpbs and N_0 equal to 0 pW/Hz. For the value 0.1 pW/Hz, higher channel coding rates are preferred for all nodes. Since the increase of the bit rate and N_0 leads to an increase of the BER at each hop, a bigger channel coding rate is necessary so that a good level of quality is maintained for the all nodes. Especially for the high motion nodes, the highest source coding rate is never chosen due to the background noise presence.

As far as the transmitted power allocation is concerned (Tables (4.3), (4.5), (4.7), (4.11), (4.13), (4.15), (4.19), (4.21), (4.23) and (4.25)) for both criteria, the transmitted powers of the relay nodes are in accordance with the motion level of the transmitted video sequences. Namely, the transmitted powers for the relay nodes of the clusters with high motion nodes are higher than the transmitted powers of the relays of low and medium motion clusters. When N_0 is 0 pW/Hz, the source nodes have the minimum available transmitted power, i.e. 100 mW. Moreover, when N_0 is not equal to 0, higher transmitted powers for all nodes is demanded in order to keep the bit error rate probability per hop low and maintain high quality. The source nodes use the maximum available transmitted power, i.e. 500 mW. In any case, it is clear that w.NBS demands lower transmitted power than MWAD.

$N_0 = 0$ pW/Hz								
Cluster	$C1$		$C2$		$C3$		$C4$	
Criterion	PSNR	CS	PSNR	CS	PSNR	CS	PSNR	CS
MWAD	36.7435	3	30.4577	1	32.6942	2	32.9295	2
w.NBS	39.1853	3	28.9987	1	29.8229	1	30.1971	1

Table 4.2: PSNR(dB) and Source and Channel Coding Rates for the case with bitrate 96kbps, $\mathbf{V} = \{high, low, medium, medium\}$ and bandwidth 5MHz for all hops.

$N_0 = 0$ pW/Hz								
Relay node	$R1$	$R2$	$R3$	$R4$	$R1$	$R2$	$R3$	$R4$
Criterion	S^{rec}	S^{rec}	S^{rec}	S^{rec}	S^{trans}	S^{trans}	S^{trans}	S^{trans}
MWAD	0.86741	0.22867	0.43951	0.45318	378.95	100	192.01	197.98
w.NBS	1.07521	0.22867	0.37774	0.39612	469.74	100	165.03	173.05

Table 4.3: Received powers (μW) and Transmitted powers (mW) for the case with bitrate 96kbps, $\mathbf{V} = \{high, low, medium, medium\}$ and bandwidth 5MHz for all hops.

$N_0 = 1$ pW/Hz								
Cluster	$C1$		$C2$		$C3$		$C4$	
Criterion	PSNR	CS	PSNR	CS	PSNR	CS	PSNR	CS
MWAD	33.4342	3	29.5509	1	31.6767	2	31.9092	2
w.NBS	33.6779	3	28.9038	1	31.3255	2	31.6311	2

Table 4.4: PSNR(dB) and Source and Channel Coding Rates for the case with bitrate 96kbps, $\mathbf{V} = \{high, low, medium, medium\}$ and bandwidth 5MHz for all hops.

$N_0 = 1$ pW/Hz								
Relay node	$R1$	$R2$	$R3$	$R4$	$R1$	$R2$	$R3$	$R4$
Criterion	S^{rec}	S^{rec}	S^{rec}	S^{rec}	S^{trans}	S^{trans}	S^{trans}	S^{trans}
MWAD	11.433	3.8573	7.0090	7.2238	4994.81	1685.16	3062.07	3155.91
w.NBS	11.433	3.6973	6.6522	6.8942	4994.81	1615.26	2906.19	3011.92

Table 4.5: Received powers (μW) and Transmitted powers (mW) for the case with bitrate 96kbps, $\mathbf{V} = \{high, low, medium, medium\}$ and bandwidth 5MHz for all hops.

$N_0 = 0$ pW/Hz								
Cluster	$C1$		$C2$		$C3$		$C4$	
Criterion	PSNR	CS	PSNR	CS	PSNR	CS	PSNR	CS
MWAD	35.2866	3	29.6871	1	35.2866	3	29.6871	1
w.NBS	35.4061	3	28.3137	1	35.4061	3	28.3137	1

Table 4.6: PSNR(dB) and Source and Channel Coding Rates for the case with bitrate 96kbps, $\mathbf{V} = \{high, low, high, low\}$ and bandwidth 5MHz for all hops.

$N_0 = 0$ pW/Hz								
Relay node	$R1$	$R2$	$R3$	$R4$	$R1$	$R2$	$R3$	$R4$
Criterion	S^{rec}	S^{rec}	S^{rec}	S^{rec}	S^{trans}	S^{trans}	S^{trans}	S^{trans}
MWAD	0.79055	0.22867	0.79055	0.22867	345.38	100	345.38	100
w.NBS	0.82750	0.22867	0.82750	0.22867	361.52	100	361.52	100

Table 4.7: Received powers (μW) and Transmitted powers (mW) for the case with bitrate 96kbps, $\mathbf{V} = \{high, low, high, low\}$ and bandwidth 5MHz for all hops.

$N_0 = 1$ pW/Hz								
Cluster	$C1$		$C2$		$C3$		$C4$	
Criterion	PSNR	CS	PSNR	CS	PSNR	CS	PSNR	CS
MWAD	33.0902	3	28.8655	1	33.0902	3	28.8655	1
w.NBS	33.1402	3	28.1284	1	33.1402	3	28.1284	1

Table 4.8: PSNR(dB) and Source and Channel Coding Rates for the case with bitrate 96kbps, $\mathbf{V} = \{high, low, high, low\}$ and bandwidth 5MHz for all hops.

$N_0 = 1$ pW/Hz								
Relay node	$R1$	$R2$	$R3$	$R4$	$R1$	$R2$	$R3$	$R4$
Criterion	S^{rec}	S^{rec}	S^{rec}	S^{rec}	S^{trans}	S^{trans}	S^{trans}	S^{trans}
MWAD	11.433	3.91538	11.433	3.91538	4994.81	1710.54	4994.81	1710.54
w.NBS	11.433	3.83021	11.433	3.83021	4994.81	3573.61	4994.81	3573.61

Table 4.9: Received powers (μW) and Transmitted powers (mW) for the case with bitrate 96kbps, $\mathbf{V} = \{high, low, high, low\}$ and bandwidth 5MHz for all hops.

$N_0 = 0$ pW/Hz								
Cluster	$C1$		$C2$		$C3$		$C4$	
Criterion	PSNR	CS	PSNR	CS	PSNR	CS	PSNR	CS
MWAD	34.0656	3	31.0071	2	34.0656	3	28.9685	1
w.NBS	34.5206	3	28.7662	1	34.5206	3	28.0804	1

Table 4.10: PSNR(dB) and Source and Channel Coding Rates for the case with bitrate 96kbps, $\mathbf{V} = \{high, medium, high, low\}$ and bandwidth 5MHz for all hops.

$N_0 = 0$ pW/Hz								
Relay node	$R1$	$R2$	$R3$	$R4$	$R1$	$R2$	$R3$	$R4$
Criterion	S^{rec}	S^{rec}	S^{rec}	S^{rec}	S^{trans}	S^{trans}	S^{trans}	S^{trans}
MWAD	0.72486	0.40094	0.72486	0.22867	316.68	175.17	316.68	100
w.NBS	0.77068	0.35313	0.77068	0.22867	336.70	154.27	336.70	100

Table 4.11: Received powers (μW) and Transmitted powers (mW) for the case with bitrate 96kbps, $\mathbf{V} = \{high, medium, high, low\}$ and bandwidth 5MHz for all hops.

$N_0 = 1$ pW/Hz								
Cluster	$C1$		$C2$		$C3$		$C4$	
Criterion	PSNR	CS	PSNR	CS	PSNR	CS	PSNR	CS
MWAD	32.2853	3	28.8654	1	32.285	3	28.1785	1
w.NBS	32.4046	3	28.3289	1	32.4046	3	27.7056	1

Table 4.12: PSNR(dB) and Source and Channel Coding Rates for the case with bitrate 96kbps, $\mathbf{V} = \{high, medium, high, low\}$ and bandwidth 5MHz for all hops.

$N_0 = 1$ pW/Hz								
Relay node	$R1$	$R2$	$R3$	$R4$	$R1$	$R2$	$R3$	$R4$
Criterion	S^{rec}	S^{rec}	S^{rec}	S^{rec}	S^{trans}	S^{trans}	S^{trans}	S^{trans}
MWAD	11.433	6.44848	11.433	4.15167	4994.81	2817.19	4994.81	1813.77
w.NBS	11.433	6.11904	11.433	4.06674	4994.81	4256.09	4994.81	3555.98

Table 4.13: Received powers (μW) and Transmitted powers (mW) for the case with bitrate 96kbps, $\mathbf{V} = \{high, medium, high, low\}$ and bandwidth 5MHz for all hops.

$N_0 = 0$ pW/Hz								
Cluster	$C1$		$C2$		$C3$		$C4$	
Criterion	PSNR	CS	PSNR	CS	PSNR	CS	PSNR	CS
MWAD	31.2047	3	27.3027	2	28.8549	1	29.1655	1
w.NBS	31.2534	3	27.2768	2	28.7429	1	29.0756	1

Table 4.14: PSNR(dB) and Source and Channel Coding Rates for the case with bitrate 144kbps, $\mathbf{V} = \{high, low, medium, medium\}$ and bandwidth 2MHz and 10MHz for the first and second hop.

$N_0 = 0$ pW/Hz								
Relay node	$R1$	$R2$	$R3$	$R4$	$R1$	$R2$	$R3$	$R4$
Criterion	S^{rec}	S^{rec}	S^{rec}	S^{rec}	S^{trans}	S^{trans}	S^{trans}	S^{trans}
MWAD	0.47377	0.22867	0.31802	0.32567	206.98	100	138.94	142.28
w.NBS	0.47802	0.22867	0.31617	0.32421	208.83	100	138.13	141.64

Table 4.15: Received powers (μW) and Transmitted powers (mW) for the case with bitrate 144kbps, $\mathbf{V} = \{high, low, medium, medium\}$ and bandwidth 2MHz and 10MHz for the first and second hop.

$N_0 = 0.1$ pW/Hz								
Cluster	$C1$		$C2$		$C3$		$C4$	
Criterion	PSNR	CS	PSNR	CS	PSNR	CS	PSNR	CS
MWAD	31.1187	2	27.0062	2	28.5560	1	28.8616	1
w.NBS	31.2271	2	27.0149	2	28.4067	1	28.7192	1

Table 4.16: PSNR(dB) and Source and Channel Coding Rates for the case with bitrate 144kbps, $\mathbf{V} = \{high, low, medium, medium\}$ and bandwidth 2MHz and 10MHz for the first and second hop.

$N_0 = 0.1$ pW/Hz								
Relay node	$R1$	$R2$	$R3$	$R4$	$R1$	$R2$	$R3$	$R4$
Criterion	S^{rec}	S^{rec}	S^{rec}	S^{rec}	S^{trans}	S^{trans}	S^{trans}	S^{trans}
MWAD	22.866	11.13061	15.33280	15.70107	9989.62	4862.71	6698.55	6859.43
w.NBS	22.866	11.01710	15.04517	15.41435	9989.62	4813.12	6572.89	6734.17

Table 4.17: Received powers (μW) and Transmitted powers (mW) for the case with bitrate 144kbps, $\mathbf{V} = \{high, low, medium, medium\}$ and bandwidth 2MHz and 10MHz for the first and second hop.

$N_0 = 0$ pW/Hz								
Cluster	$C1$		$C2$		$C3$		$C4$	
Criterion	PSNR	CS	PSNR	CS	PSNR	CS	PSNR	CS
MWAD	30.8444	3	25.7851	2	30.8444	3	25.7851	2
w.NBS	30.8204	3	26.0112	2	30.8204	3	26.0112	2

Table 4.18: PSNR(dB) and Source and Channel Coding Rates for the case with bitrate 144kbps, $\mathbf{V} = \{high, low, high, low\}$ and bandwidth 2MHz and 10MHz for the first and second hop.

$N_0 = 0$ pW/Hz								
Relay node	$R1$	$R2$	$R3$	$R4$	$R1$	$R2$	$R3$	$R4$
Criterion	S^{rec}	S^{rec}	S^{rec}	S^{rec}	S^{trans}	S^{trans}	S^{trans}	S^{trans}
MWAD	0.46950	0.22867	0.46950	0.22866	205.12	100	205.12	100
w.NBS	0.46600	0.22867	0.46600	0.22867	203.59	100	203.59	100

Table 4.19: Received powers (μW) and Transmitted powers (mW) for the case with bitrate 144kbps, $\mathbf{V} = \{high, low, high, low\}$ and bandwidth 2MHz and 10MHz for the first and second hop.

$N_0 = 0.1$ pW/Hz								
Cluster	$C1$		$C2$		$C3$		$C4$	
Criterion	PSNR	CS	PSNR	CS	PSNR	CS	PSNR	CS
MWAD	30.4943	2	25.8047	2	30.4943	2	25.8047	2
w.NBS	33.1402	2	26.0772	2	33.1402	2	26.0772	2

Table 4.20: PSNR(dB) and Source and Channel Coding Rates for the case with bitrate 144kbps, $\mathbf{V} = \{high, low, high, low\}$ and bandwidth 2MHz and 10MHz for the first and second hop.

$N_0 = 0.1$ pW/Hz								
Relay node	$R1$	$R2$	$R3$	$R4$	$R1$	$R2$	$R3$	$R4$
Criterion	S^{rec}	S^{rec}	S^{rec}	S^{rec}	S^{trans}	S^{trans}	S^{trans}	S^{trans}
MWAD	22.866	11.38761	22.866	11.38760	9989.62	4974.98	9989.62	4974.98
w.NBS	22.866	11.49150	22.866	11.49140	9989.62	6889.16	9989.62	6889.16

Table 4.21: Received powers (μW) and Transmitted powers (mW) for the case with bitrate 144kbps, $\mathbf{V} = \{high, low, high, low\}$a and bandwidth 2MHz and 10MHz for the first and second hop.

$N_0 = 0$ pW/Hz								
Cluster	$C1$		$C2$		$C3$		$C4$	
Criterion	PSNR	CS	PSNR	CS	PSNR	CS	PSNR	CS
MWAD	31.7421	2	29.3133	1	31.7421	2	27.8243	2
w.NBS	31.8172	2	28.9909	1	31.8172	2	27.526612	2

Table 4.22: PSNR(dB) and Source and Channel Coding Rates for the case with bitrate 144kbps, $\mathbf{V} = \{high, medium, high, low\}$ and bandwidth 2MHz and 10MHz for the first and second hop.

$N_0 = 0$ pW/Hz								
Relay node	$R1$	$R2$	$R3$	$R4$	$R1$	$R2$	$R3$	$R4$
Criterion	S^{rec}	S^{rec}	S^{rec}	S^{rec}	S^{trans}	S^{trans}	S^{trans}	S^{trans}
MWAD	0.49598	0.32618	0.49598	0.22867	216.69	142.50	216.69	100
w.NBS	0.50446	0.32239	0.50446	0.22867	220.39	140.84	220.39	100

Table 4.23: Received powers (μW) and Transmitted powers (mW) for the case with bitrate 144kbps, $\mathbf{V} = \{high, medium, high, low\}$ and bandwidth 2MHz and 10MHz for the first and second hop.

$N_0 = 0.1$ pW/Hz								
Cluster	$C1$		$C2$		$C3$		$C4$	
Criterion	PSNR	CS	PSNR	CS	PSNR	CS	PSNR	CS
MWAD	31.3392	2	29.1870	1	31.3392	2	27.6976	2
w.NBS	31.3952	2	28.9293	1	31.3952	2	27.4771	2

Table 4.24: PSNR(dB) and Source and Channel Coding Rates for the case with bitrate 144kbps, $\mathbf{V} = \{high, medium, high, low\}$ and bandwidth 2MHz and 10MHz for the first and second hop.

$N_0 = 0.1$ pW/Hz								
Relay node	$R1$	$R2$	$R3$	$R4$	$R1$	$R2$	$R3$	$R4$
Criterion	S^{rec}	S^{rec}	S^{rec}	S^{rec}	S^{trans}	S^{trans}	S^{trans}	S^{trans}
MWAD	22.866	15.25769	22.866	10.74254	9989.62	6665.73	9989.62	4693.17
w.NBS	22.866	14.91755	22.866	10.60633	9989.62	8410.16	9989.62	7002.87

Table 4.25: Received powers (μW) and Transmitted powers (mW) for the case with bitrate 144kbps, $\mathbf{V} = \{high, medium, high, low\}$ and bandwidth 2MHz and 10MHz for the first and second hop.

WVSN topology 2:

As in the previous topology, w.NBS and MWAD favor the high motion nodes. Both criteria offer better quality to nodes that transmit high motion video, although MWAD can also achieve better PSNRs than w.NBS for low and medium motion videos. This criterion results in higher average PSNR than w.NBS in all cases, too.

Particularly, when N_0 is equal to 0 pW/Hz and w.NBS is used, the high motion nodes have a gain of 0.061–0.335 dB in comparison with the case that MWAD is used. The low and medium motion nodes have a gain of 0.027–3.1652 dB when MWAD is employed. On the contrary, if N_0 is equal to 0.1 pW/Hz the difference of gain between the two criteria is smaller. The high motion nodes have a gain of 0.054–0.3 dB in comparison with the case that MWAD is used; the low and medium motion nodes have a gain of 0.02–2.93 dB when MWAD is employed. Furthermore, in this topology, the differences between the two criteria that concern the offered PSNRs are more evident when the bit rate is equal to 144 kbps.

As for the choices of the source and channel coding rates, they are not affected by the background noise; the most of them are the same for both $N_0 = 0$ and $N_0 \neq 0$. Generally, the higher the motion level of the videos is, the higher source coding rate is preferred. However, when bit rate increases from 96 to 144 kbps, a lower source coding rate is chosen for the high motion videos, if $\mathbf{V} = \{low, high, medium\}$ and a higher one for the low and medium motion videos for $\mathbf{V} = \{low, low, high\}$ and $\mathbf{V} = \{low, high, medium\}$.

Moreover, it is important to mention that the choice of transmitted powers depends on the arrangement of the source nodes, i.e. whether the high motion nodes transmit

via multiple hops to the CCU or not. The level of the background noise affects the power allocation as well. As an illustration of this remark, we can refer to the case with $\mathbf{V} = \{low, high, medium\}$. As shown in Tables (4.31), (4.33), (4.39) and (4.41) , the transmitted powers allocated to $R2$ are bigger than those allocated to $R1$. This can be explained by the fact that w.NBS and MWAD aim at maintaining a very good quality for the high motion videos of the source nodes in cluster $C2$, which are transmitted via the relay node $R2$. Also, the relay node $R1$ transmits low motion videos which are not favored by these two criteria. In contrast, when $\mathbf{V} = \{low, low, high\}$, the relay node $R1$ transmits the videos using bigger power than $R2$, as depicted in Tables (4.27), (4.29), (4.35) and (4.37). The relay node $R1$ tries to achieve a good quality for the videos of cluster $C1$ that are transmitted via more hops than the videos of the cluster $C2$.

By all means, when $N_0 \neq 0$, an increase in transmitted powers of both source and relay nodes is observed in all set–ups tested in this topology. In either case, w.NBS uses lower average transmitted power comparing to MWAD. As in the first topology, when N_0 is 0 pW/Hz, the source nodes have the minimum available transmitted power, i.e. 100 mW, but when N_0 is not equal to 0, they use the maximum available transmitted power, i.e. 500 mW.

$N_0 = 0$ pW/Hz						
Cluster	$C1$		$C2$		$C3$	
Criterion	PSNR	CS	PSNR	CS	PSNR	CS
MWAD	34.9328	1	34.9328	1	37.4323	3
w.NBS	33.8502	1	33.8502	1	37.5271	3

Table 4.26: PSNR(dB) and Source and Channel Coding Rates for the case with bitrate 96kbps, $\mathbf{V} = \{low, low, high\}$ and bandwidth 4MHz for all hops.

$N_0 = 0$ pW/Hz				
Relay node	$R1$	$R2$	$R1$	$R2$
Criterion	S^{rec}	S^{rec}	S^{trans}	S^{trans}
MWAD	0.75200	0.46667	160.98	100
w.NBS	0.66383	0.46667	142.11	100

Table 4.27: Received powers (μW) and Transmitted powers (mW) for the case with bitrate 96kbps, $\mathbf{V} = \{low, low, high\}$ and bandwidth 4MHz for all hops.

$N_0 = 0.1$ pW/Hz						
Cluster	$C1$		$C2$		$C3$	
Criterion	PSNR	CS	PSNR	CS	PSNR	CS
MWAD	34.8149	1	34.8149	1	37.1414	3
w.NBS	33.8178	1	33.8178	1	37.2262	3

Table 4.28: PSNR(dB) and Source and Channel Coding Rates for the case with bitrate 96kbps, $\mathbf{V} = \{low, low, high\}$ and bandwidth 4MHz for all hops.

$N_0 = 0.1$ pW/Hz				
Relay node	$R1$	$R2$	$R1$	$R2$
Criterion	S^{rec}	S^{rec}	S^{trans}	S^{trans}
MWAD	5.18048	1.69982	1108.98	363.88
w.NBS	5.18335	1.56981	1109.60	336.05

Table 4.29: Received powers (μW) and Transmitted powers (mW) for the case with bitrate 96kbps, $\mathbf{V} = \{low, low, high\}$ and bandwidth 4MHz for all hops.

$N_0 = 0$ pW/Hz						
Cluster	$C1$		$C2$		$C3$	
Criterion	PSNR	CS	PSNR	CS	PSNR	CS
MWAD	35.2118	1	37.9638	3	37.8328	2
w.NBS	34.0044	1	38.0252	3	37.8056	2

Table 4.30: PSNR(dB) and Source and Channel Coding Rates for the case with bitrate 96kbps, $\mathbf{V} = \{low, high, medium\}$ and bandwidth 4MHz for all hops.

$N_0 = 0$ pW/Hz				
Relay node	$R1$	$R2$	$R1$	$R2$
Criterion	S^{rec}	S^{rec}	S^{trans}	S^{trans}
MWAD	0.46667	6.53989	100	1399.99
w.NBS	0.46667	4.80180	100	1027.92

Table 4.31: Received powers (μW) and Transmitted powers (mW) for the case with bitrate 96kbps, $\mathbf{V} = \{low, high, medium\}$ and bandwidth 4MHz for all hops.

$N_0 = 0.1$ pW/Hz						
Cluster	$C1$		$C2$		$C3$	
Criterion	PSNR	CS	PSNR	CS	PSNR	CS
MWAD	35.0804	1	37.6632	3	37.6921	2
w.NBS	33.9648	1	37.7172	3	37.6723	2

Table 4.32: PSNR(dB) and Source and Channel Coding Rates for the case with bitrate 96kbps, $\mathbf{V} = \{low, high, medium\}$ and bandwidth 4MHz for all hops.

$N_0 = 0.1$ pW/Hz				
Relay node	$R1$	$R2$	$R1$	$R2$
Criterion	S^{rec}	S^{rec}	S^{trans}	S^{trans}
MWAD	0.87017	9.92741	186.28	2125.16
w.NBS	0.79350	9.98489	169.86	2137.46

Table 4.33: Received powers (μW) and Transmitted powers (mW) for the case with bitrate 96kbps, $\mathbf{V} = \{low, high, medium\}$ and bandwidth 4MHz for all hops.

$N_0 = 0$ pW/Hz						
Cluster	$C1$		$C2$		$C3$	
Criterion	PSNR	CS	PSNR	CS	PSNR	CS
MWAD	37.7660	2	37.7660	2	40.9630	2
w.NBS	35.8419	2	35.8419	2	41.2947	2

Table 4.34: PSNR(dB) and Source and Channel Coding Rates for the case with bitrate 144kbps, $\mathbf{V} = \{low, low, high\}$ and bandwidth 6MHz for all hops.

$N_0 = 0$ pW/Hz				
Relay node	$R1$	$R2$	$R1$	$R2$
Criterion	S^{rec}	S^{rec}	S^{trans}	S^{trans}
MWAD	1.02970	0.46667	220.43	100
w.NBS	0.72913	0.46667	156.08	100

Table 4.35: Received powers (μW) and Transmitted powers (mW) for the case with bitrate 144kbps, $\mathbf{V} = \{low, low, high\}$ and bandwidth 6MHz for all hops.

$N_0 = 0.1$ pW/Hz						
Cluster	$C1$		$C2$		$C3$	
Criterion	PSNR	CS	PSNR	CS	PSNR	CS
MWAD	37.51120	2	37.5120	2	40.4563	2
w.NBS	35.7520	2	35.75120	2	40.7473	2

Table 4.36: PSNR(dB) and Source and Channel Coding Rates for the case with bitrate 144kbps, $\mathbf{V} = \{low, low, high\}$ and bandwidth 6MHz for all hops.

$N_0 = 0.1$ pW/Hz				
Relay node	$R1$	$R2$	$R1$	$R2$
Criterion	S^{rec}	S^{rec}	S^{trans}	S^{trans}
MWAD	4.64465	2.58805	994.28	554.02
w.NBS	4.64711	2.20355	994.81	471.71

Table 4.37: Received powers (μW) and Transmitted powers (mW) for the case with bitrate 144kbps, $\mathbf{V} = \{low, low, high\}$ and bandwidth 6MHz for all hops.

$N_0 = 0$ pW/Hz						
Cluster	$C1$		$C2$		$C3$	
Criterion	PSNR	CS	PSNR	CS	PSNR	CS
MWAD	37.1332	2	41.5427	3	39.8589	2
w.NBS	33.9680	2	41.8777	3	38.3350	1

Table 4.38: PSNR(dB) and Source and Channel Coding Rates for the case with bitrate 144kbps, $\mathbf{V} = \{low, high, medium\}$ and bandwidth 6MHz for all hops.

$N_0 = 0$ pW/Hz				
Relay node	$R1$	$R2$	$R1$	$R2$
Criterion	S^{rec}	S^{rec}	S^{trans}	S^{trans}
MWAD	0.46667	9.30838	100	1992.64
w.NBS	0.46667	4.27369	100	914.87

Table 4.39: Received powers (μW) and Transmitted powers (mW) for the case with bitrate 144kbps, $\mathbf{V} = \{low, high, medium\}$ and bandwidth 6MHz for all hops.

$N_0 = 0.1$ pW/Hz						
Cluster	$C1$		$C2$		$C3$	
Criterion	PSNR	CS	PSNR	CS	PSNR	CS
MWAD	36.8245	2	40.9769	3	39.5515	2
w.NBS	33.8957	2	41.2750	3	38.1315	1

Table 4.40: PSNR(dB) and Source and Channel Coding Rates for the case with bitrate 144kbps, $\mathbf{V} = \{low, high, medium\}$ and bandwidth 6MHz for all hops.

$N_0 = 0.1$ pW/Hz				
Relay node	$R1$	$R2$	$R1$	$R2$
Criterion	S^{rec}	S^{rec}	S^{trans}	S^{trans}
MWAD	1.21070	9.331070	259.17	1997.50
w.NBS	0.95809	10.15077	205.10	2172.97

Table 4.41: Received powers (μW) and Transmitted powers (mW) for the case with bitrate 144kbps, $\mathbf{V} = \{low, high, medium\}$ and bandwidth 6MHz for all hops.

4.3 Non–prioritized Resource Allocation in Multihop DS–CDMA Visual Sensor Networks

The aforementioned topologies were also tested using three criteria, namely e.NBS, MAD and MMD, that do not take into account the motion level of the users. Thus, high motion

nodes do not obtain any priority and consequently all nodes are treated equally. On the hand, e.NBS and MAD seem to favor the low and medium motion videos. On the other hand, MMD does not imply a content–aware approach, thus it achieves similar quality levels for all videos.

WVSN topology 1:

To begin with, Tables (4.42), (4.44), (4.46), (4.48), (4.50), (4.52), (4.54), (4.56), (4.58), (4.60), (4.62) and (4.64) clearly show that e.NBS achieves higher PSNR for the low motion nodes in all cases. However, MAD offers better PSNRs to the high and medium motion nodes than e.NBS does. As expected, MMD achieves the same quality level for all nodes, regardless of the level of motion and the background noise. The higher average PSNR is achieved when e.NBS is used, although the differences between the average PSNRs of these three criteria reduce when background noise is taken into account.

Using MAD, when N_0 is equal to 0 pW/Hz, the high motion nodes have a gain of 0.13–0.94 dB in comparison with the case that e.NBS is used. At the same time, the medium motion nodes have a small gain of 0.08–0.2 dB when MAD is employed. The videos of the low motion nodes have better PSNRs if e.NBS is chosen instead of MAD(gain 0.41–2.69 dB). If N_0 is equal to 1 pW/Hz, using MAD the high motion nodes have a gain of 0.12–0.83 dB. With e.NBS, low motion nodes have gain of 0.39–2.54 dB, whereas the medium motion nodes have a gain of 0.08–0.11 dB when MAD is employed.

With regard to the choices of source and channel coding rates, we can see that in most cases they are not affected by the background noise when e.NBS and MAD are used. However, MMD tends to assign a lower source coding rate to the high motion nodes, in order to keep the influence of the background noise at a low level. In general, the highest available source coding rate is preferred for the high motion nodes, except some cases with $N_0 \neq 0$ pW/Hz and transmitted power equal to 144 kbps that the second higher source coding rate is chosen. Even though the high motion videos are encoded using more bits, their PSNRs are not better than the PSNRs of the low or medium motion videos.

Concerning the power allocation for the three criteria, the source nodes transmit their videos with the lowest available power if N_0 is equal to 0 pW/Hz, whereas the highest transmitted powers are used when $N_0 \neq 0$ pW/Hz, as illustrated in Tables (4.43), (4.45), (4.47), (4.49), (4.51), (4.53), (4.55), (4.57), (4.59), (4.61), (4.63) and (4.65). In particular, e.NBS allocates lower powers than MAD and MMD allocate to the relay nodes, if $N_0 = 0$ pW/Hz. Conversely, when $N_0 \neq 0$ pW/Hz, MAD and MMD allocate lower powers to the relay nodes than e.NBS does. It should also be noted that the transmitted powers of the relay nodes are allocated with respect to the motion levels of the videos of their corresponding clusters, when e.NBS, MAD and MMD are used.

$N_0 = 0$ pW/Hz								
Cluster	$C1$		$C2$		$C3$		$C4$	
Criterion	PSNR	CS	PSNR	CS	PSNR	CS	PSNR	CS
e.NBS	32.5422	3	40.5004	3	33.7773	2	33.8292	2
MAD	33.2506	3	37.9803	3	33.9849	2	34.0238	2
MMD	34.1722	3	34.1722	1	34.1722	2	34.1722	2

Table 4.42: PSNR(dB) and Source and Channel Coding Rates for the case with bitrate 96kbps, $\mathbf{V} = \{high, low, medium, medium\}$ and bandwidth 5MHz for all hops.

$N_0 = 0$ pW/Hz								
Relay node	$R1$	$R2$	$R3$	$R4$	$R1$	$R2$	$R3$	$R4$
Criterion	S^{rec}	S^{rec}	S^{rec}	S^{rec}	S^{trans}	S^{trans}	S^{trans}	S^{trans}
e.NBS	0.33959	0.22867	0.27305	0.27663	148.36	100	119.29	120.86
MAD	0.42386	0.22867	0.32628	0.33002	185.18	100	142.54	144.18
MMD	0.58237	0.22867	0.42035	0.42337	254.43	100	183.64	184.96

Table 4.43: Received powers (μW) and Transmitted powers (mW) for the case with bitrate 96kbps, $\mathbf{V} = \{high, low, medium, medium\}$ and bandwidth 5MHz for all hops.

$N_0 = 1$ pW/Hz								
Cluster	$C1$		$C2$		$C3$		$C4$	
Criterion	PSNR	CS	PSNR	CS	PSNR	CS	PSNR	CS
e.NBS	30.2792	3	39.1806	3	32.8664	2	32.9030	2
MAD	31.0197	3	36.6365	2	32.9555	3	32.9825	2
MMD	32.5255	3	32.5255	1	32.5255	3	32.5255	1

Table 4.44: PSNR(dB) and Source and Channel Coding Rates for the case with bitrate 96kbps, $\mathbf{V} = \{high, low, medium, medium\}$ and bandwidth 5MHz for all hops.

$N_0 = 1$ pW/Hz								
Relay node	$R1$	$R2$	$R3$	$R4$	$R1$	$R2$	$R3$	$R4$
Criterion	S^{rec}	S^{rec}	S^{rec}	S^{rec}	S^{trans}	S^{trans}	S^{trans}	S^{trans}
e.NBS	11.433	8.54780	10.2229	10.3581	4994.81	3734.33	4466.15	4525.21
MAD	11.433	6.95720	6.65220	9.70860	9.8273	3039.45	4241.45	4293.32
MMD	11.433	4.72200	8.19590	8.28280	4994.81	2062.94	3580.62	3618.55

Table 4.45: Received powers (μW) and Transmitted powers (mW) for the case with bitrate 96kbps, $\mathbf{V} = \{high, low, medium, medium\}$ and bandwidth 5MHz for all hops.

$N_0 = 0$ pW/Hz								
Cluster	$C1$		$C2$		$C3$		$C4$	
Criterion	PSNR	CS	PSNR	CS	PSNR	CS	PSNR	CS
e.NBS	32.3489	3	40.2768	3	32.3489	3	40.2768	3
MAD	33.2883	3	28.3137	3	33.2883	3	38.0134	3
MMD	34.4121	3	34.4121	1	34.4121	3	34.4121	1

Table 4.46: PSNR(dB) and Source and Channel Coding Rates for the case with bitrate 96kbps, $\mathbf{V} = \{high, low, high, low\}$ and bandwidth 5MHz for all hops.

$N_0 = 0$ pW/Hz								
Relay node	$R1$	$R2$	$R3$	$R4$	$R1$	$R2$	$R3$	$R4$
Criterion	S^{rec}	S^{rec}	S^{rec}	S^{rec}	S^{trans}	S^{trans}	S^{trans}	S^{trans}
e.NBS	0.33891	0.22867	0.33892	0.22867	148.06	100	148.06	100
MAD	0.42452	0.22867	0.42452	0.22867	185.46	100	185.46	100
MMD	0.58526	0.22867	0.58526	0.22867	255.69	100	255.69	100

Table 4.47: Received powers (μW) and Transmitted powers (mW) for the case with bitrate 96kbps, $\mathbf{V} = \{high, low, high, low\}$ and bandwidth 5MHz for all hops.

$N_0 = 1$ pW/Hz								
Cluster	$C1$		$C2$		$C3$		$C4$	
Criterion	PSNR	CS	PSNR	CS	PSNR	CS	PSNR	CS
e.NBS	30.6544	3	38.9495	3	30.6544	3	38.9495	3
MAD	31.4849	3	36.6788	2	31.4849	3	36.6788	2
MMD	32.6312	3	32.6312	1	32.6312	3	32.6312	1

Table 4.48: PSNR(dB) and Source and Channel Coding Rates for the case with bitrate 96kbps, $\mathbf{V} = \{high, low, high, low\}$ and bandwidth 5MHz for all hops.

$N_0 = 1$ pW/Hz								
Relay node	$R1$	$R2$	$R3$	$R4$	$R1$	$R2$	$R3$	$R4$
Criterion	S^{rec}	S^{rec}	S^{rec}	S^{rec}	S^{trans}	S^{trans}	S^{trans}	S^{trans}
e.NBS	11.433	8.1799	11.433	8.1799	4994.81	3573.61	4994.81	3573.61
MAD	11.433	6.70503	11.433	6.70503	4994.81	3573.61	4994.81	3573.61
MMD	11.433	4.70160	11.433	4.70160	4994.81	2929.27	4994.81	2929.27

Table 4.49: Received powers (μW) and Transmitted powers (mW) for the case with bitrate 96kbps, $\mathbf{V} = \{high, low, high, low\}$ and bandwidth 5MHz for all hops.

$N_0 = 0$ pW/Hz								
Cluster	$C1$		$C2$		$C3$		$C4$	
Criterion	PSNR	CS	PSNR	CS	PSNR	CS	PSNR	CS
e.NBS	31.8984	3	33.2362	2	31.8984	3	39.7192	3
MAD	32.4108	3	33.3183	2	32.4108	3	37.0507	2
MMD	33.1297	3	33.1297	1	33.1297	3	33.1297	1

Table 4.50: PSNR(dB) and Source and Channel Coding Rates for the case with bitrate 96kbps, $\mathbf{V} = \{high, medium, high, low\}$ and bandwidth 5MHz for all hops.

$N_0 = 0$ pW/Hz								
Relay node	$R1$	$R2$	$R3$	$R4$	$R1$	$R2$	$R3$	$R4$
Criterion	S^{rec}	S^{rec}	S^{rec}	S^{rec}	S^{trans}	S^{trans}	S^{trans}	S^{trans}
e.NBS	0.3379	0.2733	0.3379	0.22867	147.65	119.40	147.65	100
MAD	0.4141	0.3225	0.4141	0.22867	180.91	154.27	140.88	100
MMD	0.5652	0.4054	0.5652	0.22867	246.92	177.12	246.92	100

Table 4.51: Received powers (μW) and Transmitted powers (mW) for the case with bitrate 96kbps, $\mathbf{V} = \{high, medium, high, low\}$ and bandwidth 5MHz for all hops.

$N_0 = 1$ pW/Hz								
Cluster	$C1$		$C2$		$C3$		$C4$	
Criterion	PSNR	CS	PSNR	CS	PSNR	CS	PSNR	CS
e.NBS	30.2270	3	32.2616	2	30.2270	3	38.2981	3
MAD	30.8539	3	32.4026	3	30.8539	3	34.7708	1
MMD	31.5500	3	31.5500	3	31.5500	3	31.5500	1

Table 4.52: PSNR(dB) and Source and Channel Coding Rates for the case with bitrate 96kbps, $\mathbf{V} = \{high, medium, high, low\}$ and bandwidth 5MHz for all hops.

$N_0 = 1$ pW/Hz								
Relay node	$R1$	$R2$	$R3$	$R4$	$R1$	$R2$	$R3$	$R4$
Criterion	S^{rec}	S^{rec}	S^{rec}	S^{rec}	S^{trans}	S^{trans}	S^{trans}	S^{trans}
e.NBS	11.433	9.74208	11.433	8.13956	4994.81	4256.09	4994.81	3555.98
MAD	11.433	9.37788	11.433	6.27198	4994.81	4096.98	4994.81	2740.08
MMD	11.433	8.25026	11.433	14.92122	4994.81	3604.35	4994.81	2149.97

Table 4.53: Received powers (μW) and Transmitted powers (mW) for the case with bitrate 96kbps, $\mathbf{V} = \{high, medium, high, low\}$ and 5MHz for all hops.

$N_0 = 0$ pW/Hz								
Cluster	$C1$		$C2$		$C3$		$C4$	
Criterion	PSNR	CS	PSNR	CS	PSNR	CS	PSNR	CS
e.NBS	29.1757	3	32.6403	2	29.5210	1	29.6455	1
MAD	29.3051	3	32.0405	2	29.6423	1	29.7517	1
MMD	29.8871	3	29.8871	2	29.8871	1	29.8871	1

Table 4.54: PSNR(dB) and Source and Channel Coding Rates for the case with bitrate 144kbps, $\mathbf{V} = \{high, low, medium, medium\}$ and bandwidth 2MHz and 10MHz for the first and second hop.

$N_0 = 0$ pW/Hz								
Relay node	$R1$	$R2$	$R3$	$R4$	$R1$	$R2$	$R3$	$R4$
Criterion	S^{rec}	S^{rec}	S^{rec}	S^{rec}	S^{trans}	S^{trans}	S^{trans}	S^{trans}
e.NBS	0.33192	0.22867	0.27287	0.27611	145.01	100	119.21	120.63
MAD	0.34362	0.22867	0.31617	0.28564	150.12	100	123.47	124.79
MMD	0.38767	0.22867	0.31281	0.31387	169.36	100	136.66	137.12

Table 4.55: Received powers (μW) and Transmitted powers (mW) for the case with bitrate 144kbps, $\mathbf{V} = \{high, low, medium, medium\}$ and bandwidth 2MHz and 10MHz for the first and second hop.

$N_0 = 0.1$ pW/Hz								
Cluster	$C1$		$C2$		$C3$		$C4$	
Criterion	PSNR	CS	PSNR	CS	PSNR	CS	PSNR	CS
e.NBS	28.7231	2	32.4143	2	29.3420	1	29.4606	1
MAD	28.8465	3	31.8477	2	29.4504	1	29.5564	1
MMD	29.5866	2	29.5866	2	29.5866	1	29.5866	1

Table 4.56: PSNR(dB) and Source and Channel Coding Rates for the case with bitrate 144kbps, $\mathbf{V} = \{high, low, medium, medium\}$ and bandwidth 2MHz and 10MHz for the first and second hop.

$N_0 = 0.1$ pW/Hz								
Relay node	$R1$	$R2$	$R3$	$R4$	$R1$	$R2$	$R3$	$R4$
Criterion	S^{rec}	S^{rec}	S^{rec}	S^{rec}	S^{trans}	S^{trans}	S^{trans}	S^{trans}
e.NBS	22.866	15.8683	18.9274	19.1527	9989.62	6932.51	8268.96	8367.40
MAD	22.866	15.3638	18.9239	19.1306	9989.62	6712.09	8267.42	8357.73
MMD	22.866	13.4488	18.2432	18.3204	9989.62	5875.49	7970.04	8003.76

Table 4.57: Received powers (μW) and Transmitted powers (mW) for the case with bitrate 144kbps, $\mathbf{V} = \{high, low, medium, medium\}$ and bandwidth 2MHz and 10MHz for the first and second hop.

$N_0 = 0$ pW/Hz								
Cluster	$C1$		$C2$		$C3$		$C4$	
Criterion	PSNR	CS	PSNR	CS	PSNR	CS	PSNR	CS
e.NBS	29.0080	3	32.3730	2	29.0080	3	32.3730	2
MAD	29.2415	3	31.9602	2	29.2415	3	31.9602	2
MMD	30.0408	3	30.0408	2	30.0408	3	30.0408	2

Table 4.58: PSNR(dB) and Source and Channel Coding Rates for the case with bitrate 144kbps, $\mathbf{V} = \{high, low, high, low\}$ and bandwidth 2MHz and 10MHz for the first and second hop.

$N_0 = 0$ pW/Hz								
Relay node	$R1$	$R2$	$R3$	$R4$	$R1$	$R2$	$R3$	$R4$
Criterion	S^{rec}	S^{rec}	S^{rec}	S^{rec}	S^{trans}	S^{trans}	S^{trans}	S^{trans}
e.NBS	0.3330	0.22867	0.3330	0.22866	145.52	100	145.52	100
MAD	0.3436	0.22867	0.3436	0.22867	150.13	100	150.13	100
MMD	0.3894	0.22867	0.3894	0.22867	170.13	100	170.13	100

Table 4.59: Received powers (μW) and Transmitted powers (mW) for the case with bitrate 144kbps, $\mathbf{V} = \{high, low, high, low\}$ and bandwidth 2MHz and 10MHz for the first and second hop.

$N_0 = 0.1$ pW/Hz								
Cluster	$C1$		$C2$		$C3$		$C4$	
Criterion	PSNR	CS	PSNR	CS	PSNR	CS	PSNR	CS
e.NBS	28.6154	3	32.1490	2	28.6154	3	32.1489	2
MAD	28.8237	3	31.7610	2	28.8237	3	31.7610	2
MMD	29.6512	2	29.6512	2	29.6512	2	29.6512	2

Table 4.60: PSNR(dB) and Source and Channel Coding Rates for the case with bitrate 144kbps, $\mathbf{V} = \{high, low, high, low\}$ and bandwidth 2MHz and 10MHz for the first and second hop.

$N_0 = 0.1$ pW/Hz								
Relay node	$R1$	$R2$	$R3$	$R4$	$R1$	$R2$	$R3$	$R4$
Criterion	S^{rec}	S^{rec}	S^{rec}	S^{rec}	S^{trans}	S^{trans}	S^{trans}	S^{trans}
e.NBS	22.866	15.7691	22.866	15.7691	9989.62	6889.16	9989.62	6889.16
MAD	22.866	15.3255	22.866	15.3255	9989.62	6695.37	9989.62	6695.37
MMD	22.866	13.4246	22.866	13.4246	9989.62	5864.92	9989.62	5864.92

Table 4.61: Received powers (μW) and Transmitted powers (mW) for the case with bitrate 144kbps, $\mathbf{V} = \{high, low, high, low\}$a and bandwidth 2MHz and 10MHz for the first and second hop.

$N_0 = 0$ pW/Hz								
Cluster	$C1$		$C2$		$C3$		$C4$	
Criterion	PSNR	CS	PSNR	CS	PSNR	CS	PSNR	CS
e.NBS	30.1870	3	31.1942	1	30.1870	3	34.7884	2
MAD	30.3731	3	31.3365	1	30.3731	3	33.8264	2
MMD	30.9893	2	30.9893	1	30.9893	2	30.9893	2

Table 4.62: PSNR(dB) and Source and Channel Coding Rates for the case with bitrate 144kbps, $\mathbf{V} = \{high, medium, high, low\}$ and bandwidth 2MHz and 10MHz for the first and second hop.

$N_0 = 0$ pW/Hz								
Relay node	$R1$	$R2$	$R3$	$R4$	$R1$	$R2$	$R3$	$R4$
Criterion	S^{rec}	S^{rec}	S^{rec}	S^{rec}	S^{trans}	S^{trans}	S^{trans}	S^{trans}
e.NBS	0.32038	0.27468	0.32038	0.22867	139.97	120.0	139.97	100
MAD	0.34349	0.29340	0.34349	0.22867	128.18	140.84	150.06	100
MMD	0.41440	0.32750	0.41440	0.22867	181.06	143.09	181.06	100

Table 4.63: Received powers (μW) and Transmitted powers (mW) for the case with bitrate 144kbps, $\mathbf{V} = \{high, medium, high, low\}$ and bandwidth 2MHz and 10MHz for the first and second hop.

$N_0 = 0.1$ pW/Hz								
Cluster	$C1$		$C2$		$C3$		$C4$	
Criterion	PSNR	CS	PSNR	CS	PSNR	CS	PSNR	CS
e.NBS	29.9211	2	30.8542	1	29.9211	2	34.3665	2
MAD	30.1312	2	30.9402	1	30.1312	2	33.4155	2
MMD	30.7002	2	30.7002	1	30.7002	2	30.7002	2

Table 4.64: PSNR(dB) and Source and Channel Coding Rates for the case with bitrate 144kbps, $\mathbf{V} = \{high, medium, high, low\}$ and bandwidth 2MHz and 10MHz for the first and second hop.

$N_0 = 0.1$ pW/Hz								
Relay node	$R1$	$R2$	$R3$	$R4$	$R1$	$R2$	$R3$	$R4$
Criterion	S^{rec}	S^{rec}	S^{rec}	S^{rec}	S^{trans}	S^{trans}	S^{trans}	S^{trans}
e.NBS	22.866	19.2506	22.866	16.023	9989.62	8410.16	9989.62	7002.87
MAD	22.866	19.0875	22.866	14.986	9989.62	8338.89	9989.62	6547.04
MMD	22.866	17.9557	22.866	12.6516	9989.62	7844.45	9989.62	5527.22

Table 4.65: Received powers (μW) and Transmitted powers (mW) for the case with bitrate 144kbps, $\mathbf{V} = \{high, medium, high, low\}$ and bandwidth 2MHz and 10MHz for the first and second hop.

WVSN topology 2:

Firstly, we can see from Tables (4.66), (4.68), (4.70), (4.72), (4.74), (4.76) (4.78) and (4.80) that in this topology e.NBS achieves higher PSNR for the low motion nodes in all cases. However, MAD offers better PSNRs to the high and medium motion nodes. The MMD critetion offers the same PSNRs to all of the nodes.

Regarding the high motion nodes, they have a gain of 0.4–2.23 dB when N_0 is equal to 0 pW/Hz, if MAD is employed. The low motion nodes have a gain of 1.34–5.29 dB when e.NBS is used. On the other hand, medium motion nodes are not always favored by e.NBS, as they have a loss of 0.85 dB when the bit rate is equal to 144 kbps and a small gain of 0.2 dB when the bit rate is 96 kbps. Moreover, if N_0 is equal to 0.1 pW/Hz the high motion nodes have a gain of 0.34–2.13 dB with MAD; the low motion nodes have a gain of 1.28–5.17 dB when e.NBS is employed. As in the case with $N_0 = 0$, with e.NBS the medium motion nodes have a loss of 0.8 dB when the bit rate is equal to 144 kbps and a gain of 0.2 dB when the bit rate is 96 kbps. The e.NBS criterion achieves higher average PSNR compared to MAD for both values of N_0.

Furthermore, the choices of source and channel coding rates are not affected by the background noise. In general, for all three criteria, if the bit rate is 96 kbps, the higher possible source coding rates are preferred. In the case that the bit rate is equal to 144 kbps, the higher the motion level is, the lower channel coding rate is chosen.

The power allocation for these criteria is quite similar to that of w.NBS and MWAD, as can be seen in Tables (4.67), (4.69), (4.71), (4.73), (4.75), (4.77), (4.79) and (4.81). For the case with $\mathbf{V} = \{low, high, medium\}$, all criteria allocate higher transmitted power to the relay node $R2$ comparing to that allocated to R_1. If $N_0 = 0$ pW/Hz, MMD allocates higher transmitted power to R_2 than the other criteria. For $N_0 = 0.1$ pW/Hz, e.NBS is the criterion that allocates higher transmitted power to R_2. Nevertheless, when $\mathbf{V} = \{low, low, high\}$, the relay node $R1$ transmits the videos using higher power than $R2$ only if MMD is used. The opposite happens with e.NBS and MAD that allocate higher transmitted power to the relay node R_2. This is necessary, as the transmitted of the low motion videos by R_2 interfere with the transmitted of the high motion videos of the cluster $C3$. As in previous test cases, when $N_0 \neq 0$, an increase in transmitted powers of both source and relay nodes is observed using all set–ups. Last, when N_0 is 0 pW/Hz, the source nodes have the minimum available transmitted power, i.e. 100 mW, but when N_0 is not equal to 0, they use the maximum available transmitted power, i.e. 500 mW.

$N_0 = 0$ pW/Hz						
Cluster	$C1$		$C2$		$C3$	
Criterion	PSNR	CS	PSNR	CS	PSNR	CS
e.NBS	49.8116	3	49.0224	2	33.8598	3
MAD	44.5212	3	44.5212	3	36.0861	3
MMD	37.2351	2	37.2351	2	37.2351	3

Table 4.66: PSNR(dB) and Source and Channel Coding Rates for the case with bitrate 96kbps, $\mathbf{V} = \{low, low, high\}$ and bandwidth 4MHz for all hops.

$N_0 = 0$ pW/Hz				
Relay node	$R1$	$R2$	$R1$	$R2$
Criterion	S^{rec}	S^{rec}	S^{trans}	S^{trans}
e.NBS	0.46667	0.85864	100	183.81
MAD	0.46667	0.57568	100	123.23
MMD	1.01041	0.46667	216.30	100

Table 4.67: Received powers (μW) and Transmitted powers (mW) for the case with bitrate 96kbps, $\mathbf{V} = \{low, low, high\}$ and bandwidth 4MHz for all hops.

$N_0 = 0.1$ pW/Hz						
Cluster	$C1$		$C2$		$C3$	
Criterion	PSNR	CS	PSNR	CS	PSNR	CS
e.NBS	49.5739	3	48.8019	2	33.6992	3
MAD	44.4041	3	44.4035	3	35.8308	3
MMD	36.9584	2	36.9584	2	36.9584	3

Table 4.68: PSNR(dB) and Source and Channel Coding Rates for the case with bitrate 96kbps, $\mathbf{V} = \{low, low, high\}$ and bandwidth 4MHz for all hops.

$N_0 = 0.1$ pW/Hz				
Relay node	$R1$	$R2$	$R1$	$R2$
Criterion	S^{rec}	S^{rec}	S^{trans}	S^{trans}
e.NBS	4.69249	3.93497	1004.52	1842.08
MAD	3.78696	0.57568	810.67	842.36
MMD	4.45129	1.98610	952.89	425.16

Table 4.69: Received powers (μW) and Transmitted powers (mW) for the case with bitrate 96kbps, $\mathbf{V} = \{low, low, high\}$ and bandwidth 4MHz for all hops.

$N_0 = 0$ pW/Hz						
Cluster	$C1$		$C2$		$C3$	
Criterion	PSNR	CS	PSNR	CS	PSNR	CS
e.NBS	48.8810	3	36.0427	3	38.6263	2
MAD	45.3237	3	36.9588	3	38.4188	2
MMD	37.8481	3	37.8481	3	37.8481	2

Table 4.70: PSNR(dB) and Source and Channel Coding Rates for the case with bitrate 96kbps, $\mathbf{V} = \{low, high, medium\}$ and bandwidth 4MHz for all hops.

$N_0 = 0$ pW/Hz				
Relay node	$R1$	$R2$	$R1$	$R2$
Criterion	S^{rec}	S^{rec}	S^{trans}	S^{trans}
e.NBS	0.46667	0.94709	100	202.74
MAD	0.46667	4.14622	100	887.58
MMD	0.46667	5.02894	100	1076.54

Table 4.71: Received powers (μW) and Transmitted powers (mW) for the case with bitrate 96kbps, $\mathbf{V} = \{low, high, medium\}$ and bandwidth 4MHz for all hops.

$N_0 = 0.1$ pW/Hz						
Cluster	$C1$		$C2$		$C3$	
Criterion	PSNR	CS	PSNR	CS	PSNR	CS
e.NBS	48.7015	3	35.8090	3	38.4489	2
MAD	45.1654	3	36.6940	3	38.2606	2
MMD	37.5721	2	37.5721	3	37.5721	2

Table 4.72: PSNR(dB) and Source and Channel Coding Rates for the case with bitrate 96kbps, $\mathbf{V} = \{low, high, medium\}$ and bandwidth 4MHz for all hops.

$N_0 = 0.1$ pW/Hz				
Relay node	$R1$	$R2$	$R1$	$R2$
Criterion	S^{rec}	S^{rec}	S^{trans}	S^{trans}
e.NBS	3.85771	7.83469	825.82	1677.17
MAD	2.18458	8.33628	467.65	1784.54
MMD	1.03536	10.27815	221.64	2200.24

Table 4.73: Received powers (μW) and Transmitted powers (mW) for the case with bitrate 96kbps, $\mathbf{V} = \{low, high, medium\}$ and bandwidth 4MHz for all hops.

$N_0 = 0$ pW/Hz						
Cluster	$C1$		$C2$		$C3$	
Criterion	PSNR	CS	PSNR	CS	PSNR	CS
e.NBS	47.1708	3	46.3362	3	37.6186	2
MAD	45.0178	3	44.9916	3	38.7605	2
MMD	40.3839	3	40.3839	3	40.3839	2

Table 4.74: PSNR(dB) and Source and Channel Coding Rates for the case with bitrate 144kbps, $\mathbf{V} = \{low, low, high\}$ and bandwidth 6MHz for all hops.

$N_0 = 0$ pW/Hz				
Relay node	$R1$	$R2$	$R1$	$R2$
Criterion	S^{rec}	S^{rec}	S^{trans}	S^{trans}
e.NBS	0.46667	0.86196	100	184.52
MAD	0.46667	0.70220	100	150.32
MMD	0.46667	0.47191	100	101.02

Table 4.75: Received powers (μW) and Transmitted powers (mW) for the case with bitrate 144kbps, $\mathbf{V} = \{low, low, high\}$ and bandwidth 6MHz for all hops.

$N_0 = 0.1$ pW/Hz						
Cluster	$C1$		$C2$		$C3$	
Criterion	PSNR	CS	PSNR	CS	PSNR	CS
e.NBS	46.8543	3	45.9618	3	37.2431	2
MAD	44.7132	3	44.6792	3	38.3526	2
MMD	39.9336	3	39.9336	3	39.9336	2

Table 4.76: PSNR(dB) and Source and Channel Coding Rates for the case with bitrate 144kbps, $\mathbf{V} = \{low, low, high\}$ and bandwidth 6MHz for all hops.

$N_0 = 0.1$ pW/Hz				
Relay node	$R1$	$R2$	$R1$	$R2$
Criterion	S^{rec}	S^{rec}	S^{trans}	S^{trans}
e.NBS	4.10713	7.68114	879.21	1644.30
MAD	3.80667	5.73647	814.89	1228.00
MMD	3.54137	3.30848	758.10	708.25

Table 4.77: Received powers (μW) and Transmitted powers (mW) for the case with bitrate 144kbps, $\mathbf{V} = \{low, low, high\}$ and bandwidth 6MHz for all hops.

$N_0 = 0$ pW/Hz						
Cluster	$C1$		$C2$		$C3$	
Criterion	PSNR	CS	PSNR	CS	PSNR	CS
e.NBS	48.5202	3	39.3198	2	39.8910	2
MAD	45.9069	3	39.7126	3	40.7435	2
MMD	40.5804	3	40.5804	3	40.5804	2

Table 4.78: PSNR(dB) and Source and Channel Coding Rates for the case with bitrate 144kbps, $\mathbf{V} = \{low, high, medium\}$ and bandwidth 6MHz for all hops.

$N_0 = 0$ pW/Hz				
Relay node	$R1$	$R2$	$R1$	$R2$
Criterion	S^{rec}	S^{rec}	S^{trans}	S^{trans}
e.NBS	0.46667	1.08464	100	232.19
MAD	0.46667	1.11487	100	238.66
MMD	0.46667	2.20755	100	472.57

Table 4.79: Received powers (μW) and Transmitted powers (mW) for the case with bitrate 144kbps, $\mathbf{V} = \{low, high, medium\}$ and bandwidth 6MHz for all hops.

$N_0 = 0.1$ pW/Hz						
Cluster	$C1$		$C2$		$C3$	
Criterion	PSNR	CS	PSNR	CS	PSNR	CS
e.NBS	48.0926	3	38.9132	2	39.5777	2
MAD	45.5455	3	39.2533	3	40.3832	2
MMD	40.1784	3	40.1784	3	40.1784	2

Table 4.80: PSNR(dB) and Source and Channel Coding Rates for the case with bitrate 144kbps, $\mathbf{V} = \{low, high, medium\}$ and bandwidth 6MHz for all hops.

$N_0 = 0.1$ pW/Hz				
Relay node	$R1$	$R2$	$R1$	$R2$
Criterion	S^{rec}	S^{rec}	S^{trans}	S^{trans}
e.NBS	4.61059	9.27758	986.99	1986.05
MAD	3.20353	7.69318	685.78	1646.88
MMD	1.69310	8.08470	362.44	1730.69

Table 4.81: Received powers (μW) and Transmitted powers (mW) for the case with bitrate 144kbps, $\mathbf{V} = \{low, high, medium\}$ and bandwidth 6MHz for all hops.

Chapter 5

CONCLUSIONS AND FUTURE WORK

5.1 Conclusions

In the present thesis, we proposed a method for the optimal allocation of the resources of a Wireless Visual Sensor Network. The overall goal was to allocate the available source coding rates, channel coding rates and transmitted powers among the nodes of the WVSN in a way that the quality of the transmitted videos is maximized.

In particular, we applied our method in a multihop DS–CDMA based WVSN. The WVSN nodes can either monitor different scenes (source nodes) or retransmit videos of other sensors (relay nodes). A node's transmissions cause interference to other transmitting nodes within its transmission range, leading to degradation of the quality of the received videos. Moreover, the nodes may record scenes with different amounts of motion, so their resource requirements are different. Due to all these factors, resources (transmitted power, source coding rate, channel coding rate) have to be optimally allocated using a quality–aware joint strategy, in order to maintain the end–to–end distortion at a low level for all nodes.

In order to tackle the aforementioned problems, we proposed a cross–layer resource allocation scheme that can be used with five optimization criteria. Two of the criteria we tested, i.e. w.NBS and MWAD, are priority–based and allocate the resources with respect to the motion level of the recorded video scenes. The first (w.NBS) maximizes the distortion–related Nash Product by using motion–based bargaining powers, while the second (MWAD) minimizes the weighted aggregation of the expected end–to–end video distortions by using motion–based weights. Three other criteria that are not taking into account the motion levels of the videos were also tested. The e.NBS criterion uses the

Nash Bargaining Solution with equal bargaining powers. The MAD criterion aims at minimizing the average distortion of the videos transmitted through the network, while the MMD criterion minimizes the maximum distortion so as to achieve an overall good quality for the videos.

The conducted experiments have illustrated that both priority–based criteria achieve their goal even in the case that the background noise is considered, resulting in higher video quality (in terms of PSNR) for the source nodes that view scenes of high motion compared to e.NBS, MAD and MMD. However, MWAD achieves higher average PSNR, whereas w.NBS demands lower transmission power. Thus, for the purpose of enhancing the delivered video quality of the source nodes with respect to their content and its importance, we suggest the use of priority–based optimization criteria. The weights used in MWAD and the bargaining powers of w.NBS can be changed in order to demonstrate different levels of priorities.

Otherwise, e.NBS, MAD or MMD should be employed. MAD and e.NBS generally favor low motion videos, as they offer better quality to these videos comparing to high motion videos. Nevertheless, MAD is more fair to high motion videos as it keeps their quality at a better level than e.NBS does. If the same quality is needed for all of the videos, MMD is the criterion that should be preferred. In conclusion, the appropriate optimization criterion should be chosen by the system designer according to the requirements of each application.

5.2 Future Work

Undoubtedly, three fundamental constraints shape the WVSN design, namely the power supply, the need for delivery of multimedia content with a certain level of QoS and the lossy and transient behavior of wireless communication. Under this consideration, there are many directions for future work.

One interesting direction can be the perpetual adaptation of the allocation of the powers and the rates to the dynamically changing source and network condition. Instead of relying on stable allocations, our resource allocation technique could be modified in order to consider both the dynamic source characteristics and the network conditions. This feature is desirable for real–time multiuser multimedia applications. Another useful extension to our method can be the use of a TDMA–like network; in this case, the video streams should share in an efficient way the transmission time over the links so that the video quality received by the CCU is maximized.

Further improvement of the quality of the videos that are transmitted over WVSNs can be achieved by employing scalable video coding, as the one provided by the H.246/MPEG-4 SVC standard. The objective of the SVC standardization has been to enable the encoding of a high-quality video bitstream that contains one or more subset bitstreams that can themselves be decoded with a complexity and reconstruction quality similar to that achieved using the existing H.264/MPEG-4 AVC design with the same quantity of data

as in the subset bitstream. The subset bitstream is derived by dropping packets from the larger bitstream and can have several modalities:

(a) Temporal (frame rate) scalability: the motion compensation dependencies are structured so that complete pictures (i.e. their associated packets) can be dropped from the bitstream.

(b) Spatial (picture size) scalability: video is coded at multiple spatial resolutions. The data and decoded samples of lower resolutions can be used to predict data or samples of higher resolutions in order to reduce the bit rate to code the higher resolutions.

(c) SNR/Quality/Fidelity scalability: video is coded at a single spatial resolution but at different qualities. The data and decoded samples of lower qualities can be used to predict data or samples of higher qualities in order to reduce the bit rate to code the higher qualities.

Our method could be extended so as to use scalable videos, consisting of different layers that have different priority and resource requirements. Therefore, a different video rate-distortion model should be used in order to estimate both the encoding distortion and the distortion due to errors of transmission through a lossy channel for each layer of the transmitted video. Last, instead of PSNR, a more objective metric for quality can be chosen. Specifically, we could use the structural similarity (SSIM) index which is a well–known quality measurement metric that has been proved to be more consistent with human eye perception.

Bibliography

[1] I. F. Akyildiz, T. Melodia and K.R. Chowdhury, A survey on wireless multimedia sensor networks, *Comput. Netw.*, **vol.51, no.4** (2007) 921–960.

[2] J. N. Al-Karaki and A. E. Kamal, Routing techniques in wireless sensor networks: a survey, *IEEE Wireless Communications*, **vol.35, no.3** (2004) 6–28.

[3] E. S. Bentley, L. P. Kondi, J. D. Matyjas, M. J. Medley and B. W. Suter, Spread Spectrum Visual Sensor Network Resource Management Using an End–to–End Cross–Layer Design, *IEEE Transactions on Multimedia*, **vol.13, no.1** (2011) 125–131.

[4] D. Bertsekas and R. Gallager, *Data Networks*, 2nd ed. Englewood Cliffs, NJ:Prentice Hall, 1992.

[5] S. Betz and H. V. Poor, Energy efficiency in multihop DS–CDMA networks: A game theoretic analysis considering operating costs, *Proc. of IEEE International Conference on Acoustics, Speech and Signal Processing* (2008).

[6] K. Binmore, *Playing for Real: A Text on Game Theory*, Oxford University Press, 2007.

[7] Y. S. Chan and J. W. Modestino, A joint source coding-power control approach for video transmission over CDMA networks, *IEEE Journ. on Selected Areas in Communications*, **vol.21, no.10** (2003) 1516–1525.

[8] K. Y. Chow, K. S. Lui and E. Y. Lam, Balancing Image Quality and Energy Consumption in Visual Sensor Networks, *1st Int. Symp. on Wireless Pervasive Computing*, (2006).

[9] M. Clerc and J. Kennedy, The particle swarm–explosion, stability and convergence in a multidimensional complex space, *IEEE Trans. Evol. Comput.*, **vol.6, no.1** (2002) 58–73.

[10] J. Dowling, E. Curran, R. Cunningham and V. Cahill, sing feedback in collaborative reinforcement learning to adaptively optimize MANET routing, *IEEE Trans. Syst., Man, Cybern., Part A* (2007).

[11] E. Forster and A. Murphy, A feedback–enhanced learning approach for routing in WSN, *4th WMAN* (2005).

[12] J. Haapola, Z. Shelby, C. Pomalaza–Ráez, and P. Mähönen, Cross-layer Energy Analysis of Multi-hop Wireless Sensor Networks, *Proc. of the Second European Workshop on Wireless Sensor Networks* (2005) 33–44.

[13] J. Hagenauer, Rate-compatible punctured convolutional codes (RCPC codes) and their applications, *IEEE Trans. on Communications*, **vol.36, no.4** (1988) 389–400.

[14] P. Jayachandran and T. Abdelzaher, Bandwidth Allocation for Elastic Real-Time Flows in Multihop Wireless Networks Based on Network Utility Maximization, *International Conference on Distributed Computing Systems* (2008) 849–857.

[15] A. V. Katsenou, L. P. Kondi and K. E. Parsopoulos, Resource management for wireless visual sensor networks based on individual video characteristics, *IEEE Intern. Conf. on Image Processing* (2011) 149–152.

[16] L. P. Kondi and A .K. Katsaggelos, Joint source–channel coding for scalable video using models of rate distortion functions, *Proc. IEEE Intern. Conf. on Acoustics, Speech and Signal Processing*, **vol.3** (2001) 1377–1380.

[17] L. P. Kondi and E. S. Bentley, Game–Theory–based cross–layer optimization for Wireless DS–CDMA Visual Sensor Networks, *IEEE Int. Conf. on Image Processing* (2010).

[18] H. Kwon, T. H. Kim, S. Choi and B. G. Lee, A Cross–Layer Strategy for Energy Efficient Reliable Delivery in Wireless Sensor Networks, *IEEE Transactions on Wireless Communications*, **vol.5** (2006) 3689–3699.

[19] C. Li, J. Zou, H. Xiong and C. Wen Chen, Joint Coding/Routing Optimization for Distributed Video Sources in Wireless Visual Sensor Networks, *IEEE Transactions on Circuits and Systems for Video Technology*, **vol.21, no.2** (2011) 141–155.

[20] R. C. de Lamare, Joint Interference Suppression and Group-Based Power Allocation via Alternating Optimization for DS-CDMA Networks with Multihop Relaying, *11th European Wireless Conference–Sustainable Wireless Technologies* (2011) 1–5.

[21] Z. Lin and M. van der Schaar, Autonomic and Distributed Joint Routing and Power Control for Delay-Sensitive Applications in Multi-Hop Wireless Networks, *IEEE Transactions on Wireless Communications*, **vol.10, no.1** (2011) 102–113.

[22] R. Madan, S. Cui, S. Lall and N A. Goldsmith, Cross–Layer Design for Lifetime Maximization in Interference–Limited Wireless Sensor Networks, *IEEE Transactions on Wireless Communications*, **vol.5** (2006) 3142–3152.

[23] M. Meghji and D. Habibi, Transmission Power Control in multihop wireless sensor networks, *3rd Intern. Conf. on Ubiquitous and Future Networks* (2011) 25–30.

[24] G. Messier, J. Hartwell and R. Davies, A Sensor Network Cross–Layer Power Control Algorithm that Incorporates Multiple Access Interference, *IEEE Transactions on Signal Processing*, **vol.55** (2007).

[25] H. Park and M. van der Schaar, Bargaining strategies for networked multimedia resource management, *IEEE Transactions on Signal Processing* **vol.55** (2007).

[26] H. Park and M. van der Schaar, Faireness Strategies for Multi–user Multimedia Applications in Competitive Environments using the Kalai–Smorodinsky Bargaining Solution, *Proc. IEEE Int. Conf. Acoust., Speech, Signal Processing* **vol.2** (2007) 713–716.

[27] K. E. Parsopoulos and M. N. Vrahatis, *Particle Swarm Optimization and Intelligence: Advances and Applications*, Information Science Publishing (IGI Global), 2010.

[28] S. S. Rao, *Engineering Optimization: Theory and Practice*, John Wiley & Sons, 2009.

[29] T. S. Rappaport, *Wireless Communications: Principles and Practice*, Prentice Hall PTR, 1996.

[30] H. Schwarz, D. Marpe and T. Weigand, Overview of the Scalable Video Coding Extension of the H.264/AVC Standard, *IEEE Trans. on Circuits and Systems for Video Technology*, **vol.17, no.9** (2007) 1103–1120.

[31] H. Shiang and M. van der Schaar, Multi-user video streaming over multi-hop wireless networks: a distributed, cross-layer approach based on priority queuing, *IEEE Journal on Selected Areas in Communications* (2007) 770–785.

[32] H. Shiang and M. van der Schaar, Information-Constrained Resource Allocation in Multicamera Wireless Surveillance Networks, *IEEE Transactions on Circuits and Systems for Video Technology* **vol.10, no.4** (2010) 505–517.

[33] W. Stallings, *Wireless Communications and Networks*, Prentice Hall PTR, 2005.

[34] T. Stockhammer, M. N. Hannuksela and T. Wiegand, H.264/AVC in Wireless Environments, *IEEE Transactions on Circuits and Systems for Video Technology*, **vol.13** (2003) 657–672.

[35] A. S. Tanenbaum, *Computer Networks*, Prentice Hall PTR, 2003.

[36] H. Wang, L. P. Kondi, A. Luthra and S. Ci, *4G Wireless Video Communications*, John Wiley & Sons, Ltd, 2009.

[37] F. Zhai, Y. Eisenberg, T. N. Pappas, R. Berry and A. K. Katsaggelos, Joint source–channel coding and power allocation for energy efficient wireless video communications, *Proc. 41st Allerton Conf. Communication, Control and Computing*, (2003).

[38] R. Zhang, S. L. Regunathan and K. Rose, Video coding with optimal inter/intra-mode switching for packet loss resilience, *IEEE Journ. on Selected Areas in Communications*, **vol.18, no.6** (2000) 966–976.

Short CV

Eftychia Datsika was born in Ioannina in 1987. She was admitted at the Department of Computer Science of University of Ioannina in September 2005 and graduated in March 2010. She began her postgraduate studies at the same department in March 2010. Her research interests focus on Wireless Video Optimization and Wireless Visual Sensor Networks.